



**HAL**  
open science

## Feeding ecology of the last European colobine monkey, *Dolichopithecus ruscinensis*

Christos Alexandros Plastiras, Ghislain Thiery, Franck Guy, Dimitris  
Kostopoulos, Vincent Lazzari, Gildas Merceron

► **To cite this version:**

Christos Alexandros Plastiras, Ghislain Thiery, Franck Guy, Dimitris Kostopoulos, Vincent Lazzari, et al.. Feeding ecology of the last European colobine monkey, *Dolichopithecus ruscinensis*. *Journal of Human Evolution*, 2022, 168, pp.103199. 10.1016/j.jhevol.2022.103199 . hal-03758462

**HAL Id: hal-03758462**

**<https://hal.science/hal-03758462>**

Submitted on 22 Jul 2024

**HAL** is a multi-disciplinary open access archive for the deposit and dissemination of scientific research documents, whether they are published or not. The documents may come from teaching and research institutions in France or abroad, or from public or private research centers.

L'archive ouverte pluridisciplinaire **HAL**, est destinée au dépôt et à la diffusion de documents scientifiques de niveau recherche, publiés ou non, émanant des établissements d'enseignement et de recherche français ou étrangers, des laboratoires publics ou privés.



Distributed under a Creative Commons Attribution - NonCommercial 4.0 International License

## Feeding ecology of the last European colobine monkey, *Dolichopithecus*

Christos Alexandros Plastiras<sup>a,b,\*</sup>, Ghislain Thiery<sup>b</sup>, Franck Guy<sup>b</sup>, Dimitris S. Kostopoulos<sup>a</sup>,  
Lazzari Vincent<sup>b</sup>, Gildas Merceron<sup>b</sup>

<sup>a</sup> *Laboratory of Geology and Palaeontology, Aristotle University of Thessaloniki, 54 124 Thessaloniki, Greece*

<sup>b</sup> *PALEVOPRIM – UMR 7262 CNRS-INEE, Université de Poitiers, 86073 Poitiers Cedex, France*

**\*Corresponding author.**

*Email address:* [caplasti@geo.auth.gr](mailto:caplasti@geo.auth.gr) (C.A. Plastiras)

## **Acknowledgments**

The authors thank A. Mille, curator and D. Mary musées de Perpignan (France), D. Berthet from the Musée des Confluences, E. Robert from the Université Claude Bernard (Lyon, France), N. Spassov from the Natural History Museum of Sofia (Bulgaria), G.D Koufos from the Laboratory of Geology and Paleontology of Aristotle University of Thessaloniki (LGPUT, Greece), B. Haiduc and B. Ratoi and P. Tibuleac from Department of Geology of Alexandru Ioan Cuza University of Iasi (Romania), T. D. Nishimura and M. Takai from the Primate Research Institute University of Kyoto (PRI, Japan), the Royal Museum of Central Africa (Tervuren, Belgium), the Seckenberg Museum of Frankfurt (Frankfurt, Germany) and Laboratory Paleontology Evolution Paleoecosystems Paleoprimatology, University of Poitiers (PALEVOPRIM, France). We are also grateful to Arnaud Mazurier (PALEVOPRIM) (Centre de Microtomographie of Poitiers) for his help with the acquisition of the micro-CT scans. This research is co-financed by Greece and the European Union (European Social Fund-ESF) through the Operational Programme «Human Resources Development, Education and Lifelong Learning» in the context of the project “Strengthening Human Resources Research Potential via Doctorate Research” (MIS-5000432), implemented by the State Scholarships Foundation (IKY); the Eiffel Excellence Scholarship Programme of the French Ministry of Foreign and European Affairs; and the Diet Scratches Project (ANR-17CE27-0002-01; PI: G. Merceron).

## Feeding ecology of the last European colobine monkey, *Dolichopithecus ruscinensis*

### **Abstract**

Currently, very little is known about the ecology of extinct Eurasian cercopithecids. Dietary information is crucial in understanding the ecological adaptations and diversity of extinct cercopithecids and the evolution of this family. For example, the colobine genus *Dolichopithecus* is represented by multiple large bodied species that inhabited Eurasia during the Pliocene-Early Pleistocene. The available evidence, though limited, suggests semi-terrestrial locomotion, which contrasts with most extant African and Asian colobines that exhibit morphological and physiological adaptations for arboreality and folivory. These differences raise questions regarding the dietary specialization of early colobine taxa and how/if that influenced their dispersion out of Africa and into Eurasia. To further our understanding of the ecology of Plio-Pleistocene cercopithecids, we characterized the dental capabilities and potential dietary adaptations of *Dolichopithecus ruscinensis* through dental topographic and enamel thickness analyses on an M<sup>1</sup> from the locality of Serrat d'en Vacquer–Perpignan (France). We also assessed the feeding behavior of *Dolichopithecus ruscinensis* through dental microwear texture analysis on a broad sample of fossil molars from fossil sites in France, Greece, Bulgaria, and Romania. Dental topographic and enamel thickness analyses suggest that *Dolichopithecus ruscinensis* could efficiently process a wide range of foods. Results of the dental microwear texture analysis suggest that its diet ranged from folivory to the consumption of more mechanically challenging foods. Collectively, this suggests a more opportunistic feeding behavior for *Dolichopithecus* than characteristic of most extant colobines.

**Keywords:** Cercopithecidae; Dental microwear; Texture analysis; Dental topography; Plio-Pleistocene; Paleoecology

## 1. Introduction

The Colobinae subfamily has been long described as a group of highly folivorous monkeys (Davies and Oates, 1994 and references therein). All extant colobines possess a multi-chambered stomach with an enlarged forestomach adapted to microbial food fermentation (Chivers, 1994; Lambert, 1998; Matsuda et al., 2019). Furthermore, colobines possess robust jaws with bilophodont molars with higher and sharper cusps compared to the other cercopithecoid subfamily (Cercopithecinae). These features enable colobines to effectively process and digest large amounts of tough and fibrous material (e.g., most leaves; Ravosa, 1996; Daegling and McGraw, 2001; see also Onoda et al., 2011). Moreover, with the exception of *Semnopithecus entellus*, which spends significant amounts of time on terrestrial substrates (Sayers and Norconk, 2008), extant African and Asian colobines are arboreal. Despite their primarily folivorous diets, some extant African and Asian colobines (i.e., Colobini and Presbytini respectively) consume significant amounts of nonleafy plant parts like seeds and fruits. This behavior is likely influenced by the availability of preferred food resources and competition with sympatric colobines and cercopithecines (Maisels et al., 1994; Tutin et al., 1997; Daegling and McGraw, 2001; Vandercone et al., 2012).

The first occurrence of Colobinae in the fossil record dates to the Middle Miocene of Kenya (12.5–10 Ma; Rossie et al., 2013). During the Late Miocene, colobine presence in Europe is recorded by *Mesopithecus*, whose first appearance is recorded in early Turolian (8.7–8.2 Ma) localities of northern Greece (de Bonis et al., 1990; Koufos, 2009, 2019). In the Pliocene, the European fossil record shows the presence of two colobine genera, *Mesopithecus* and *Dolichopithecus*, coexisting temporally and occurring sympatrically in fossil sites of France (Montpellier, Perpignan), Bulgaria (Dorkovo), and Romania (Mălușteni; Eronen and Rook, 2004; Delson et al., 2005). After the Early Pleistocene, colobines disappear from the European fossil record, though they persist in Asia, with some extinct species

possibly being related to the living Asian species (Andrews et al., 1996; Jablonski, 1998; Pan et al., 2004). While the phylogenetic relationships of *Mesopithecus* and *Dolichopithecus* with extant Asian colobines remain unclear, the numerous modern representatives combined with fossil evidence in Africa and Eurasia attest to the evolutionary success of this subfamily.

Early colobines may have differed ecologically from extant representatives (e.g., Leakey, 1982; Davies, 1994; Rowe et al., 1996). In the Plio-Pleistocene of Africa, colobines are represented by at least six genera (i.e., *Microcolobus*, *Rhinocolobus*, *Paracolobus*, *Libypithecus*, *Kuseracolobus*, and *Cercopithecoides*). These genera exhibit postcranial and dental morphologies not seen among their extant African counterparts (Leakey, 1982), which suggests that they were considerably more ecologically diverse than the extant colobine radiation (Williams and Geissler, 2014; Frost et al., 2015; Frost, 2017; Merceron et al., 2021). Furthermore, there are contrasting opinions concerning the locomotor adaptations of early colobines. Some suggest that early African colobines were mainly arboreal and that the semi-terrestrial locomotion in some Late Miocene and Plio-Pleistocene taxa (e.g., *Cercopithecoides williamsi*, *C. kimeui*, *C. bruneti*, *Paracolobus mutiwa*, *Pa. chemeroni*) is secondarily derived (Hlusko, 2006; Gilbert et al., 2010; Nakatsukasa et al., 2010).

The ecological diversity of early African colobines raises questions about whether dietary specialization may have played a role in their Out-of-Africa dispersion. The evidence for the earliest Eurasian colobine, *Mesopithecus pentelicus*, suggests that it was an opportunistic feeder, possibly consuming seeds, and was semi-terrestrial (Youlatos, 2003; Merceron et al., 2009b; Youlatos and Koufos, 2010; Thiery et al., 2017a, 2021; Ji et al., 2020). The available dietary information for other extinct Eurasian cercopithecoid taxa is limited, however, hampering our understanding of colobine dietary evolution. *Dolichopithecus* is a suitable taxon to address such questions, as it is geographically widespread and coexisted in

some places with *Mesopithecus*, thus providing insight into possible niche partitioning between colobines.

### 1.1. *Dolichopithecus fossil record and paleoecology*

The genus *Dolichopithecus* includes large bodied (22 to 28kg for males and 15 to 17kg for females; Delson et al., 2000) colobines found at Plio-Pleistocene sites in France, Greece, and Ukraine (Koufos et al., 1991; Eronen and Rook, 2004). It is mostly represented by a single species, *Dolichopithecus ruscinensis* (Depéret 1889), without apparent differences in size or morphology across geography and time (Maschenko, 1991; Delson et al., 2005). Two additional species, *Dolichopithecus balcanicus* and *Dolichopithecus hypsilophus*, have been proposed; however, the limited material assigned to these taxa does not currently allow for clear distinctions among *Dolichopithecus* species (Gremiatskiy, 1958; Maschenko, 2005; Spassov and Geraads, 2007). Most specimens of *D. ruscinensis* are from the type locality of Serrat d'en Vacquer—Perpignan (France), with the biochronological range of this fossil species spanning from approximately 5.3 to 2.0 Ma. Nevertheless, phylogenetic relationships among the western Eurasian species of *Dolichopithecus*, extinct Asian taxa (e.g., *Kanagawapithecus*, *Parapresbytis*), and extant colobines remain unclear (Kalmykov, 1992, 1995; Jablonski, 2002; Iwamoto et al., 2005; Egi et al., 2007; Nishimura et al., 2012).

The available ecological information for *D. ruscinensis* is derived mostly from analyses of postcranial morphology (Depéret, 1890; Gabis, 1961; Jolly, 1967, 1970; Szalay and Delson, 1979; Ingicco, 2008). Given postcranial similarities to *Mandrillus sphinx* and *Macaca sylvanus*, early interpretations suggested semiterrestrial locomotor adaptations (Depéret, 1890; Jolly, 1967), while other studies interpreted the evidence to suggest a fully terrestrial lifestyle similar to savannah baboons (Gabis, 1960, 1961). The degree of terrestriality inferred for *D. ruscinensis* is not observed in any extant colobine. The

environment in which *D. ruscinensis* lived has been briefly discussed (e.g., Delson, 1994; Tobien, 1970), but a detailed investigation is still pending. *Dolichopithecus ruscinensis* appeared in Europe following the refilling of the Mediterranean Basin, which prompted the development of woodland and humid forests across the northern Mediterranean (Delson, 1994; Koufos and Vasileiadou, 2015) and might have facilitated adaptations associated with a variable locomotor repertoire in *Dolichopithecus*.

In this paper we investigate the dietary ecology of the last known European colobine, *D. ruscinensis*. We combine data on dental morphology (i.e., enamel thickness, occlusal relief) and dental microwear (microwear textures) to test the hypothesis that *D. ruscinensis* exhibited molar morphology and dietary behavior similar to that of extant colobines. This study has important implications for understanding the evolution of Colobinae. If the dietary ecology of early colobines appears to be more opportunistic, it may indicate that specialized adaptations towards folivorous diets shown by most extant colobines may have occurred as evolved traits used as a strategy to withstand periods of food shortage and/or to avoid interspecific competition for food resources (Napier, 1970).

### 1.2. *The functional significance of enamel thickness and studies of tooth shape*

Previous work has linked variation in enamel thickness among mammals, and especially primates, to adaptations to diet (Grine et al., 2005; Lucas et al., 2008; Vogel et al., 2008). However, disentangling the contributions of adaptation from phylogeny on trait variation is not always straightforward (e.g., Smith et al., 2012; McGraw et al., 2012). Whether primate enamel thickness is adapted to food mechanical properties is a matter of debate (King et al., 2005; Rabenold and Pearson, 2011; Pampush et al., 2013; Kato et al., 2014). For example, primates that consume hard food items (e.g., hard-shelled nuts) often have relatively thicker enamel compared to primates that feed on softer foods (Kay, 1981;

Dumont, 1995; Shellis et al., 1998; Martin et al., 2003; Lambert et al., 2004). The thicker enamel is expected to increase tooth resistance to high stress (Lucas et al., 2008). Martin (1983) devised relative enamel thickness as a scale-free metric to quantify enamel distribution over the tooth crown, which was later adopted and modified by other researchers (e.g., Kono, 2004; Lucas et al., 2008; Olejniczak et al., 2008). However, size is an important factor in certain aspects of feeding biology (Davies et al., 1983; Kay and Covert, 1984); the size of the food item that a given tooth can process depends to some extent on the size of the tooth itself, which is correlated with body size among species (Lucas et al., 1986). Thus, larger primates may be able to process a wider array of food resources, in terms of both size and mechanical properties, compared to smaller species (Gingerich, 1977; Wood, 1979; Norconk et al., 2009).

Three-dimensional topographical analyses have now moved into landmark-free methods using geographic information systems to quantify tooth shape (Zuccotti et al., 1998; Ungar and Williamson, 2000). These methods have generally been successful at correlating tooth shape with diet (e.g., King et al., 2005; Godfrey et al., 2012; Ledogar et al., 2013; Winchester et al., 2014; Berthaume and Schroer, 2017; Berthaume et al., 2018). Dental topography can quantify morphologies across stages of dental wear (Ungar and M'Kirera, 2003; Winchester et al., 2014). Dental topography has also been used to investigate niche partitioning among primate taxa (Godfrey et al., 2012; Berthaume and Schroer, 2017), to assess the relationship between enamel and dentine morphology (Skinner et al., 2010; Guy et al., 2015), to explore the relationship between tooth shape and food breakdown (Berthaume, 2016a, 2016b; Thiery et al., 2017a, 2017b), and to assign a fossil primate to a new species (Boyer et al., 2012). Several measures have been used to quantify aspects of tooth shape, including relief, curvature/sharpness, complexity of the tooth surface, and ambient occlusion (Evans et al., 2007; Bunn et al., 2011; Guy et al., 2013; Winchester et al., 2014; Allen et al., 2015; Berthaume et al., 2019a; Shan et al., 2019). These

morphological characteristics are important in characterizing tooth function associated with a specific type of diet (Bunn et al., 2011; Ledogar et al., 2013; Allen et al., 2015; Ungar et al., 2018). For instance, folivorous primates usually possess taller crowned/cusped molars with more curved/sharper features (i.e., shearing crests) compared to more durophagous primates (Bunn et al., 2011; Winchester et al., 2014), whereas high values of dental complexity have been shown to correlate with the degree of herbivory in some mammalian clades (Evans et al., 2007; see Berthaume et al., 2020 for a review in dental topography).

### 1.3. *Dental microwear texture analysis*

Dental microwear, the study of microscopic use-wear scars in enamel, reveals information about what an individual ate over a short period of time before death (Baker et al., 1959; Rensberger, 1978; Walker et al., 1978; Teaford and Oyen, 1989; Ungar and Teaford, 1996; Ungar et al., 2008). Dental Microwear Texture Analysis (DMTA) provides repeatable and quantitative characterization of 3D microwear surfaces (Scott et al., 2006; Teaford, 2007; Merceron et al., 2009b; Percher et al., 2018) and has proven to be a valuable tool for reconstructing the dietary ecology of extant and extinct mammals (for an extended discussion on application and comparisons with previous methods, see Calandra and Merceron, 2016; DeSantis, 2016; Green and Croft, 2018). Dental microwear texture variables characterize properties such as roughness, the orientation and direction of microwear features (e.g., pits and striations), and their variation across a microwear surface. Primates reported to regularly consume hard foods have been shown to display more complex and heterogeneous microwear textures, whereas primates that feed on less hard but tougher foods have been associated with striated microwear features and overall more anisotropic and less heterogeneous textures (Merceron et al., 2006; Scott et al., 2006, 2012; Ragni et al., 2017; Percher et al., 2018). In addition to the mechanical properties of food objects, exogenous

abrasives and attrition potentially affect microwear patterns (Ungar, 1995; Teaford and Lytle, 1996; Nystrom et al., 2004; Lucas et al., 2014; Ackermans et al., 2020; Schulz-Kornas et al., 2020; van Casteren et al., 2020; Winkler et al., 2020). However, controlled experiments have shown that even if dust can affect microwear textures, there is no need to invoke grit to explain tooth wear (Merceron et al., 2016; Sanson et al., 2017; Teaford et al., 2017).

## 2. Materials and methods

### 2.1. Enamel thickness and dental topography

The fossil *D. ruscinensis* sample consists of a right M<sup>1</sup> of a subadult (MHNPn-PR01), as no other upper molars were available (Fig. 1A). The specimen is from Serrat d'en Vacquer—Perpignan and is stored in the Muséum d'Histoire Naturelle Perpignan, France. The specimen retains minimal wear (Fig. 1), and shows basal flaring on the lingual part, a typical feature on cercopithecoid cheek teeth (Delson, 1973; Swindler, 2002).

The extant comparative sample consists of 39 M<sup>2</sup>s belonging to 20 cercopithecoid species. We included Asian and African colobines and cercopithecines to ensure that our comparative sample encompasses a wide array of the dietary preferences seen in extant cercopithecoids. All teeth are derived from dry skulls of historical collections from museums and other public institutions (Supplementary Online Material [SOM] Table S1). Following previous standard approaches, only subadults with unworn M<sup>2</sup>s or with minimal wear were selected to ensure that no macro-elements were altered by wear (e.g., King et al., 2005; Olejniczak et al., 2008 among others).

The comparison between different molars (i.e., fossil M<sup>1</sup> with M<sup>2</sup>s of extant species) could be considered problematic in enamel thickness and dental topographic analyses (e.g., Bunn and Ungar, 2009). However, while the available M<sup>1</sup> material of extant species showed

advanced wear, prohibiting morphological comparisons, in most cases cercopithecoid first and second molars are not distinguishable from each other within a given species; the only apparent difference between them is in terms of size, with no major differences in shape and morphology evident (Delson, 1973; Swindler, 2002; Bunn et al., 2009). Furthermore, both upper and lower first and second molars have similar functions during mastication and food fragmentation; thus, they are expected to possess similar morphological adaptations (Kay and Hiimae, 1974; Kay, 1975).

## 2.2. Dental microwear texture analysis

The fossil material used for DMTA consists of 30 *Dolichopithecus* molars (SOM Table S2). All specimens belong to *D. ruscinensis*, except a single specimen from Tenevo (Bulgaria) assigned to *D. balcanicus* (Spassov and Geraads, 2007). As sample sizes are too small to explore microwear texture differences among extinct species or fossil sites, here we pool the fossil specimens at the genus level. The fossil material was collected in the fossiliferous localities of Serrat d'en Vacquer—Perpignan (France,  $n = 23$ ), Dorkovo (Bulgaria,  $n = 3$ ), Tenevo (Bulgaria,  $n = 1$ ), Vorog (Bulgaria,  $n = 1$ ), Megalo Emvolon (Greece,  $n = 1$ ), and Mălușteni (Romania,  $n = 1$ ). The fossil specimens are housed in the Museum d'Histoire Naturelle Perpignan (France), Musée des Confluences and Université de Lyon (France), Natural History Museum of Sofia (Bulgaria), Museum of Geology-Paleontology-Paleoanthropology of Aristotle University of Thessaloniki (Greece) and Department of Geology of Alexandru Ioan Cuza University of Iași (Romania).

Our extant comparative sample includes eight species with dietary behaviors that bracket the extremes of food mechanical properties (i.e., soft-tough, hard-brittle, and more diverse) usually consumed by cercopithecoids (see SOM Table S3 and citations therein): five colobines (*Colobus guereza*,  $n = 25$ ; *Ptilocolobus badius*,  $n = 16$ ; *Nasalis larvatus*,  $n = 7$ ;

*Semnopithecus entellus*,  $n = 8$ ; *Presbytis melalophos*,  $n = 19$ ) and three cercopithecines (*Lophocebus albigena*,  $n = 16$ ; *Erythrocebus patas*,  $n = 16$ ; *Chlorocebus aethiops*,  $n = 37$ ).

### 2.3. Dietary categorization

All species used in enamel thickness, dental topographic and microwear analyses were assigned to one of three general dietary categories: folivory, mixed feeders, or fruit/seed consumption. This division is based on dietary information from previously published studies on wild populations (see SOM Table S3 and citations therein). Thus, in the current study, the folivorous category includes species that primarily rely on foliage throughout the year (leaf and flower consumption >50% of their annual diet), even though the consumption of fruits, seeds, and other resources is also expected in some cases, such as in African (*Colobus polykomos*, *Colobus guereza*, *Colobus satanas*, *Procolobus verus*) and Asian colobines (*Nasalis larvatus*, *Semnopithecus entellus*, *Trachypithecus cristatus*, *Presbytis melalophos*; SOM Table S3). Species in the fruit/seed consumption category included six species that primarily exploit fruits and seeds (*Lophocebus albigena*, *Lophocebus aterrimus*, *Cercocebus torquatus*, *Cercopithecus diana*, *Cercopithecus nictitans*, and *Cercopithecus pogonias*) throughout the year (fruit and seeds >50% of their annual diet), even if they also occasionally consume leaves and animal matter (Mitani, 1989; Ham, 1994; Poulsen et al., 2001; Curtin, 2004; Buzzard, 2006; McGraw et al., 2012). Finally, a total of six species were classed as mixed feeders: (e.g., *Papio anubis*, *Papio hamadryas*, *Mandrillus leucophaeus*, *Cercopithecus campbelli*, *Chlorocebus aethiops*, and *Erythrocebus patas*) because they usually exhibit more opportunistic dietary behaviors and consume a wide array of food resources, such as leaves, fruits, seeds, gum, grass, shoots, roots and tubers, bark, and animal matter, that vary throughout the year (SOM Table S3). Although these dietary categories are relatively broad, and colobines and cercopithecines do have variable diets, we

expect these categories to reflect dental morphological and microwear texture differences among primates with contrasting diets (e.g., folivores vs. fruit/seed-eaters), as well as intermediate morphologies and microwear textures associated with mixed feeders.

#### 2.4. *Data collection*

Dental topographic and enamel thickness analyses The fossil M<sup>1</sup> and the comparative sample of M<sup>2</sup>s were scanned using EasyTom XL duo  $\mu$ CT (Plateforme PLATINA, PALEVOPRIM, University of Poitiers, France). Computed tomographic scans were processed in Avizo v. 7.0 (Visualization Sciences Group, 2011). Each enamel cap was isolated from the dentine tissue using automatic segmentation tools and then was smoothed using the ‘smoothing labels’ command (size = 3, 3D volume). Each resulting enamel cap surface was extracted using the ‘generate surface’ module with the unconstrained smoothing type (smoothing extent = 3) (Fig. 1B). The resulting enamel caps then were separated into two components, the outer enamel surface (OES) and the enamel-dentine junction surface (EDJ), using Geomagic studio 2013 (3D Systems Inc., 2013). After removing potential artifacts (e.g., small holes, intersecting triangles produced by the tessellation procedure), the resulting surfaces were set to an equivalent amount of (55 k) polygons by a re-tessellation of the original polyhedral surface, with each polygon retaining an equivalent size. This procedure does not significantly affect any macroscopic features present on the tooth crown (Fig. 1B, C).

The position and orientation of all OES/EDJ couples were standardized using a reference plane, created by a best-fit plane procedure applied on the occlusal basin of the EDJ surface, which represents the virtual space xy axis. The x-axis was then aligned with an axis formed by connecting the dentine horn tips of the paracone and protocone (SOM Fig. S1D, E). Lastly, the lowermost point of each molar cervix was set to x, y, 0 so that the crown height could be measured on a z positive scale. Following standardization, each OES and EDJ

surface for every specimen underwent a subsampling procedure (SOM Fig. S1F, G) to retain only the regions above a plane parallel to the xy reference plane passing through the lowermost point of the occlusal basin for both OES and EDJ surfaces (Ulhaas et al., 2004; Guy et al., 2015). All enamel thickness and dental topographic variables (see below) were measured on these subsampled 3D surfaces (SOM Fig. S1G), because it has been shown that some variables correlate better with diet when considering subsampled surfaces (Allen et al., 2015; Berthaume et al., 2018), as doing this minimizes the influence of tooth elements, such as the lateral parts of enamel, that do not participate actively in food comminution (Thiery et al., 2017a).

Eight variables were measured on each virtually reconstructed molar (see Table 1 and references therein). We used three variables that characterize enamel thickness. Two of these variables estimate 3D relative enamel thickness—volumetric (3DRETvol; Kono, 2004; Olejniczak et al., 2008) and geometric (3DRETgeo; Thiery et al., 2017c, 2019). Additionally, we measured a new linear measure of the thickness of enamel present on a crown, namely, absolute crown strength (ACS; Schwartz et al., 2020). This metric measures the average enamel thickness modeled as a hemisphere assuming a uniform distribution and assesses the resistance of teeth to fracture (see SOM Fig. S1 in Schwartz et al., 2020). Furthermore, we measured five variables that characterize dental topography. Dental relief was assessed by relief index (LRFI) and inclination; the former provides a more global assessment of occlusal relief (Boyer, 2008) whereas the latter documents the variation of relief across a tooth surface (Guy et al., 2013). 'Orientation patch count rotated' (OPCR) was used to quantify tooth complexity (Evans et al., 2007; Evans and Jernvall, 2009; Evans and Janis, 2014). Complexity essentially quantifies the number of locations on the tooth's surface where foods are likely to fracture, and is presumably associated with the number of occlusal features (Berthaume et al., 2020). Curvature/sharpness was assessed by Dirichlet normal energy (DNE; Bunn et al., 2011) and area-relative curvature (ARC; Guy et al., 2013, 2017;

Thiery et al, 2021). Lastly, we considered two estimates that measure the area of the molar crown: the three-dimensional occlusal enamel surface (OES 3D) of each specimen and its two-dimensional projection (OES 2D).

Calculations for 3DRETgeo, ACS, LRFI, inclination, OPCR, DNE, ARC, OES 2D and OES 3D were performed using the beta version of the 'Doolkit' package (Thiery et al., 2021) in R v. 3.6 (R Core Team, 2013), while 3DRETvol was calculated using Geomagic studio 2013 (3D Systems Inc., 2013). The values of all these metrics are given in SOM Table S1.

Dental microwear texture analysis Data for DMTA were collected on molar Phase II (crushing) and Phase I (shearing) facets (Maier, 1977). Analyses were preferentially done on upper and lower M<sup>2</sup>s in extant species, but the fossil sample also includes some M<sup>1</sup>s and M<sup>3</sup>s. Experimental work has shown no significant variation along the upper and lower molar sequences (Ramdarshan et al., 2017), and no significant differences between homologous facets of upper and lower molars (Teaford and Walker, 1984). Traditionally, microwear analyses on primates are performed on dental facets resulting from the Phase II stroke of mastication instead of Phase I, because it is suggested that they more accurately distinguish diet (Krueger et al., 2008). In this analysis, we include both Phase I and II facets (Fig. 2), as both facet types seem to bear dietary signals (Merceron et al., 2021).

Following standard protocols, teeth were cleaned and then molded with a silicone dental molding material (polyvinyl siloxane Coltene Whaledent, President Regular Body). Each dental facet was then scanned with 'TRIDENT', a confocal DCM8 Leica Microsystems surface profilometer housed at the PALEVOPRIM lab (Centre National de la Recherche Scientifique [CNRS], University of Poitiers) using a 100× lens (Merceron et al., 2016). The scanned surfaces were mirrored and automatically freed from any abnormal peaks, and a 200 × 200 μm area was then extracted and saved as a digital elevation model to be used for DMTA. The resulting data were analyzed in Toothfrax v. 1.0 (Surfract, [www.surfract.com](http://www.surfract.com)). Five variables were used to characterize microwear surface textures (see Table 1 and

references therein): complexity (Asfc; dimensionless), the scale of maximum complexity (Smc in  $\mu\text{m}^2$ ), heterogeneity (Hasfc with 9, 36, 81 cells; dimensionless), anisotropy (ePLsar at 1.8  $\mu\text{m}$ ; dimensionless) and textural fill volume (Tfv at the scale of 2  $\mu\text{m}$ ; in  $\mu\text{m}^3$ ).

## 2.5. *Statistical analysis*

Dental topographic and enamel thickness analyses Topographical estimates and enamel thickness metrics are often correlated, while the presence and the strength of such correlations could be affected by parameters such as phylogeny and dietary variation (Berthaume et al., 2020). In other words, closely related species are assumed to have similar traits because of their shared ancestry and thus produce more similar residuals from the least square regression line. Thus, some similarities in dental traits among cercopithecine and colobine species (e.g., thick/thin enamel, high/low dental relief, etc.) may be due to their phylogenetic relatedness while others may show lability or stability over time, suggesting that factors other than or in addition to phylogeny may have influenced their evolution (e.g., diet). Consequently, estimation of the phylogenetic signal can provide some insight into how particular traits have evolved (see Symonds and Blomberg, 2014). We therefore assessed the relationships among all variables (e.g., 3DRETvol, 3DRETgeo, ACS, OPCR, LRFI, inclination, DNE, ARC) using phylogenetic generalized least squares (PGLS) regression analysis, which allowed us to evaluate the potential effect of phylogeny on the distribution of the data (Winchester et al., 2014; Boyer et al., 2015; Pampush et al., 2016; Thiery, et al., 2017). The effect of phylogeny is measured using Pagel's Lambda (Pagel, 1994, 1999; Freckleton et al., 2002), henceforth referred to as  $\lambda$ , which is a measure of phylogenetic signal with values ranging from 0 to 1 (0 representing no phylogenetic structuring, 1 representing a perfect fit between data and a Brownian motion model of change in values through evolution). A phylogeny for the 20 cercopithecine species included in this study was generated using a consensus tree (100 iterations) downloaded from the

10k Trees Project website V. 3 (Arnold et al., 2010). We also included the 2D occlusal enamel surface (OES 2D) in our PGLS regression analysis to investigate the effect of size on the distribution of data. Instead of using OES 3D as a size indicator, we chose OES 2D as the latter is not influenced by dental relief. To perform the PGLS we used the 'caper' package v. 1.0.1 in R v. 3.6 (R Core Team, 2013).

To explore the dental traits of the fossil molar of *D. ruscinensis* with respect to diet, we first examined the morphological differences among the proposed dietary categories. This was achieved in SPSS v. 22.0 (SPSS, 2013) by comparing the variables among the dietary categories (i.e., 3DRETvol, 3DRETgeo, ACS, LRFI, inclination, OPCR, DNE and ARC) using the nonparametric Kruskal-Wallis followed by Dunn's post-hoc tests with Bonferroni adjustment, and a significance level set to 0.05. Next, linear discriminant analyses (LDA) were performed using several variable combinations to determine which combination(s) provides the most successful classification of individuals in the proposed dietary categories, and to determine where the fossil molar falls with respect to the range of variation of the comparative sample. Moreover, each LDA variable combination included a jack-knife resampling method and only the variables that were not correlated in the PGLS were incorporated. Lastly, in each variable combination we included the 3D occlusal enamel surface (OES 3D), as it has been shown to improve the success rate of classification (Winchester et al., 2014; Thiery et al., 2017a). Computations and visualizations for the discriminant analyses were performed using PAST v. 3.22 (Hammer et al., 2001).

Dental microwear texture analysis To identify microwear texture differences associated with diet, nonparametric Kruskal-Wallis tests were performed on modern species and *Dolichopithecus* to determine which variables differ significantly among species for each dental facet type (i.e., Phase II and Phase I). Post-hoc pairwise comparisons among extant species and *Dolichopithecus* for both dental facet types were performed using Dunn's post-hoc tests with Bonferroni adjustment, with a significance level set to 0.05. All computations

were performed using SPSS v. 22.0 (SPSS, 2013). Lastly, to assess the variation in dental microwear textures across dental facet types, we explored the values of *Asfc* and *epLsar* between facet type from one species to another.

### 3. Results

#### 3.1. Dental topographic and enamel thickness analyses

The PGLS analysis reveals significant correlations between pairs of variables with some containing a significant phylogenetic signal (Table 2). It is worth mentioning, that both measures of 3D relative enamel thickness (i.e., 3DRETvol and 3DRETgeo) are strongly correlated with both relief estimates (i.e., LRFI and inclination) with no phylogenetic effect, whereas the new linear measure of enamel thickness (i.e., ACS) shows no correlation with the relief estimates, yet with a strong phylogenetic effect (Table 2). In addition, size is significantly correlated with OES 2D, 3DRETvol, ACS, OPCR, and DNE (SOM Figs. S2–S5; Table 2). The largest species included in our extant sample (i.e., *P. anubis*, *P. hamadryas*, and *M. leucophaeus*) are separated from the rest of the sample (see specimens labeled 1 and 2 in the blue box in SOM Figs. S2–S5).

Results of the Kruskal-Wallis test indicate significant differences ( $p < 0.001$ ) among dietary categories in 3DRETvol and 3DRETgeo, LRFI, inclination, and ARC (Table 3). Folivorous species have significantly lower values of 3DRETvol and 3DRETgeo than species classified as fruit/seed consumers, and significantly lower values of 3DRETgeo than mixed feeders (Tables 4 and 5). Furthermore, the folivorous taxa exhibit significantly higher values of LRFI and ARC than mixed feeders and fruit/seed eaters (Tables 4 and 5), whereas the folivores also have significantly lower values of inclination than fruit/seed eaters (Tables 4 and 5).

While seed specialists such as *L. albigena*, *L. aterrimus*, and *C. torquatus* possess the highest values of 3DRETvol and 3DRETgeo (Fig. 3A, B; SOM Fig. S6A, B), the highest values of

ACS in our sample are shown by *Papio* (*P. hamadryas* then *P. anubis*) followed by *Mandrillus* (SOM Fig. S6C), which all possess moderate values of 3DRETvol and 3DRETgeo (SOM Fig. S6A, B). The folivorous cercopithecids exhibit the lowest ACS values (Fig. 3C; SOM Fig. S6C).

The 3DRETvol and 3DRETgeo of the MHNPn-PR01 molar falls within the range of both mixed feeders and folivores, whereas the ACS value of the fossil specimen falls within the range of mixed feeders (Fig. 3A–C). The values of LRFI, inclination and ARC of MHNPn-PR01 more closely resemble folivorous species (Fig. 4A–C; SOM Fig. S7A–C). For OPCR and DNE, the values of the fossil molar fall within the range of folivores and mixed feeders, but these two topographic metrics show considerable overlap across the three dietary categories (Figs. 3D and 4D).

The results of the LDAs are presented in Table 6. The combination of ARC, ACS, and OES 3D presents the highest rate of classification. However, the contribution of each of these variables differs depending on the axis considered. On one hand, ARC (-0.098) has the biggest effect on axis 1, followed by ACS (0.078) and OES 3D (0.053), although all with lower effects. On the other hand, OES 3D (42.185) contributes the most to the second axis, followed by ACS (0.346) then ARC (0.015) with the latter two having a much lower effect. This implies that the second axis is heavily influenced by tooth size. Indeed, the largest representatives in our sample (e.g., *Papio* and *Mandrillus*) are separated from the rest of the cercopithecids (see specimens labeled 1 and 2 in the blue box in Fig. 5). The fossil M<sup>1</sup> (MHNPn-PR01) is placed out of the range of the dietary categories, in a space between mixed feeders and folivores (Fig. 5).

### 3.2. Dental microwear texture analysis

Descriptive statistics for each microwear texture variable are given in Table 7 and the results of the Kruskal-Wallis tests in Table 8. Results for Phase II facets showed

significant differences among species in Asfc, Smc, epLsar, and Hasfc<sub>36</sub> (Table 8). Results for the Phase I facets showed significant differences in Asfc, Smc, and Tfv (Table 8).

Post-hoc pairwise comparisons indicate significant differences among species and depending on the facet type (Tables 9 and 10). For Phase II facets, the colobines *Co. guereza*, *Pi. badius*, and *P. melalophos* have significantly lower Asfc and higher epLsar than *L. albigena*, *Ch. aethiops*, and *E. patas* (Fig. 6). *Semnopithecus entellus* differs from *L. albigena* in having significantly lower values of Asfc, and both *S. entellus* and *N. larvatus* differ from *E. patas* in having significantly lower Asfc and higher epLsar (Tables 9 and 10). Additionally, *Co. guereza* has significantly lower values of Hasfc<sub>36</sub> than *L. albigena* and *S. entellus* and *P. melalophos* has significantly lower values of Hasfc<sub>36</sub> than *Ch. aethiops* (Tables 9 and 10). *Dolichopithecus* differs from *Co. guereza*, *Pi. badius* and *P. melalophos* in having significantly lower epLsar. Moreover, *Dolichopithecus* differs from *Co. guereza* and *Pi. badius* in having significantly higher Asfc, while it differs from *L. albigena* and *E. patas* in having significantly lower values of Asfc (Tables 9 and 10). Lastly, *Dolichopithecus* differs from *L. albigena* and *S. entellus* in having lower values of Hasfc<sub>36</sub> (Tables 9 and 10).

For Phase I facets, *Co. guereza* and *Pi. badius* differ from *L. albigena*, *Ch. aethiops*, and *E. patas* in having significantly lower Asfc (Fig. 6; Tables 9 and 10). *Semnopithecus entellus* differs from *L. albigena* and *E. patas* in having significantly lower values of Asfc, and *P. melalophos* differs from *L. albigena* in having significantly lower Asfc. In addition, *N. larvatus* differs from *E. patas* and *L. albigena* in having significantly lower values of Tfv, while the latter taxon also differs from *P. melalophos* in having significantly higher Tfv (Tables 9 and 10). *Dolichopithecus* differs from *Co. guereza* and *Pi. badius* in having significantly higher values of Asfc, and differs from all extant species having significantly higher values of Smc (Tables 9 and 10).

#### 4. Discussion

The results of this study suggest that the combined methodological approach followed here (i.e., enamel thickness, dental topographic and dental microwear texture analyses) may be useful in dietary investigations of extinct primate species. Specifically, analysis of the MHNPN-PR01 molar crown via enamel thickness and dental topography provides insight regarding the mechanical properties of foods it could potentially have consumed (i.e., dental capabilities). At the same time, the investigation of the dietary behavior of *Dolichopithecus* specimens from fossil sites across Europe via DMTA provides information regarding the types of foods this taxon consumed weeks prior to death (i.e., tooth use).

#### 4.1. *Dental capabilities as evidenced by dental topography and enamel structure*

Dental topographic analysis The comparisons of dental topographic measures support their utility in investigating dental morphology associated with diet. In our comparative sample, the fruit/seed eaters are separated from folivores, whereas the mixed feeders are intermediate between the two. Mixed feeders may lack specializations for the consumption of specific food resources, unlike folivores and fruit/seed eaters, or they may possess features necessary to process a wide range of food items. The wider distribution of values of some topographic variables used here may suggest the latter (Figs. 3D and 4D). Nevertheless, these results could mean that some variables more reliably reveal morphologies related to dietary adaptations than others.

Given the potential complexities, it is not surprising that the comparisons among dietary groups based on measures of curvature/sharpness (i.e., ARC and DNE) are somewhat ambiguous. Folivores generally have higher values of curvature than frugivores, indicating more curved/sharper features on the crown (e.g., Ungar and M'Kirera, 2003; Bunn et al., 2011). This is consistent with the comparisons of both ARC and DNE in this study; however, the mixed feeders exhibit slightly higher values of DNE compared to the folivores (Fig. 4D).

This might be linked with the fact that DNE is influenced by size, as the mixed feeders include the largest representatives in our sample (SOM Fig. S5; SOM Table S3). In this sense, ARC more effectively discriminates the proposed dietary categories compared to DNE (Fig. 4C). Hence, ARC seems to be quite promising and requires more investigation in future dental topographic analyses. Furthermore, both LRFI and inclination adequately discriminate the proposed dietary categories (Fig. 4A, B), whereas OPCR does not show a clear relationship to diet as all three dietary categories overlap considerably (Fig. 3D).

The overall results of the dental topographic analysis suggest that the MHNp-PR01 M<sup>1</sup> was capable of efficiently processing tough fibrous material such as some leaves, probably in a similar way to that of some extant colobines (e.g., Wright et al., 2008; Matsuda et al., 2017). Nevertheless, it has been shown that there are differences in toughness among leaves (e.g., ripe and young) and fracture toughness varies by location within single leaves (e.g., Teaford et al., 2006; Dunham and Lambert, 2016), suggesting that food toughness may strongly influence dietary choices of some primate species (see also Coiner-Collier et al., 2016).

Enamel thickness analysis The results of this study show that 3DRETvol and 3DRETgeo significantly differ between extant cercopithecids with different diets (e.g., species classified as folivores had significantly lower values than did species classified as fruit/seed consumers; SOM Table S3). Furthermore, the results from our analyses of ACS are consistent with previous suggestions that estimates of 3D relative enamel thickness (i.e., 3DRETvol and 3DRETgeo) along with ACS can potentially be combined to add new insights into the evolution of tooth form in cercopithecids (e.g., Schwartz et al., 2020). For instance, while folivorous cercopithecids in our extant sample exhibit the lowest values of ACS, 3DRETvol and 3DRETgeo, MHNp-PR01 showed higher values for ACS than all folivorous extant taxa (SOM Table S1). Thicker enamel may have enabled *Dolichopithecus* molars to withstand high forces associated with the consumption of mechanically challenging food resources, at least

seasonally, and/or to help resist wear and abrasion (e.g., Molnar and Gantt, 1977; Kay, 1981; Lambert et al., 2004; King et al., 2005; Constantino et al., 2011). However, these differences could also reflect molar size, as *D. ruscinensis* is possibly the colobine with the largest molars in this study, followed by *S. entellus* and *N. larvatus* (see SOM Tables S1 and S3).

Nevertheless, it requires further investigation to determine the extent to which the combined application of these measures can be used to discriminate species based on diet. Moreover, future studies should also focus on sorting primate species by feeding behavior and diet as reflected by food material and geometric properties, and should investigate as many primate families as possible.

Discriminant analyses of dental topography and enamel structure Although some overlap exists, the LDAs satisfactorily separate taxa by dietary categories. Notably, however, the MHNPn-PR01 M<sup>1</sup> falls entirely outside of the range of all three dietary categories, separated entirely along axis 1 from fruit/seed-eaters and intermediate between folivores and mixed feeders along axis 2 (Fig. 5). Importantly, most cercopithecoid species do not fit neatly into these three diet categories, as they typically consume various amounts of leaves, fruits, and seeds throughout the year depending on seasonal availability (Rowe, 1996). Moreover, the exact dietary composition of each species was not recorded and the dietary composition of the 'mixed feeders' category is considerably more heterogeneous compared to the other two categories. Furthermore, information is lacking on the mechanical and geometric properties of the foods ingested and masticated by many of these taxa. This, in turn, makes it difficult to assess the potential effects of some mechanically challenging resources (e.g., fallback foods) on dental morphology (Constantino and Wright, 2009; Lambert, 2009).

The position of the MHNPn-PR01 fossil molar close to folivorous and mixed feeder species indicates a molar morphology that differs from all extant colobines included in this study, and may be indicative of distinct/different selective pressures related to dietary behavior. A previous dental topographic study also found that *M. pentelicus* fell outside of

the range of a comparative sample of extant cercopithecids (see Fig. 4 in Thiery et al., 2017a and Fig. 3 in Thiery et al., 2017b). This led the authors to suggest that extinct colobines might have distinct dental topographic features, possibly related to a dietary niche not found in cercopithecids today. The present study provides some support for this idea, although additional investigation including more extant cercopithecids, additional fossil molars of *D. ruscinensis*, and, if possible, other extinct colobine species would undoubtedly be beneficial.

Notwithstanding the above observations, there are a few caveats to consider. The fossil sample we used for enamel thickness and dental topographic analyses consists of a single  $M^1$ , whereas the extant comparative sample consisted of  $M^2$ s. Previous research by Bunn and Ungar (2009) has shown that different tooth types should not be directly compared, at least in some cercopithecids. Nevertheless, the latter study was focused on variably worn lower molars unlike in the current study, where only unworn or minimally worn upper molars were considered, thus removing the potential effects of wear on the analyzed topographic variables. Even if some differences between  $M^1$  and  $M^2$  can be expected in topographic estimates already influenced by size (e.g., DNE, OPCR; SOM Figs. S4–S5), these differences are likely to be subtle, and not significant at the taxonomic scale of our study. This is further supported by preliminary comparisons between  $M^1$ s and  $M^2$ s of *D. ruscinensis* from Serrat d'en Vacquer—Perpignan, which suggests no significant variation when no and/or minimal wear is considered (Plastiras, unpub. data). Nevertheless, this requires additional investigation. Additionally, enamel thickness shows a wide range of interspecific and intrageneric variation (Macho, 1994; Shellis, et al., 1998; Schwartz, 2000; Kono, 2004; Smith et al., 2005, 2012; Olejniczak et al., 2008), even within the same tooth locus. Moreover, enamel thickness has also been demonstrated to be an evolutionarily plastic trait, capable of rapid adaptation in response to functional dietary requirements (Hlusko et al., 2004; Kelley and Swanson, 2008; Pampush et al., 2013; Kato et al., 2014).

Thus, caution is required when interpreting dental topographic and enamel thickness results for *D. ruscinensis* given that only a single tooth was analyzed.

#### 4.2. *Tooth use as evidenced by dental microwear texture analysis*

Early work using DMTA demonstrated that primate feeding habits are reflected in texture parameters on Phase II facets (Scott et al., 2005, 2006). Indeed, primate folivores have lower  $Asfc$  and higher  $epLsar$  than primates that forage on fruits and seeds (Scott et al., 2012; Ungar et al., 2012a). Furthermore, the occurrence of outliers with high complexity among a population indicates a higher frequency of hard foods (Merceron et al., 2009; Scott et al., 2012). While some studies have argued that food items are not hard enough to abrade enamel surfaces (Lucas et al., 2013; Hoffman et al., 2015; van Casteren et al., 2020) and that exogenous silica particles ('grit') may be the main cause of tooth wear (Madden, 2014), experimental work has shown that the situation is far more complex (e.g., Xia et al., 2018; Schulz-Kornas et al. 2020) and that there is no need to invoke dust to generate differences in tooth wear (Teaford et al., 2017). In fact, dust generally does not overwhelm the dietary signal (Merceron et al., 2016; Sanson et al., 2017; Merceron et al., 2021).

Setting these discussions aside, the present datasets provide several pieces of evidence that dental microwear reflects dietary habits rather than amounts of exogenous particles or their geometrical properties. For instance, among colobine monkeys, the most distinct microwear texture differences are not between arboreal and semi-terrestrial species, such as *Co. guereza* and *S. entellus*. Instead, they are between the two arboreal species, *Co. guereza* and *N. larvatus* (Fig. 6), the latter including significantly higher amounts of seeds and fruits compared to the former (Kool, 1993; Bennett, 1994; Yeager and Kool, 1994). This same trend can be seen among cercopithecine monkeys, with *L. albigena* (which feeds mostly on fruits and seeds) having similar dental microwear textures on both dental

wear facet types, and the semi-terrestrial and more opportunistic *Ch. aethiops* and *E. patas* showing higher microwear texture variation between dental wear facet types (Fig. 6). There is no doubt that the processes behind dental microwear formation are complex and need further investigation to be fully understood (Teaford et al., 2021). However, most datasets issued from wild populations as well as in vitro and in vivo experiments support the relationship between texture and proportion of hard items in the diet (Calandra et al., 2012; Daegling et al., 2016; Teaford et al., 2017; Percher et al., 2018; Merceron et al., 2021).

When evaluating the two dental facet types, the microwear texture of *Dolichopithecus* differs from both specialized folivores such as *Co. guereza* and *Pi. badius* and the hard object feeder *L. albigena*. However, the texture differences between *Dolichopithecus* and the specialized folivores (i.e., *Co. guereza* and *Pi. badius*) are distinct on both facet types (Table 10), which further suggests a lower frequency of leaf consumption for the fossil colobine. Regardless, our results suggest that Phase II dental facets seem to better distinguish taxa based on dietary categories (Fig. 6), providing support for previous research that investigated both facet types in respect to diet (e.g., Krueger et al., 2008). As expected, the higher values of *Asfc* for *Dolichopithecus* and all extant taxa are observed in Phase II facets (SOM Fig. S8). The Phase I dental facets are biomechanically involved with shearing actions during mastication and are generally expected to produce more anisotropic microwear textures (Teaford and Oyen, 1989; Krueger et al., 2008; Scott et al., 2012; Martin et al., 2018; Percher et al., 2018), thus higher values for *epLsar* on Phase I facets are predicted. However, in the current study, some folivorous species in our sample (i.e., *Co. guereza*, *Pi. badius* and *P. melalophos*) have higher *epLsar* values on Phase II dental facets, which suggests that the slicing movement is important during the two masticatory phases for leaf-eating monkeys (Walker and Murray, 2011).

It is important to note that most of the fossil sample in the present study derives from the locality of Serrat d'en Vacquer—Perpignan (France). Earlier studies have shown that diet can differ between groups of the same species in different habitats, such that the dietary behavior of one group may not be representative of the species as a whole (e.g., Chapman et al., 2002; Ganas et al., 2004; Vandercone et al., 2012). Fortunately, variation in Asfc and epLsar between the fossiliferous localities included in the current analysis provide some insights in this respect (Fig. 7). Regarding Phase II facets for both Asfc and epLsar, all individuals from the fossiliferous localities of Dorkovo, Megalo Emvolon, Tenevo, Mălușteni, and Vorog fall within the range of variation of the *Dolichopithecus* microwear sample from Serrat d'en Vacquer—Perpignan (Fig. 7). The same applies to Phase I facets, although in this case the Asfc values for one individual, from Megalo Emvolon, marginally falls outside of the range of the variation of Perpignan's sample (Fig. 7). Hopefully, additional *Dolichopithecus* fossils from other Pliocene fossil sites in Europe will enable more detailed investigations.

#### 4.3. *The ecology of Dolichopithecus*

Our results suggest that the MNHPn—PR01 M<sup>1</sup> displays a morphology that combines the masticatory capabilities that possibly enabled it to consume a wide range of foods with a wide range of mechanical properties. Its high occlusal relief and curvature are also consistent with the ability to process tough and fibrous material, while its relatively thick enamel was capable of resisting high stresses that may have been associated with ingesting more mechanically challenging foods and/or resisting wear and abrasion. Furthermore, the dental microwear textures indicate that *Dolichopithecus* occupied an intermediate ecospace between highly specialized folivorous colobines and durophagous cercopithecines.

The intermediate pattern in both molar topography and dental microwear texture suggests that *D. ruscinensis* potentially enlarged its dietary niche by falling back on food

resources other than preferred ones when needed. Combined with evidence from postcranial morphology that indicates semi-terrestrial locomotion (e.g., robust and long limb bones, short phalanges, and several aspects of the elbow joint; Delson 1973), this taxon may have exploited arboreal and terrestrial substrates and may have had the ability to transition from one micro-habitat to another. This type of locomotor adaptations may have also influenced its ranging patterns and biogeographic distribution. While leaf consumption was presumably an integral part of the dietary repertoire of *Dolichopithecus* between seasons, a wide array of foods available in the arboreal and terrestrial substrates of each habitat could have rounded out its diet. However, these ecological characteristics seem not to be a novelty in colobine ecology (Benefit, 2000; Reitz and Benefit, 2001; Jablonski et al., 2020).

Earlier Eurasian and African fossil colobine representatives were also likely mixed substrate (arboreal-terrestrial) users and opportunistic feeders (Youlatos, 2003; Codron et al., 2005; Fourie et al., 2008; Merceron et al., 2009b; Youlatos and Koufos, 2010; Youlatos et al., 2012; Williams and Geissler, 2014). Thus, early colobines were probably more diverse in terms of locomotor and dietary behavior compared to their extant African and Asian relatives (Leakey, 1982; El-Zaatari et al., 2005; Hlusko, 2006; Merceron et al., 2009b; Nakatsukasa et al., 2010; Youlatos et al., 2012; Geissler, 2013; Williams and Geissler, 2014; Frost et al., 2015; Pallas et al., 2019; Ji et al., 2020). By exploiting a wide array of food resources and/or by targeting food resources that are not primarily preferred by other sympatric primate species, such as leaves, early colobine taxa were probably able to inhabit various micro-habitats in both Africa and Eurasia. Such resources are usually abundant in most habitats with tree cover throughout the year. Hence, it is plausible that folivory may have worked as an evolutionary advantage to withstand selective ecological pressures, such as scarcity of preferred resources and large- or small-scale environmental changes, as well as interspecific competition.

Sympatric primates often exhibit different behavioral/foraging strategies to partition food resources (MacKinnon and MacKinnon, 1980; Garber, 1987; Ungar, 1995; Grueter et al., 2010; Astaras et al., 2011; Hadi et al., 2012), which may lead to morphological adaptations (Macho, 2017). It has been reported that extant colobines and cercopithecines compete for space and resources (Yeager, 1989; Singht et al., 2011; Sterck and Steenbeek, 2012; Ruslin et al., 2019). Furthermore, fossil colobines might have coexisted with the latest fossil hominoids for a short period of time in eastern Eurasia (Spassov et al., 2012; Böhme et al., 2017; Jablonski et al., 2020), and also with cercopithecines (i.e., *Macaca*) from the latest Miocene to latest Pliocene of Europe (see Eronen and Rook, 2004; Alba et al., 2014). The ecological diversity and the biogeographical expansion of the cercopithecids during the Plio-Pleistocene are usually associated with global and/or regional climatic changes that took place within this period (Cerling et al., 1993, 1998; Vrba, 1993; Frost, 2002; Jablonski, 2002; Bobe and Behrensmeyer, 2004). However, interspecific competition due to food resource variation among sympatric primates is expected. Thus, the effect of these natural processes needs to be considered more thoroughly to better explain the diversity of extinct and extant Cercopithecidae.

## 5. Conclusions

This study characterized the dietary ecology of *D. ruscinensis*, the latest surviving European colobine, by combining evidence from dental topographic and enamel thickness analyses along with dental microwear texture analysis. The results suggest a molar morphology intermediate between folivorous and mixed feeding taxa. *Dolichopithecus ruscinensis* molars were capable of processing mechanically challenging resources and sustaining high bite forces, while also being able to process tough and fibrous material efficiently. This interpretation is supported by microwear texture analysis, which suggests

neither dedicated folivory nor durophagy; rather, *D. ruscinensis* was likely dependent on seasonal and spatial variation of resources. Our reconstruction of its dietary behavior agrees with its presumed semi-terrestrial locomotor behavior. However, this ecological profile was not unusual in early colobine ecology as similar locomotor and dietary behaviors have been suggested for some earlier fossil African and Eurasian colobine taxa. This contrasting picture with most extant colobine species raises further questions regarding the diversity of early colobine paleohabitats and how the cumulative effects of resource variations and interspecific competition shaped colobine ecology as it is today. Lastly, the results of this study further support the utility of combining multiple lines of evidence to investigate extinct and extant primate dietary adaptations.

### **Acknowledgments**

The authors would like to thank, A. Mille and M. Didier from the Muséum d'Histoire Naturelle de Perpignan, E. Robert from the Université de Lyon, B. Didier from the Musée des Confluences (Lyon), G.D. Koufos from the Laboratory of Geology and Paleontology of Aristotle University of Thessaloniki (Greece), N. Spassov from the Natural History Museum of Sofia (Bulgaria), B. Haiduc, B. Ratoi and P. Tibuleac from Department of Geology of Alexandru Ioan Cuza University of Iași (Romania), T. D. Nishimura and M. Takai from Primate Research Institute of Kyoto University, Inuyama (Japan), and the Royal Museum of Central Africa, Tervuren (Belgium), the Seckenberg Museum of Frankfurt (Germany), and Laboratory Paleontology Evolution Paleoecosystems Paleoprimatology (PALEVOPRIM), – CNRS University of Poitiers (France). We are also grateful to A. Mazurier (Centre de Microtomographie of Poitiers) for his help with the acquisition of the micro-CT scans. Finally, we are grateful to the two anonymous reviewers, the Associate Editor, and the Editor-in-Chief for providing constructive and insightful comments which improved significantly the clarity and quality of

this scientific paper. This research was co-financed by Greece and the European Union (European Social Fund) through the Operational Program “Human Resources Development, Education and Lifelong Learning” in the context of the project “Strengthening Human Resources Research Potential via Doctorate Research” (MIS-5000432), implemented by the State Scholarships Foundation (IKY); the Eiffel Excellence Scholarship Programme of the French Ministry of Foreign and European Affairs; and the Diet Scratches Project (ANR-17CE27-0002-01; PI: G. Merceron).

## References

- Ackermans, N.L., Winkler, D.E., Martin, L.F., Kaiser, T.M., Clauss, M., Hatt, J.M., 2020. Dust and grit matter: Abrasives of different size lead to opposing dental microwear textures in experimentally fed sheep (*Ovis aries*). *J. Exp. Biol.* 223, jeb.220442.
- Alba, D.M., Delson, E., Carnevale, G., Colombero, S., Delfino, M., Giuntelli, P., Pavia, M., Pavia, G., 2014. First joint record of *Mesopithecus* and cf. *Macaca* in the Miocene of Europe. *J. Hum. Evol.* 67, 1–18.
- Allen, K.L., Cooke, S.B., Gonzales, L.A., Kay, R.F., 2015. Dietary inference from upper and lower molar morphology in platyrrhine primates. *PLoS One* 10, e0118732.
- Andrews, P., 1982. Ecological polarity in primate evolution. *Zool. J. Linn. Soc.* 74, 233–244.
- Andrews, P., Harrison, T., Delson, E., Bernor, R.L., Martin, L.B., 1996. Distribution and Biochronology of European and Southwest Asian Miocene Catarrhines. In: Bernor R.L., Fahlbusch V., Mittmann, H.W. (Eds.), *The Evolution of Western Eurasian Neogene Mammal Faunas*. Columbia University Press, New York pp. 168–207.
- Arnold, C., Matthews, L.J., Nunn, C.L., 2010. The 10kTrees website: A new online resource for primate phylogeny. *Evol. Anthropol.* 19, 114–118.

- Astaras, C., Krause, S., Mattner, L., Rehse, C., Waltert, M., 2011. Associations between the drill (*Mandrillus leucophaeus*) and sympatric monkeys in Korup National Park, Cameroon. *Am. J. Primatol.* 73, 127–134.
- Astaras, C., Mühlenberg, M., Waltert, M., 2008. Note on drill (*Mandrillus leucophaeus*) ecology and conservation status in Korup National Park, Southwest Cameroon. *Am. J. Primatol.* 70, 306–310.
- Baker, G., Jones, L.H.P., Wardrop, I.D., 1959. Cause of wear in sheep's teeth. *Nature* 184, 1583–1584.
- Barrett, A.S., 2005. Foraging ecology of the vervet monkey (*Chlorocebus aethiops*) in mixed lowveld bushveld and sour lowveld bushveld of the Blydeberg Conservancy, Northern Province, South Africa. Ph.D. Dissertation, University of South Africa.
- Benefit, B.R., 1999. *Victoriapithecus*: The key to old world monkey and catarrhine origins. *Evol. Anthropol.* 7, 155–174.
- Benefit, B.R., 2000. Old World monkey origins and diversification: An evolutionary study of diet and dentition. Old world monkeys. In: Bromage, T.G. and Schrenk, F. (Eds.), *African Biogeography, Climate Change, and Early Hominid Evolution*, Oxford University Press, Oxford, pp. 133–179.
- Bennett, E.L., 1994. The ecology of Asian colobines. In: Davies, G.E., Oates, J.F. (Eds.), *Colobine Monkeys: Their Ecology, Behaviour and Evolution*. Cambridge University Press, Cambridge, 129-171
- Berthaume, M.A., 2016a. Food mechanical properties and dietary ecology. *Am. J. Phys. Anthropol.* 159, S79–S104.
- Berthaume, M.A., 2016b. On the relationship between tooth shape and masticatory efficiency: A finite element study. *Anat. Rec.* 299, 679–687.

- Berthaume, M.A., Schroer, K., 2017. Extant ape dental topography and its implications for reconstructing the emergence of early *Homo*. *J. Hum. Evol.* 112, 15–29.
- Berthaume, M.A., Delezene, L.K., Kupczik, K., 2018. Dental topography and the diet of *Homo naledi*. *J. Hum. Evol.* 118, 14–26.
- Berthaume, M.A., Winchester, J., Kupczik, K., 2019a. Ambient occlusion and PCV (portion de ciel visible): A new dental topographic metric and proxy of morphological wear resistance. *PLoS One* 14, e0215436.
- Berthaume, M.A., Winchester, J., Kupczik, K., 2019b. Effects of cropping, smoothing, triangle count, and mesh resolution on 6 dental topographic metrics, *PLoS One*, 14, e0216229.
- Berthaume, M.A., Lazzari, V., Guy, F., 2020. The landscape of tooth shape: Over 20 years of dental topography in primates. *Evol. Anthropol.* 29, 245–262.
- Bobe, R., Behrensmeyer, A.K., 2004. The expansion of grassland ecosystems in Africa in relation to mammalian evolution and the origin of the genus *Homo*. *Palaeogeogr. Palaeoclimatol. Palaeoecol.* 207, 399–420.
- Böhme, M., Spassov, N., Ebner, M., Geraads, D., Hristova, L., Kirscher, U., Kötter, S., Linnemann, U., Prieto, J., Roussiakis, S., Theodorou, G., Uhlig, G., Winklhofer, M., 2017. Messinian age and savannah environment of the possible hominin *Graecopithecus* from Europe. *PLoS One* 12, e0177347.
- Boyer, D.M., 2008. Relief index of second mandibular molars is a correlate of diet among prosimian primates and other euarchontan mammals. *J. Hum. Evol.* 55, 1118–1137.
- Boyer, D.M., Costeur, L., Lipman, Y., 2012. Earliest record of *Platychoerops* (Primates, Plesiadapidae), a new species from Mouras Quarry, Mont de Berru, France. *Am. J. Phys. Anthropol.* 149, 329–346.

- Boyer, D.M., Winchester, J., Kay, R.F. 2015. Technical note: The effect of differences in methodology among some recent applications of shearing quotients. *Am. J. Phys. Anthropol.* 156, 166–178.
- Bunn, J.M., Boyer, D.M., Lipman, Y., St. Clair, E.M., Jernvall, J., Daubechies, I., 2011. Comparing Dirichlet normal surface energy of tooth crowns, a new technique of molar shape quantification for dietary inference, with previous methods in isolation and in combination. *Am. J. Phys. Anthropol.* 145, 247–261.
- Bunn, J.M., Ungar, P.S., 2009. Dental topography and diets of four old world monkey species. *Am. J. Primatol.* 71, 466–477.
- Buzzard, P.J., 2006. Ecological partitioning of *Cercopithecus campbelli*, *C. petaurista*, and *C. diana* in the Taï Forest. *Int. J. Primatol.* 27, 529–558.
- Calandra, I., Merceron, G., 2016. Dental microwear texture analysis in mammalian ecology. *Mamm. Rev.* 46, 215–228.
- Calandra, I., Schulz, E., Pinnow, M., Krohn, S., Kaiser, T.M., 2012. Teasing apart the contributions of hard dietary items on 3D dental microtextures in primates. *J. Hum. Evol.* 63, 85–98.
- Cerling, T.E., Wang, Y., Quade, J., 1993. Expansion of C<sub>4</sub> ecosystems as an indicator of global ecological change in the late Miocene. *Nature* 361, 344–345.
- Cerling, T.E., Ehleringer, J.E., Harris, J.M., 1998. Carbon dioxide starvation, the development of C<sub>4</sub> ecosystems, and mammalian evolution. *Philos. Trans. R. Soc. B Biol. Sci.* 353, 159–171.
- Chapman, C.A., Chapman, L.J., Gillespie, T.R., 2002. Scale issues in the study of primate foraging: Red colobus of Kibale National Park. *Am. J. Phys. Anthropol.* 117, 349–363.
- Chivers, D.J., 1994. Functional anatomy of the gastrointestinal tract. In: Davies, G.E., Oates,

- J.F. (Eds.), *Colobine Monkeys: Their Ecology, Behaviour and Evolution*. Cambridge University Press, Cambridge, pp. 205–227.
- Codron, D., Luyt, J., Lee-Thorp, J.A., Sponheimer, M., De Ruiter, D., Codron, J., 2005. Utilization of savanna-based resources by Plio-Pleistocene baboons. *S. Afr. J. Sci.* 101, 245–248.
- Coiner-Collier, S., Scott, R.S., Chalk-Wilayto, J., Cheyne, S.M., Constantino, P., Dominy, N.J., Elgart, A.A., Glowacka, H., Loyola, L.C., Ossi-Lupo, K., Raguette-Schofield, M., Talebi, M.G., Sala, E.A., Sieradzy, P., Taylor, A.B., Vinyard, C.J., Wright, B.W., Yamashita, N., Lucas, P.W., Vogel, E.R., 2016. Primate dietary ecology in the context of food mechanical properties. *J. Hum. Evol.* 98, 103–118.
- Constantino, P.J., Wright, B.W., 2009. The importance of fallback foods in primate ecology and evolution. *Am. J. Phys. Anthropol.* 140, 599–602.
- Constantino, P.J., Markham, K., Lucas, P.W., 2012. Tooth chipping as a tool to reconstruct diets of great apes (*Pongo*, *Gorilla*, *Pan*). *Int. J. Primatol.* 33, 661–672.
- Curtin, S.H., 2004. Diet of the Roloway Monkey, *Cercopithecus diana roloway*, in Bia National Park, Ghana. In: Glenn, M.E. and Cords, M. (Eds.), *The Guenons: Diversity and Adaptation in African Monkeys*. Kluwer Academic Press, New York, 351–371.
- Daegling, D. J., McGraw, W. S. (2001). Feeding, diet, and jaw form in West African *Colobus* and *Procolobus*. *Int. J. Primatol.* 22, 1033–1055.
- Davies, A.G., Caldecott, J.O., Chivers, D.J., 1983. Natural foods as a guide to nutrition of Old World primates. *Stand. Lab. Anim. Manag.* 225–241.
- Davies, A.G., Bennett, E.L., Waterman, P.G., 1988. Food selection by two South-east Asian colobine monkeys (*Presbytis rubicunda* and *Presbytis melalophos*) in relation to plant chemistry. *Biol. J. Linn. Soc.* 34, 33–56.

- Davies, G.E., Oates, J.F. (Eds.) 1994. Colobine Monkeys: Their Ecology, Behaviour and Evolution. Cambridge University Press, Cambridge.
- de Bonis, L., Bouvrain, G., Geraads, D., Koufos, G., 1990. New remains of *Mesopithecus* (Primates, Cercopithecoidea) from the late Miocene of Macedonia (Greece), with the description of a new species. *J. Vertebr. Paleontol.* 10, 473–483.
- Delson, 1973. Fossil Colobine Monkeys of the circum-Mediterranean Region and the Evolutionary History of the Cercopithecidae (Primates, Mammalia). Ph.D. Dissertation, Columbia University.
- Delson, E., 1994. Evolutionary history of the colobine monkeys in paleoenvironmental perspective. In: Davies, G.E., Oates, J.F. (Eds.), *Colobine Monkeys: Their Ecology, Behaviour, and Evolution*. Cambridge University Press, pp. 11–48.
- Delson, E., Terranova, C.J., Jungers, W.L., Sargis, E.J., Jablonski, N.G., Dechow, P.C., 2000. Body mass in Cercopithecidae (Primates, Mammalia): Estimation and scaling in extinct and extant taxa. *Anthropol. Pap. Am. Mus. Nat. Hist.* 83, 1–159.
- Delson, E., Thomas, H., Spassov, N., 2005. Fossil Old World monkeys (Primates, Cercopithecidae) from the Pliocene of Dorkovo, Bulgaria. *Geodiversitas* 27, 159–166.
- Depéret, C., 1890. *Les Animaux Pliocènes du Roussillon*. Baudry, Paris
- DeSantis, L.R.G., 2016. Dental microwear textures: Reconstructing diets of fossil mammals. *Surf. Topogr. Metrol. Prop.* 4, 023002.
- Dumont, E.R., 1995. Enamel thickness and dietary adaptation among extant primates and chiropterans. *J. Mammal.* 76, 1127–1136.
- Dunham, N.T., Lambert, A.L., 2016. The role of leaf toughness on foraging efficiency in Angola black and white colobus monkeys (*Colobus angolensis palliatus*). *Am. J. Phys. Anthropol.*

161, 343–354.

Egi, N., Nakatsukasa, M., Kalmykov, N.P., Maschenko, E.N., Takai, M., 2007. Distal humerus and ulna of *Parapresbytis* (Colobinae) from the Pliocene of Russia and Mongolia: Phylogenetic and ecological implications based on elbow morphology. *Anthropol. Sci.* 115, 107–117.

El-Zaatari, S., Grine, F.E., Teaford, M.F., Smith, H.F., 2005. Molar microwear and dietary reconstructions of fossil Cercopithecoidea from the Plio-Pleistocene deposits of South Africa. *J. Hum. Evol.* 49, 180–205.

Elton, S., 2007. Environmental correlates of the cercopithecoid radiations. *Folia Primatol.* 78, 344–364.

Eronen, J.T., Rook, L., 2004. The Mio-Pliocene European primate fossil record: Dynamics and habitat tracking. *J. Hum. Evol.* 47, 323–341.

Evans, A.R., Janis, C.M., 2014. The evolution of high dental complexity in the horse lineage. *Ann. Zool. Fenn.* 51, 73–79.

Evans, A.R., Jernvall, J., 2009. Patterns and constraints in carnivoran and rodent dental complexity and tooth size. *J. Vertebr. Paleontol.* 29, 24A.

Evans, A.R., Wilson, G.P., Fortelius, M., Jernvall, J., 2007. High-level similarity of dentitions in carnivorans and rodents. *Nature* 445, 78–81.

Fourie, N.H., Lee-Thorp, J.A., Ackermann, R.R., 2008. Biogeochemical and craniometric investigation of dietary ecology, niche separation, and taxonomy of Plio-Pleistocene cercopithecoids from the Makapansgat limeworks. *Am. J. Phys. Anthropol.* 135, 121–135.

Freckleton, R.P., Harvey, P.H., Pagel, M., 2002. Phylogenetic analysis and comparative data: A

- test and review of evidence. *Am. Nat.* 160, 712–725.
- Frost, S.R., 2002. East African cercopithecoid fossil record and its relationship to global climatic change. *Am. J. Phys. Anthropol, Suppl.* 32, 72–73.
- Frost, S.R., 2017. Evolution of the Cercopithecidae. In: Fuentes, A. (Eds.), *The International Encyclopedia of Primatology*, John Wiley and Sons, Inc., Vol. 2, pp. 1–3.
- Frost, S.R., Gilbert, C.C., Pugh, K.D., Guthrie, E.H., Delson, E., 2015. The hand of *Cercopithecoides williamsi* (Mammalia, Primates): Earliest evidence for thumb reduction among colobine monkeys. *PLoS One* 10, e0125030.
- Gabis, R. V., 1960. Les os des membres des singes cynomorphes. *Mammalia* 24, 577–607.
- Gabis, R. V., 1961. Bones of the extremities of *Dolichopithecus*, fossil monkey of the Pliocene period from Roussillon. *C. R. Hebd. Seances Acad. Sci.* 252, 1368–1370.
- Gamarra, B., Nova Delgado, M., Romero, A., Galbany, J., Pérez-Pérez, A., 2016. Phylogenetic signal in molar dental shape of extant and fossil catarrhine primates. *J. Hum. Evol.* 94, 13–27.
- Ganas, J., Robbins, M.M., Nkurunungi, J.B., Kaplin, B.A., McNeilage, A., 2004. Dietary variability of mountain gorillas in Bwindi Impenetrable National Park, Uganda. *Int. J. Primatol.* 25, 1043–1072.
- Garber, P.A., 1987. Foraging strategies among living primates. *Annu. Rev. Anthropol.* 16, 339–364.
- Geissler, E., 2013. Dental microwear analysis of *Cercopithecoides williamsi*. Masters Thesis, Georgia State University.
- Gilbert, C.C., Goble, E.D., Hill, A., 2010. Miocene Cercopithecoidea from the Tugen Hills, Kenya. *J. Hum. Evol.* 59, 465–483.

- Gingerich, P.D., 1977. Correlation of tooth size and body size in living hominoid primates, with a note on relative brain size in *Aegyptopithecus* and *Proconsul*. *Am. J. Phys. Anthropol.* 47, 395–398.
- Gingerich, P.D., Smith, B.H., Rosenberg, K., 1982. Allometric scaling in the dentition of primates and prediction of body weight from tooth size in fossils. *Am. J. Phys. Anthropol.* 58, 81–100.
- Godfrey, L.R., Winchester, J.M., King, S.J., Boyer, D.M., Jernvall, J., 2012. Dental topography indicates ecological contraction of lemur communities. *Am. J. Phys. Anthropol.* 148, 215–227.
- Green, J.L., Croft, D.A., 2018. Using dental mesowear and microwear for dietary inference: A review of current techniques and applications. In: Croft, D.A., Su, D.F., Simpson, S.W. (Eds.), *Methods in Paleoecology: Reconstructing Cenozoic Terrestrial Environments and Ecological Communities*. Springer, Cham, pp. 53–73.
- Gremiatskiy, M.A., 1958. Fossil primates from the territory of the Soviet Union (with relationships of the phylogenic question of the higher primates). In: *Treatises of the VI All Union Conference of Anatomists, Gistologysts and Embryologists, July 14-18, 1958, Kiev*. pp. 576–579.
- Grine, F.E., Spencer, M.A., Demes, B., Smith, H.F., Strait, D.S., Constant, D.A., 2005. Molar enamel thickness in the chacma baboon, *Papio ursinus* (Kerr 1792). *Am. J. Phys. Anthropol.* 128, 812–822.
- Grueter, C.C., Li, D.Y., Feng, S.K., Ren, B.P., 2010. Niche partitioning between sympatric rhesus macaques and Yunnan snub-nosed monkeys at Baimaxueshan Nature Reserve, China. *Zool. Res.* 31, 516–522.
- Guy, F., Gouvard, F., Boistel, R., Euriat, A., Lazzari, V., 2013. Prospective in (primate) dental

- analysis through tooth 3D topographical quantification. PLoS One 8, e0066142.
- Guy, F., Lazzari, V., Gilissen, E., Thiery, G., 2015. To what extent is primate second molar enamel occlusal morphology shaped by the enamel-dentine junction? PLoS One 10, e013880A.
- Guy, F., Thiery, G., Lazzari, V., 2017. 3D quantification of the occlusal enamel curvature: A decisive feature in dental function analysis and diet in Primates. 17<sup>th</sup> International Symposium on Dental Morphology, 2<sup>nd</sup> Congress of International Association for Paleodontology, p. 104.
- Hadi, S., Ziegler, T., Waltert, M., Syamsuri, F., Mühlenberg, M., Hodges, J.K., 2012. Habitat use and trophic niche overlap of two sympatric colobines, *Presbytis potenziani* and *Simias concolor*, on Siberut Island, Indonesia. Int. J. Primatol. 33, 218–232.
- Ham, R.M., 1994. Behaviour and ecology of grey-cheeked mangabeys (*Cercocebus albigena*) in the Lope Reserve, Gabon. Ph.D. Dissertation, University of Stirling.
- Hammer, Ø., Harper, D.A., Ryan, P.D., 2001. PAST: Paleontological statistics software package for education and data analysis. Palaeontol. Electron. 4, 9.
- Happel, R., 1988. Seed-eating by West African cercopithecines, with reference to the possible evolution of bilophodont molars. Am. J. Phys. Anthropol. 75, 303–327.
- Harris, T.R., Chapman, C.A., 2007. Variation in diet and ranging of black and white colobus monkeys in Kibale National Park, Uganda. Primates 48, 208–221.
- Hlusko, L.J., 2006. A new large Pliocene colobine species (Mammalia: Primates) from Asa Issie, Ethiopia. Geobios 39, 57–69.
- Hoffman, J.M., Fraser, D., Clementz, M.T., 2015. Controlled feeding trials with ungulates: A new application of in vivo dental molding to assess the abrasive factors of microwear. J.

- Exp. Biol. 218, 1538–1547.
- Hongo, S., Nakashima, Y., Akomo-Okoue, E.F., Mindonga-Nguelet, F.L., 2018. Seasonal change in diet and habitat use in wild mandrills (*Mandrillus sphinx*). Int. J. Primatol. 39, 27–48.
- Hoshino, J., 1985. Feeding ecology of mandrills (*Mandrillus sphinx*) in campo animal reserve, Cameroon. Primates. 26, 248–273.
- IBM Corp., 2013. IBM SPSS Statistics for Windows, Version 22.0. Armonk, New York.
- Ingicco, T., 2008. Analyse morphofonctionnelle des os longs de deux colobes fossiles: *Mesopithecus* et *Dolichopithecus*. Sez. di Museol. Sci. e Nat. 3, 1–7.
- Isbell, L.A., 1998. Diet for a small primate: insectivory and gummivory in the (large) patas monkey (*Erythrocebus patas pyrrhonotus*). Am. J. Primatol. 45, 381–398.
- Iwamoto, M., Hasegawa, Y., Koizumi, A., 2005. A Pliocene colobine from the Nakatsu Group, Kanagawa, Japan. Anthropol. Sci. 113, 123–137.
- Jablonski, N.G., 1998. The evolution of the doucs and snub-nosed monkeys and the question of the phyletic unity of the odd-nosed colobines. In: Jablonski, N.G. (Eds.), The Natural History of the Doucs and Snub-Nosed Monkeys. World Scientific Publishing, Singapore, pp. 13–52.
- Jablonski, N.G., 2002. Fossil Old World monkeys: The late Neogene radiation. In: Hartwig, E.C. (Eds.), The Primate Fossil Record. Cambridge University Press, Cambridge pp. 255–299.
- Jablonski, N.G., Ji, X., Kelley, J., Flynn, L.J., Deng, C., Su, D.F., 2020. *Mesopithecus pentelicus* from Zhaotong, China, the easternmost representative of a widespread Miocene cercopithecoid species. J. Hum. Evol. 146, 102851.
- Ji, X., Youlatos, D., Jablonski, N.G., Pan, R., Zhang, C., Li, P., Tang, M., Yu, T., Li, W., Deng, C., Li, S., 2020. Oldest colobine calcaneus from East Asia (Zhaotong, Yunnan, China). J. Hum.

Evol. 147, 102866.

Jolly, C.J., 1967. The evolution of baboons. In: Vagtborg, H. (Eds.), *The Baboon in Medical Research*. University Texas Press, Texas, pp. 23–50.

Jolly, C.J., 1970. The large African monkeys as an adaptive array. In: Napier, J.R., Napier, P.H. (Eds.), *Old World Monkeys*. Academic Press, New York, pp. 139–174.

Kalmykov, N.P., 1992. The northernmost early Pliocene Cercopithecidae from Asia. *Paleontol. J.* 26, 178–181.

Kalmykov, N.P., 1995. New cercopithecoid genus (Cercopithecidae, primates) from Pliocene of Transbaikalian. *Vopr. Antropol.* 88, 91–114.

Kato, A., Tang, N., Borries, C., Papakyrikos, A.M., Hinde, K., Miller, E., Kunimatsu, Y., Hirasaki, E., Shimizu, D., Smith, T.M., 2014. Intra- and interspecific variation in macaque molar enamel thickness. *Am. J. Phys. Anthropol.* 155, 447–459.

Kay, R.F., 1975. The functional adaptations of primate molar teeth. *Am. J. Phys. Anthropol.* 43, 195–215.

Kay, R.F., 1981. The nut-crackers—a new theory of the adaptations of the ramapithecinae. *Am. J. Phys. Anthropol.* 55, 141–151.

King, S.J., Arrigo-Nelson, S.J., Pochron, S.T., Semprebon, G.M., Godfrey, L.R., Wright, P.C., Jernvall, J., 2005. Dental senescence in a long-lived primate links infant survival to rainfall. *Proc. Natl. Acad. Sci. USA* 102, 16579–16583.

Kono, R.T., 2004. Molar enamel thickness and distribution patterns in extant great apes and humans: New insights based on a 3-dimensional whole crown perspective. *Anthropol. Sci.* 112, 121–146.

Kool, K.M., 1993. The diet and feeding behavior of the silver leaf monkey (*Trachypithecus*

- auratus sondaicus*) in Indonesia. *Int. J. Primatol.* 14, 667–700.
- Koufos, G.D., 2009. The genus *Mesopithecus* (Primates, Cercopithecidae) in the late Miocene of Greece. *Boll. della Soc. Paleontol. Ital.* 48, 157–166.
- Koufos, G.D., Vasileiadou, K., 2015. Miocene/Pliocene mammal faunas of southern Balkans: Implications for biostratigraphy and palaeoecology. *Palaeobio. Palaeoenv.* 95, 285–303.
- Koufos, G.D., 2019. Late Turolian *Mesopithecus* (Mammalia: Cercopithecidae) from Axios Valley (Macedonia, Greece): Earliest presence of *M. monspessulanus* in Europe. *C. R. Palevol* 18, 1057–1072.
- Koufos, G.D., Syrides, G.E., Kalliopi, K., 1991. A Pliocene primate from Macedonia (Greece). *J. Hum. Evol.* 21, 283–294.
- Krueger, K.L., Scott, J.R., Kay, R.F., Ungar, P.S., 2008. Technical note: Dental microwear textures of “Phase I” and “Phase II” facets. *Am. J. Phys. Anthropol.* 137, 485–490.
- Lambert, J.E., 1998. Primate digestion: Interactions among anatomy, physiology, and feeding ecology. *Evol. Anthropol.* 7, 8–20.
- Lambert, J.E., 2009. Summary to the symposium issue: Primate fallback strategies as adaptive phenotypic plasticity-scale, pattern, and process. *Am. J. Phys. Anthropol.* 140, 759–766.
- Lambert, J.E., Chapman, C.A., Wrangham, R.W., Conklin-Brittain, N. Lou, 2004. Hardness of cercopithecine foods: Implications for the critical function of enamel thickness in exploiting fallback foods. *Am. J. Phys. Anthropol.* 125, 363–368.
- Leakey, M.G., 1982. Extinct large colobines from the Plio-Pleistocene of Africa. *Am. J. Phys. Anthropol.* 58, 153–172.
- Leakey, M.G., Teaford, M.F., Ward, C.V., 2003. Cercopithecidae from Lothagam. In: Leakey, M.G., Harris, J.M. (Eds.), *Lothagam: The Dawn of Humanity in Eastern Africa*. Columbia

University Press, New York, pp. 201–235.

Ledogar, J.A., Winchester, J.M., St. Clair, E.M., Boyer, D.M., 2013. Diet and dental topography in pitheciine seed predators. *Am. J. Phys. Anthropol.* 150, 107–121.

Lucas, P.W., Corlett, R.T., Luke, D.A., 1986. Postcanine tooth size and diet in anthropoid primates. *Z. Morphol. Anthropol.* 76, 253–276.

Lucas, P.W., Constantino, P., Wood, B., Lawn, B., 2008. Dental enamel as a dietary indicator in mammals. *BioEssays* 30, 374–385.

Lucas, P.W., Casteren, A. Van, Al-Fadhalah, K., Almusallam, A.S., Henry, A.G., Michael, S., Watzke, J., Reed, D.A., Diekwisch, T.G.H., Strait, D.S., Atkins, A.G., 2014. The role of dust, grit and phytoliths in tooth wear. *Ann. Zool. Fenn.* 51, 143–152.

Lucas, P.W., Omar, R., Al-Fadhalah, K., Almusallam, A.S., Henry, A.G., Michael, S., Thai, L.A., Watzke, J., Strait, D.S., Atkins, A.G., 2013. Mechanisms and causes of wear in tooth enamel: Implications for hominin diets. *J. R. Soc. Interface.* 10, 20120923.

Macho, G.A., 2017. Niche partitioning. In: Fuentes, A. (Eds.), *The International Encyclopedia of Primatology*, John Wiley and Sons, Inc, Vol. 2, pp. 1–4.

MacKinnon, J.R., MacKinnon, K.S., 1980. Niche Differentiation in a Primate Community. In Chivers D.J. (Eds.), *Malayan Forest Primates*, Springer, New York, 167–190.

Madden, R.H., 2014. *Hypsodonty in mammals: Evolution, geomorphology, and the role of earth surface processes*. Cambridge University Press, New York.

Maier, W., 1977. Die evolution der bilophodonten molaren der Cercopithecoidea: Eine funktionsmorphologische untersuchung. *Z. Morphol. Anthropol.* 26–56.

Maisels, F., Gautier-Hion, A., Gautier, J. P., 1994. Diets of two sympatric colobines in Zaire: More evidence on seed-eating in forests on poor soils. *Int. J. Primatol.* 15, 681–701.

- Marshall, A.J., Wrangham, R.W., 2007. Evolutionary consequences of fallback foods. *Int. J. Primatol.* 28, 1219–1235.
- Martin, L.B., 1983. The relationships of the later Miocene Hominoidea. Ph.D. Dissertation, University College London.
- Martin, L., 1985. Significance of enamel thickness in hominoid evolution. *Nature* 314, 260–263.
- Martin, L.B., Olejniczak, A.J., Maas, M.C., 2003. Enamel thickness and microstructure in pitheciin primates, with comments on dietary adaptations of the middle Miocene hominoid *Kenyapithecus*. *J. Hum. Evol.* 45, 351–367.
- Maschenko, E.N., 1991. Tooth system and taxonomic status of early Pliocene cercopithecoid monkey *Dolichopithecus hipsulophus* (Primates, Cercopithecidae). *Biol. Moscow Ov. Ist. Prir. Geol.* 66, 61–74.
- Maschenko, E.N., 2005. Cenozoic Primates of eastern Eurasia (Russia and adjacent areas). *Anthropol. Sci.* 113, 103–115.
- Matsuda, I., Chapman, C.A., Clauss, M., 2019. Colobine forestomach anatomy and diet. *J. Morphol.* 280, 1608–1616.
- Matsuda, I., Clauss, M., Tuuga, A., Sugau, J., Hanya, G., Yumoto, T., Bernard, H., Hummel, J., 2017. Factors affecting leaf selection by foregut-fermenting proboscis monkeys: New insight from in vitro digestibility and toughness of leaves. *Sci. Rep.* 7, 1–10.
- McGraw, W.S., Pampush, J.D., Daegling, D.J., 2012. Brief communication: Enamel thickness and durophagy in mangabeys revisited. *Am. J. Phys. Anthropol.* 147, 326–333.
- Merceron, G., Taylor, S., Scott, R., Chaimanee, Y., Jaeger, J.J., 2006. Dietary characterization of the hominoid *Khoratpithecus* (Miocene of Thailand): Evidence from dental

- topographic and microwear texture analyses. *Naturwissenschaften* 93, 329–333.
- Merceron, G., Koufos, G.D., Valentin, X., 2009a. Habitudes alimentaires du premier colobiné européen, *Mesopithecus*: Apports de l'analyse comparative des micro-usures dentaires avec des cercopithecidés actuels. *Geodiversitas* 31, 865–878.
- Merceron, G., Scott, J., Scott, R.S., Geraads, D., Spassov, N., Ungar, P.S., 2009b. Folivory or fruit/seed predation for *Mesopithecus*, an earliest colobine from the late Miocene of Eurasia? *J. Hum. Evol.* 57, 732–738.
- Merceron, G., Ramdarshan, A., Blondel, C., Boisserie, J.R., Brunetiere, N., Francisco, A., Gautier, D., Milhet, X., Novello, A., Pret, D., 2016. Untangling the environmental from the dietary: Dust does not matter. *Proc. R. Soc. Lond. B Biol. Sci.* 283.
- Merceron, G., Kallend, A., Francisco, A., Louail, M., Martin, F., Plastiras, C.-A., Thiery, G., Noûs, C., Boisserie, J.-R., 2021. Further away with dental microwear analysis: food resource partitioning among Plio-Pleistocene monkeys from the Shungura Formation, Ethiopia. *Palaeogeogr. Palaeoclimatol. Palaeoecol.* 572, 110414.
- Mitani, M., 1989. *Cercocebus torquatus*: Adaptive feeding and ranging behaviors related to seasonal fluctuations of food resources in the tropical rain forest of south-western Cameroon. *Primates* 30, 307–323.
- Nakagawa, N., 2000. Seasonal, sex, and interspecific differences in activity time budgets and diets of patas monkeys (*Erythrocebus patas*) and tantalus monkeys (*Cercopithecus aethiops tantalus*), living sympatrically in Northern Cameroon. *Primates* 41, 161–174.
- Nakagawa, N., 2003. Difference in food selection between patas monkeys (*Erythrocebus patas*) and tantalus monkeys (*Cercopithecus aethiops tantalus*) in Kala Maloue National Park, Cameroon, in relation to nutrient content. *Primates* 44, 3–11.
- Nakatsukasa, M., Mbua, E., Sawada, Y., Sakai, T., Nakaya, H., Yano, W., Kunimatsu, Y., 2010.

- Earliest colobine skeletons from Nakali, Kenya. *Am. J. Phys. Anthropol.* 143, 365–382.
- Napier, J. 1970. Paleocology and catarrhine evolution. In: Napier, J.R., Napier P.H. (Eds.), *Old World Monkeys*. London , Academic Press, pp. 55-95.
- Nishimura, T.D., Takai, M., Senut, B., Taru, H., Maschenko, E.N., Prieur, A., 2012. Reassessment of *Dolichopithecus (Kanagawapithecus) leptopostorbitalis*, a colobine monkey from the Late Pliocene of Japan. *J. Hum. Evol.* 62, 548–561.
- Norconk, M.A., Wright, B.W., Conklin-brittain, N.L., Vinyard, C.J., 2009. Mechanical and nutritional properties of food as factors in platyrrhine dietary adaptations. In: Garber, P.A., Estrada, A., Bicca-Marques, J.C., Heymann, E.W., Strier, K.B. (Eds.), *South American Primates: Testing New Theories in the Study of Primate Behavior, Ecology and Conservation*. Springer, New York, pp. 279–319.
- Nystrom, P., Phillips-Conroy, J.E., Jolly, C.J., 2004. Dental microwear in anubis and hybrid baboons (*Papio hamadryas*, sensu lato) living in Awash national park, Ethiopia. *Am. J. Phys. Anthropol.* 125, 279–291.
- Olejniczak, A.J., Smith, T.M., Skinner, M.M., Grine, F.E., Feeney, R.N.M., Thackeray, J.F., Hublin, J.J., 2008. Three-dimensional molar enamel distribution and thickness in *Australopithecus* and *Paranthropus*. *Biol. Lett.* 4, 406–410.
- Onoda, Y., Westoby, M., Adler, P. B., Choong, A. M. F., Clissold, F. J., Cornelissen, J. H. C., Díaz, S., Dominy, N. J., Elgart, A., Enrico, L., Fine, P. V. A., Howard, J. J., Jalili, A., Kitajima, K., Kurokawa, H., McArthur, C., Lucas, P. W., Markesteijn, L., Pérez-Harguindeguy, N., Poorter, L., Richards, L., Santiago, L.S., Sosinski, E.E., Van Bael, S.A., Warton D.I., Wright, I.J., Joseph, W.S., Yamashita, N., 2011. Global patterns of leaf mechanical properties. *Ecol. Lett.* 14, 301–312
- Owens, J.R., Honarvar, S., Nessel, M., Hearn, G.W., 2015. From frugivore to folivore: Altitudinal

- variations in the diet and feeding ecology of the Bioko Island drill (*Mandrillus leucophaeus poensis*). *Am. J. Primatol.* 77, 1263–1275.
- Pagel, M., 1994. Detecting correlated evolution on phylogenies: A general method for the comparative analysis of discrete characters. *Proc. R. Soc. B Biol. Sci.* 255, 37–45.
- Pagel, M., 1999. Inferring the historical patterns of biological evolution. *Nature* 401, 877–884.
- Pallas, L., Daver, G., Mackaye, H.T., Likius, A., Vignaud, P., Guy, F., 2019. A window into the early evolutionary history of Cercopithecidae: Late Miocene evidence from Chad, Central Africa. *J. Hum. Evol.* 132, 61–79.
- Pampush, J.D., Duque, A.C., Burrows, B.R., Daegling, D.J., Kenney, W.F., McGraw, W.S., 2013. Homoplasy and thick enamel in primates. *J. Hum. Evol.* 64, 216–224.
- Pampush, J. D., Spradley, J. P., Morse, P. E., Harrington, A. R., Allen, K. L., Boyer, D. M., Kay, R. F., 2016. Wear and its effects on dental topography measures in howling monkeys (*Alouatta palliata*). *Am. J. Phys. Anthropol.* 161, 705–721.
- Pan, R., Groves, C., Oxnard, C., 2004. Relationships between the fossil colobine *Mesopithecus pentelicus* and extant cercopithecoids, based on dental metrics. *Am. J. Primatol.* 62, 287–299.
- Percher, A.M., Merceron, G., Nsi Akoue, G., Galbany, J., Romero, A., Charpentier, M.J.E., 2018. Dental microwear textural analysis as an analytical tool to depict individual traits and reconstruct the diet of a primate. *Am. J. Phys. Anthropol.* 165, 123–138.
- Philippe, M., Bourgat, R., 1985. La collection de vertébrés pliocènes du Muséum de Perpignan. *Bull. Mens. Soc. Linn. Lyon.* 54, 146–160.
- Poulsen, J.R., Clark, C.J., Smith, T.B., 2001. Seasonal variation in the feeding ecology of the grey-cheeked mangabey (*Lophocebus albigena*) in Cameroon. *Am. J. Primatol.* 54, 91–

105.

- Pruetz, J.D., Isbell, L.A., 2000. Correlations of food distribution and patch size with agonistic interactions in female vervets (*Chlorocebus aethiops*) and patas monkeys (*Erythrocebus patas*) living in simple habitats. *Behav. Ecol. Sociobiol.* 38–47.
- R Core Team, 2013. R: A language and environment for statistical computing. R Foundation for Statistical Computing, Vienna.
- Rabenold, D., Pearson, O.M., 2011. Abrasive, silica phytoliths and the evolution of thick molar enamel in primates, with implications for the diet of *Paranthropus boisei*. *PLoS One* 6, e0028379.
- Ragni, A.J., Teaford, M.F., Ungar, P.S., 2017. A molar microwear texture analysis of pitheciid primates. *Am. J. Primatol.* 79, 1–12.
- Ramdarshan, A., Blondel, C., Gautier, D., Surault, J., Merceron, G., 2017. Overcoming sampling issues in dental tribology: Insights from an experimentation on sheep. *Palaeontol. Electron.* 20, 1-19.
- Ravosa, M.J., 1996. Jaw morphology and function in living and fossil Old World monkeys. *Int. J. Primatol.* 17, 909–932.
- Reitz, J.J., Benefit, B.R., 2001. Dental microwear in *Mesopithecus pentelici* from the late Miocene of Pikermi, Greece. *Am. J. Phys. Anthropol.* 114 (S32), 125.
- Rensberger, J.M., 1978. Scanning electron microscopy of wear and occlusal events in some small herbivores. In: Butler, P.M., Joysey, K.A. (Eds.), *Development, Function and Evolution of Teeth*. Academic Press, New York, pp. 415–438.
- Rogers, M.E., Abernethy, K., Bermejo, M., Cipolletta, C., Doran, D., Mcfarland, K., Nishihara, T., Remis, M., Tutin, C.E.G., 2004. Western gorilla diet: A synthesis from six sites. *Am. J.*

- Primatol. 64, 173–192.
- Rossie, J.B., Gilbert, C.C., Hill, A., 2013. Early cercopithecoid monkeys from the Tugen Hills, Kenya. *Proc. Natl. Acad. Sci. USA* 110, 5818–5822.
- Rowe, N., Goodall, J., Mittermeier, R., 1996. *The Pictorial Guide to the Living Primates*. Pogonias Press East Hampton, New York.
- Rowell, T.E., 1966. Hierarchy in the organization of a captive baboon group. *Anim. Behav.* 14, 430–443.
- Ruslin, F., Matsuda, I., Md-Zain, B.M., 2019. The feeding ecology and dietary overlap in two sympatric primate species, the long-tailed macaque (*Macaca fascicularis*) and dusky langur (*Trachypithecus obscurus obscurus*), in Malaysia. *Primates* 60, 41–50.
- Sanson, G.D., Kerr, S., Read, J., 2017. Dietary exogenous and endogenous abrasives and tooth wear in African buffalo. *Biosurf. Biotribol.* 3, 211–223.
- Sayers, K., Norconk, M.A., 2008. Himalayan *Semnopithecus entellus* at Langtang National Park, Nepal: Diet, activity patterns, and resources. *Int. J. Primatol.* 29, 509–530.
- Schreier, A.L., Schlaht, R.M., Swedell, L., 2019. Meat eating in wild hamadryas baboons: Opportunistic trade-offs between insects and vertebrates. *Am. J. Primatol.* 81, 1–12.
- Schulz-Kornas, E., Winkler, D.E., Clauss, M., Carlsson, J., Ackermans, N.L., Martin, L.F., Hummel, J., Müller, D.W.H., Hatt, J.M., Kaiser, T.M., 2020. Everything matters: Molar microwear texture in goats (*Capra aegagrus hircus*) fed diets of different abrasiveness. *Palaeogeogr. Palaeoclimatol. Palaeoecol.* 552, 109783.
- Schwartz, G.T., McGrosky, A., Strait, D.S., 2020. Fracture mechanics, enamel thickness and the evolution of molar form in hominins. *Biol. Lett.* 16, 3–8.
- Scott, R.S., Teaford, M.F., Ungar, P.S., 2012. Dental microwear texture and anthropoid diets.

- Am. J. Phys. Anthropol. 147, 551–579.
- Scott, R.S., Ungar, P.S., Bergstrom, T.S., Brown, C.A., Grine, F.E., Teaford, M.F., Walker, A., 2005. Dental microwear texture analysis shows within-species diet variability in fossil hominins. *Nature* 436, 693–695.
- Scott, R.S., Ungar, P.S., Bergstrom, T.S., Brown, C.A., Childs, B.E., Teaford, M.F., Walker, A., 2006. Dental microwear texture analysis: Technical considerations. *J. Hum. Evol.* 51, 339–349.
- Shan, S., Kovalsky, S.Z., Winchester, J.M., Boyer, D.M., Daubechies, I., 2019. ariaDNE: A robustly implemented algorithm for Dirichlet energy of the normal. *Methods Ecol. Evol.* 10, 541–552.
- Shellis, R.P., Beynon, A.D., Reid, D.J., Hiiemae, K.M., 1998. Variations in molar enamel thickness among primates. *J. Hum. Evol.* 35, 507–522.
- Singh, M., Roy, K., Singh, M., 2011. Resource partitioning in sympatric langurs and macaques in tropical rainforests of the central Western Ghats, south India. *Am. J. Primatol.* 73, 335–346.
- Skinner, M.M., Evans, A., Smith, T., Jernvall, J., Tafforeau, P., Kupczik, K., Olejniczak, A.J., Rosas, A., Radovčić, J., Thackeray, J.F., Toussaint, M., Hublin, J.J., 2010. Brief communication: Contributions of enamel-dentine junction shape and enamel deposition to primate molar crown complexity. *Am. J. Phys. Anthropol.* 142, 157–163.
- Smith, R.J., Jungers, W.L., 1997. Body mass in comparative primatology. *J. Hum. Evol.* 32, 523–559.
- Smith, T.M., Kupczik, K., MacHanda, Z., Skinner, M.M., Zermeno, J.P., 2012. Enamel thickness in Bornean and Sumatran orangutan dentitions. *Am. J. Phys. Anthropol.* 147, 417–426.

- Spassov, N., Geraads, D., 2007. *Dolichopithecus balcanicus* sp. nov., a new Colobinae (Primates, Cercopithecidae) from the early Pliocene of southeastern Europe, with a discussion on the taxonomy of the genus. *J. Hum. Evol.* 52, 434–442.
- Spassov, N., Geraads, D., Hristova, L., Markov, G.N., Merceron, G., Tzankov, T., Stoyanov, K., Böhme, M., Dimitrova, A., 2012. A hominid tooth from Bulgaria: The last pre-human hominid of continental Europe. *J. Hum. Evol.* 62, 138–145.
- Spradley, J.P., Pampush, J.D., Morse, P.E., Kay, R.F., 2017. Smooth operator: The effects of different 3D mesh retriangulation protocols on the computation of Dirichlet normal energy. *Am. J. Phys. Anthropol.* 163, 94–109.
- Sterck, E.H.M., Steenbeek, R., 1997. Female dominance relationships and food competition in the sympatric thomas langur and long-tailed macaque. *Behaviour* 134, 749–774.
- Struhsaker, T., 1967. Ecology of vervet monkeys (*Cercopithecus aethiops*) in the Masai-Amboseli game reserve, Kenya. *Ecology* 48, 891–904.
- Swedell, L., Hailemeskel, G., Schreier, A., 2008. Composition and seasonality of diet in wild hamadryas baboons: Preliminary findings from filoha. *Folia Primatol.* 79, 476–490.
- Swindler, D.R., 2002. *Primate Dentition: An Introduction to the Teeth of Non-human Primates*. Cambridge University Press, Cambridge.
- Symonds, M.R.E., Blomberg, S.P., 2014. Modern phylogenetic comparative methods and their application in evolutionary biology. In: Garamszegi, L.Z. (Eds.), *Modern Phylogenetic Comparative Methods and Their Application in Evolutionary Biology*. Springer, Heidelberg, pp. 105–130.
- Szalay, F.S., Delson, E., 1979. *Evolutionary History of the Primates*. Academic Press, New York.
- Teaford, M.F., 2007. Dental microwear and paleoanthropology: Cautions and possibilities. In:

- Bailey, S.E., Hublin, J.J. (Eds.), Dental Perspectives on Human Evolution. Springer, Dordrecht, 345–368.
- Teaford, M.F., Lytle, J.D., 1996. Brief communication: Diet-induced changes in rates of human tooth microwear: A case study involving stone-ground maize. *Am. J. Phys. Anthropol.* 100, 143–147.
- Teaford, M.F., Oyen, O.J., 1989. In vivo and in vitro turnover in dental microwear. *Am. J. Phys. Anthropol.* 80, 447–460.
- Teaford, M.F., Walker, A., 1984. Quantitative differences in dental microwear between primate species with different diets and a comment on the presumed diet of *Sivapithecus*. *Am. J. Phys. Anthropol.* 64, 191–200.
- Teaford, M.F., Lucas, P.W., Ungar, P.S., Glander, K.E., 2006. Mechanical defenses in leaves eaten by Costa Rican howling monkeys (*Alouatta palliata*). *Am. J. Phys. Anthropol.* 129, 99–104.
- Teaford, M.F., Ungar, P.S., Taylor, A.B., Ross, C.F., Vinyard, C.J., 2017. In vivo rates of dental microwear formation in laboratory primates fed different food items. *Biosurf. Biotrib.* 3, 166–173.
- Teelen, S., 2007. Primate abundance along five transect lines at Ngogo, Kibale national park, Uganda. *Am. J. Primatol.* 69, 1030–1044.
- Thiery, G., Gillet, G., Lazzari, V., Merceron, G., Guy, F., 2017a. Was *Mesopithecus* a seed eating colobine? Assessment of cracking, grinding and shearing ability using dental topography. *J. Hum. Evol.* 112, 79–92.
- Thiery, G., Guy, F., Lazzari, V., 2017b. Investigating the dental toolkit of primates based on food mechanical properties: Feeding action does matter. *Am. J. Primatol.* 79, 1–15.

- Thiery, G., Lazzari, V., Ramdarshan, A., Guy, F., 2017c. Beyond the map: Enamel distribution characterized from 3D dental topography. *Front. Physiol.* 8,524.
- Thiery, G., Guy, F., Lazzari, V., 2019. Enamel distribution in 3D: Is enamel thickness more uneven in the upper second molars of durophagous hominoids? *Bull. Mem. Soc. Anthropol. Paris.* 31, 52–59.
- Thiery, G., Gibert, C., Guy, F., Lazzari, V., Geraads, D., Spassov, N., Merceron, G., 2021. From leaves to seeds? The dietary shift in late Miocene colobine monkeys of southeastern Europe. *Evolution* 75, 1983–1997.
- Tobien, H., 1970. Biostratigraphy of the mammalian faunas at the Pliocene-Pleistocene boundary in Middle and Western Europe. *Palaeogeogr. Palaeoclimatol. Palaeoecol.* 8, 77–93.
- Tutin, C.E.G., Ham, R.M., White, L.J.T., Harrison, M.J.S., 1997. The primate community of the Lope Reserve, Gabon: Diets, responses to fruit scarcity, and effects on biomass. *Am. J. Primatol.* 42, 1–24.
- Ulhaas, L., Kullmer, O., Schrenk, F., Henke, W., 2004. A new 3-d approach to determine functional morphology of cercopithecoid molars. *Ann. Anat.* 186, 487–493.
- Ungar, P.S., 1995. Fruit preferences of four sympatric primate species at Ketambe, northern Sumatra, Indonesia. *Int. J. Primatol.* 16, 221–245.
- Ungar, P.S., M'Kirera, F., 2003. A solution to the worn tooth conundrum in primate functional anatomy. *Proc. Natl. Acad. Sci. USA* 100, 3874–3877.
- Ungar, P.S., Teaford, M.F., 1996. Preliminary examination of non-occlusal dental microwear in anthropoids: Implications for the study of fossil primates. *Am. J. Phys. Anthropol.* 100, 101–113.

- Ungar, P.S., Williamson, M., 2000. Exploring the effects of tooth wear on functional morphology: A preliminary study using dental topographic analysis. *Palaeontol. Electron.* 3, 1.
- Ungar, P.S., Scott, R.S., Scott, J.R., Teaford, M.F., 2008. Dental microwear analysis: historical perspectives and new approaches. In: Irish, J.D., Nelson, G.C. (Eds.), *Technique and Application in Dental Anthropology*. Cambridge University Press, Cambridge, pp. 389–425.
- Ungar, P.S., Krueger, K.L., Blumenschine, R.J., Njau, J., Scott, R.S., 2012. Dental microwear texture analysis of hominins recovered by the Olduvai Landscape Paleoanthropology Project, 1995-2007. *J. Hum. Evol.* 63, 429–437.
- Ungar, P.S., Healy, C., Karme, A., Teaford, M., Fortelius, M., 2018. Dental topography and diets of platyrrhine primates. *Hist. Biol.* 30, 64–75.
- van Casteren, A., Wright, E., Kupczik, K., Robbins, M.M., 2019. Unexpected hard-object feeding in Western lowland gorillas. *Am. J. Phys. Anthropol.* 170, 433–438.
- van Casteren, A., Strait, D.S., Swain, M. V., Michael, S., Thai, L.A., Philip, S.M., Saji, S., Al-Fadhlah, K., Almusallam, A.S., Shekeban, A., McGraw, W.S., Kane, E.E., Wright, B.W., Lucas, P.W., 2020. Hard plant tissues do not contribute meaningfully to dental microwear: Evolutionary implications. *Sci. Rep.* 10, 582.
- Vandercone, R.P., Dinadh, C., Wijethunga, G., Ranawana, K., Rasmussen, D.T., 2012. Dietary diversity and food selection in hanuman langurs (*Semnopithecus entellus*) and purple-faced langurs (*Trachypithecus vetulus*) in the Kaludiyapokuna forest reserve in the dry zone of Sri Lanka. *Int. J. Primatol.* 33, 1382–1405.
- Visualization Sciences Group, 2011. Avizo® 7.0.0. Berlin, Germany: Konrad-Zuse-Zentrum für Informationstechnik.

- Vrba, E.S., Denton, G.H., Partridge, T.C., Burckle, L.H. (Eds.), 1995. *Paleoclimate and Evolution, with Emphasis on Human Origins*. Yale University Press, New Haven.
- Walker, A., Hoeck, H.N., Perez, L., 1978. Microwear of mammalian teeth as an indicator of diet. *Science* 201, 908–910.
- Walker, P., Murray, P., 2011. An assessment of masticatory efficiency in a series of anthropoid primates with special reference to the Colobinae and Cercopithecinae. In: Tuttle, R.H. (Eds.), *Primate Functional Morphology and Evolution*. De Gruyter Mouton, Berlin, New York, p. 135-150.
- Williams, F.L.E., Geissler, E., 2014. Reconstructing the diet and paleoecology of Plio-Pleistocene *Cercopithecoides williamsi* from Sterkfontein, South Africa. *Palaios* 29, 483–494.
- Winchester, J.M., Boyer, D.M., St. Clair, E.M., Gosselin-Ildari, A.D., Cooke, S.B., Ledogar, J.A., 2014. Dental topography of platyrrhines and prosimians: Convergence and contrasts. *Am. J. Phys. Anthropol.* 153, 29–44.
- Winkler, D.E., Tütken, T., Schulz-Kornas, E., Kaiser, T.M., Müller, J., Leichliter, J., Weber, K., Hatt, J.M., Clauss, M., 2020. Shape, size, and quantity of ingested external abrasives influence dental microwear texture formation in guinea pigs. *Proc. Natl. Acad. Sci. USA* 117, 22264–22273.
- Wood, B.A., 1979. An analysis of tooth and body size relationships in five primate taxa. *Folia Primatol.* 31, 187–211.
- Wright, B.W., Willis, M.S., 2012. Relationships between the diet and dentition of Asian leaf monkeys. *Am. J. Phys. Anthropol.* 148, 262–275.
- Wright, B.W., Ulibarri, L., O'Brien, J., Sadler, B., Prodhan, R., Covert, H.H., Nadler, T., 2008. It's tough out there: Variation in the toughness of ingested leaves and feeding behavior

- among four colobinae in Vietnam. *Int. J. Primatol.* 29, 1455–1466.
- Xia, J., Zhou, Z., Qian, L., Ungar, P.S., 2018. Comment on Van Casteren et al. (2018): Softer metallic spheres do abrade harder enamel. *R. Soc. Open Sci.* 5, 181376.
- Yeager, C.P., 1989. Feeding ecology of the proboscis monkey (*Nasalis larvatus*). *Int. J. Primatol.* 10, 497–530.
- Yeager, C.P., Kool, K., 1994. The behavioral ecology of Asian colobines. In: Davies, G.E., Oates, J.F. (Eds.), *Colobine Monkeys: Their Ecology, Behaviour, and Evolution*, Cambridge University Press, Cambridge, pp. 496–521.
- Youlatos, D., 2003. Caractères calcanéens du primate du Miocène de Grèce *Mesopithecus pentelicus* (Cercopithecoidea: Colobinae). *Geobios* 36, 229–239.
- Youlatos, D., Koufos, G.D., 2010. Locomotor evolution of *Mesopithecus* (Primates: Colobinae) from Greece: Evidence from selected astragalar characters. *Primates* 51, 23–35.
- Youlatos, D., Couette, S., Koufos, G.D., 2012. A functional multivariate analysis of *Mesopithecus* (Primates: Colobinae) humeri from the Turolian of Greece. *J. Hum. Evol.* 63, 219–230.
- Zuccotti, L.F., Williamson, M.D., Limp, W.F., Ungar, P.S., 1998. Technical note: Modeling primate occlusal topography using geographic information systems technology. *Am. J. Phys. Anthropol.* 107, 137–142.

## Figure legends

**Figure 1.** Virtual reconstruction of the palate of the *Dolichopithecus ruscinensis* (MHNPn-PR01) specimen in (A1) occlusal, (A2) lateral left, (A3) lateral right, and

(A4) facial views. Right M<sup>1</sup> virtual reconstruction before (B) and after (C) processing in (B1, C1) occlusal, (B2, C2) mesial, (B3, C3) distal, (B4, C4) lingual, and (B5, C5) buccal views.

**Figure 2.** Virtual reconstruction of the palate of the *Dolichopithecus ruscinensis* specimen (MHNPn-PR01) showing the M<sup>1</sup> selected for study (A), the subsampled outer enamel (OES) and enamel-dentine junction surfaces (EDJ) of the right fossil M<sup>1</sup> cropped on their lowermost points with localization of Phase I (f3) and Phase II (f9) dental wear facets (B), and their 3D surface representation (C and D, respectively).

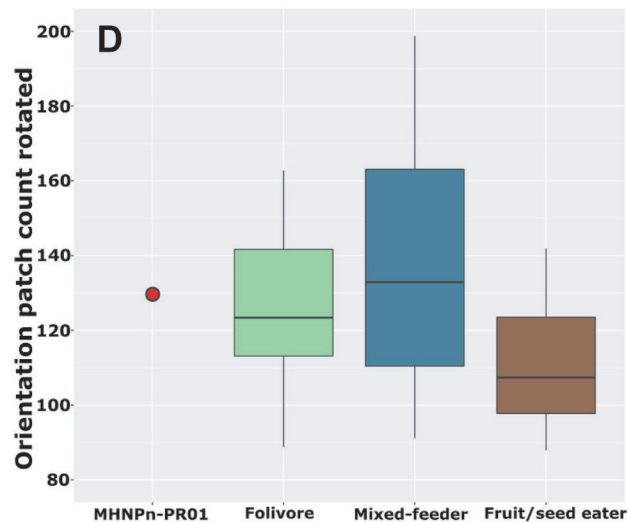
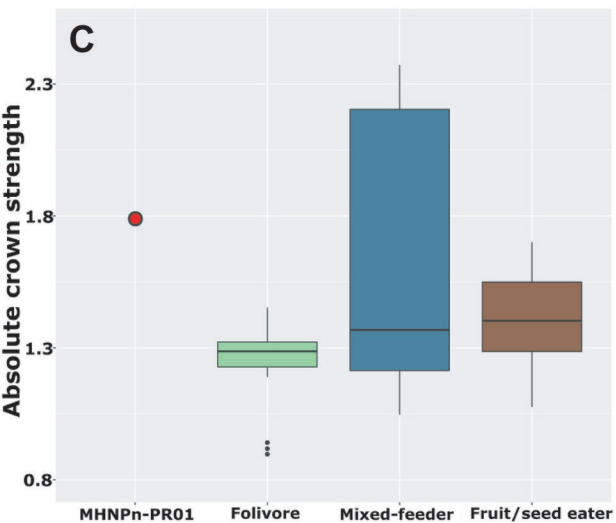
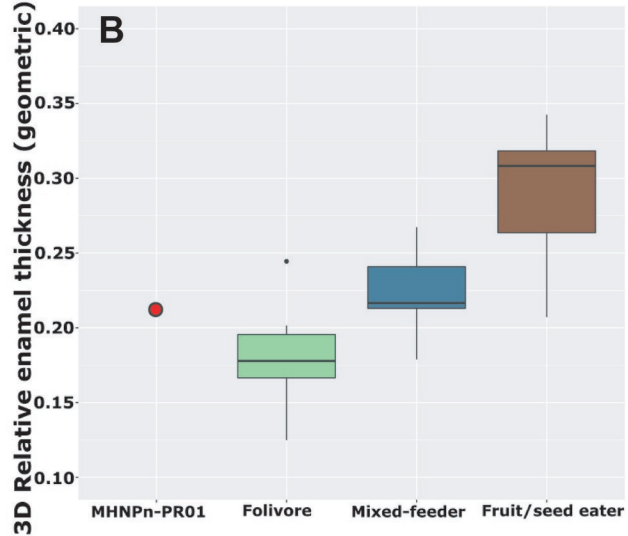
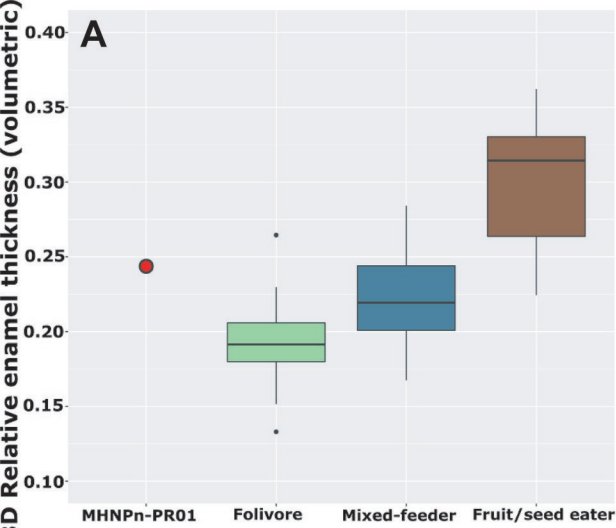
**Figure 3.** Boxplots of A) 3D relative enamel thickness (volumetric), B) 3D relative enamel thickness (geometric), C) absolute crown strength (ACS), and D) orientation patch count rotated (OPCR), for the three dietary categories represented by the extant colobine and cercopithecine comparative samples and *Dolichopithecus ruscinensis* (MHNPn-PR01). The fossil M<sup>1</sup> exhibits 3D relative enamel thickness (volumetric and geometric) similar to mixed feeders though it is closer to folivores than to fruit/seed eaters, while ACS is similar only to mixed feeders. Complexity (as indicated by OPCR) shows a high degree of overlap among the three diet categories and does not distinguish MHNPn-PR01. The horizontal center line marks the median, the lower and upper bounds of the box mark the 25<sup>th</sup> and 75<sup>th</sup> percentiles, whiskers represent the minimum and maximum interquartiles (1.5\*interquartile range), and filled circles represent outliers.

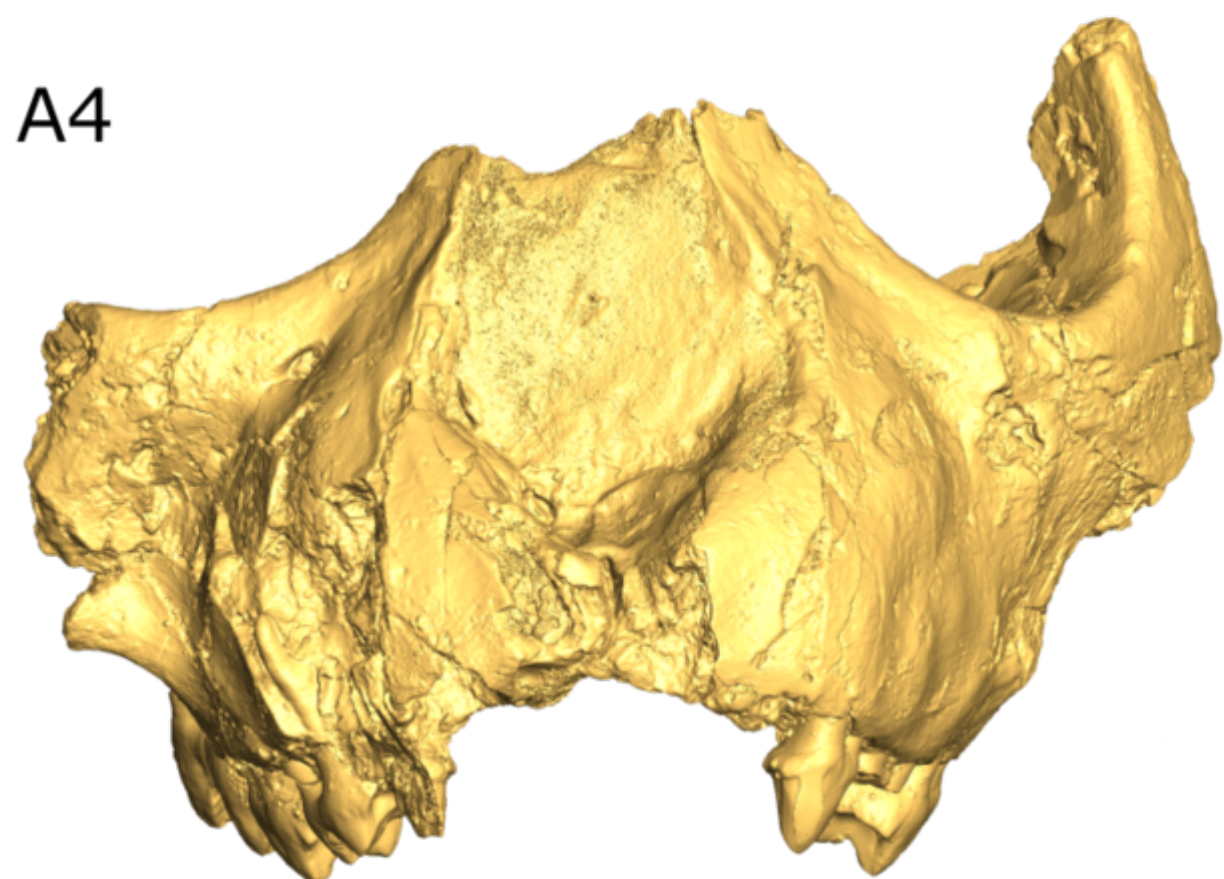
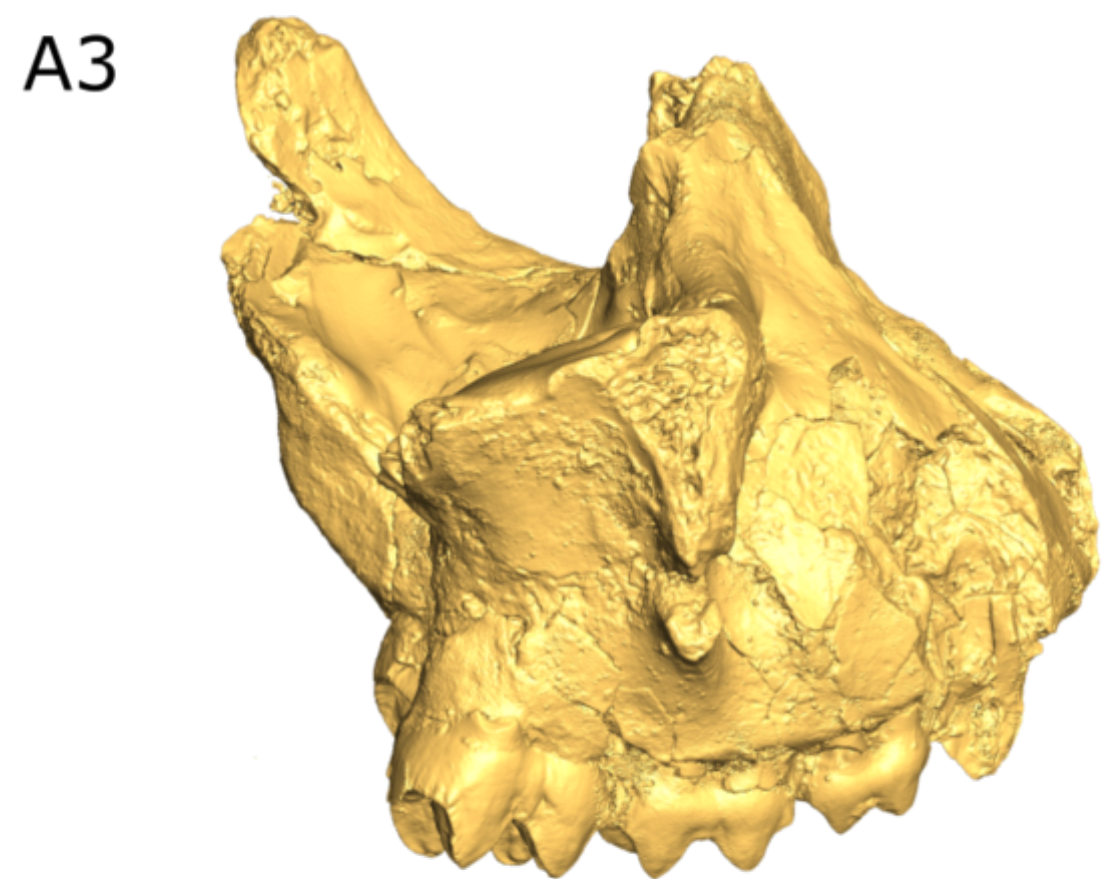
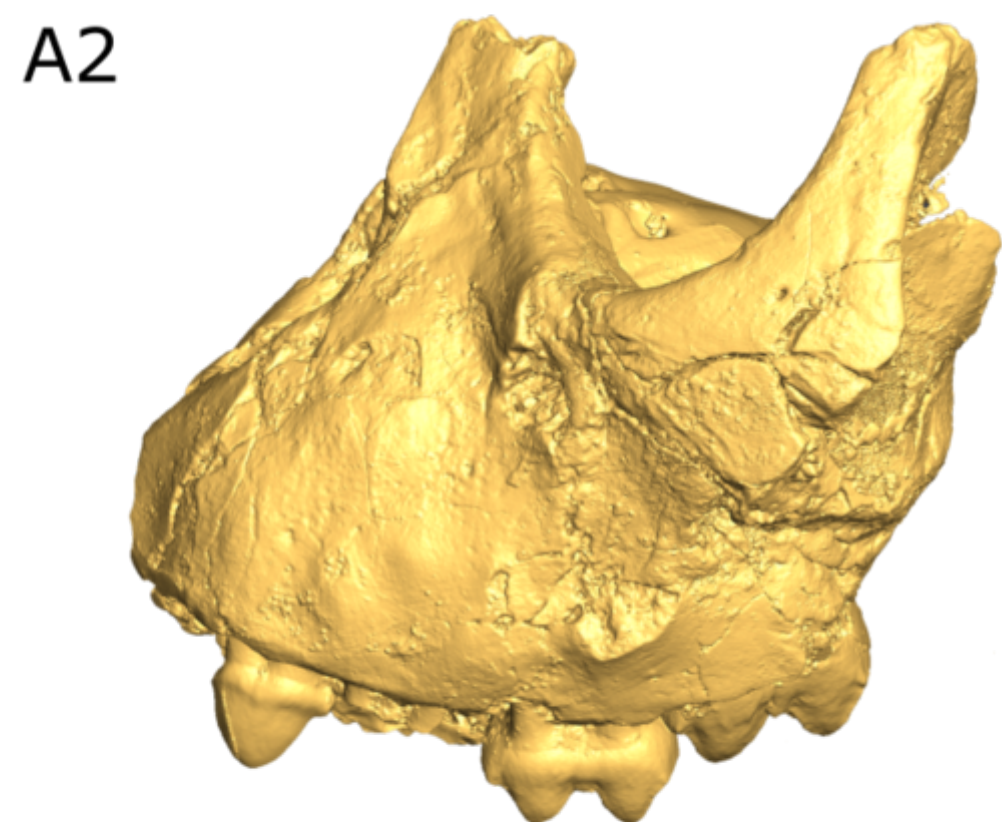
**Figure 4.** Boxplots of A) relief index (LRFI), B) inclination, C) area-relative curvature (ARC), and D) Dirichlet normal energy (DNE), for the dietary categories represented by the extant colobine and cercopithecine comparative samples and *Dolichopithecus ruscinensis* (MHNPn-PR01). The fossil M<sup>1</sup> exhibits an occlusal relief index, inclination, and ARC most similar to folivores. Dirichlet normal energy shows considerable overlap among the three diet categories and does not distinguish MHNPn-PR01. The horizontal center line marks the median, the lower and upper bounds of the box mark the 25<sup>th</sup> and 75<sup>th</sup> percentiles, whiskers represent the minimum and maximum interquartiles (1.5\*interquartile range), and filled circles represent outliers.

**Figure 5.** Plot of the linear discriminant analysis (A) with the best classification rate for inferring diet based on the three diet categories based on absolute crown strength, area-relative curvature (ARC), and 3D outer enamel surface. B) enamel distribution maps retaining original size (top) and depicting ARC (bottom) based on the lowest (*Lophocebus albigena*) and the highest value in our sample (*Piliocolobus badius*). Blue = mixed feeders (1: *Papio*, 2: *Mandrillus*; 3: *Cercopithecus campbelli*, 4: *Chlorocebus aethiops*, 5: *Erythrocebus patas*); orange = fruit/seed eaters (1: *Lophocebus albigena*, 2: *Cercocebus torquatus*, 3: *Lophocebus aterrimus*; 4: *Cercopithecus diana*, 5: *Cercopithecus pogonias*, 6: *Cercopithecus nictitans*); green = folivores (1: *Colobus polykomos*, 2: *Colobus guereza*, 3: *Procolobus verus*, 4: *Piliocolobus badius*, 5: *Colobus satanas*; 6: *Trachypithecus cristatus*, 7: *Semnopithecus entellus*, 8: *Nasalis larvatus*).

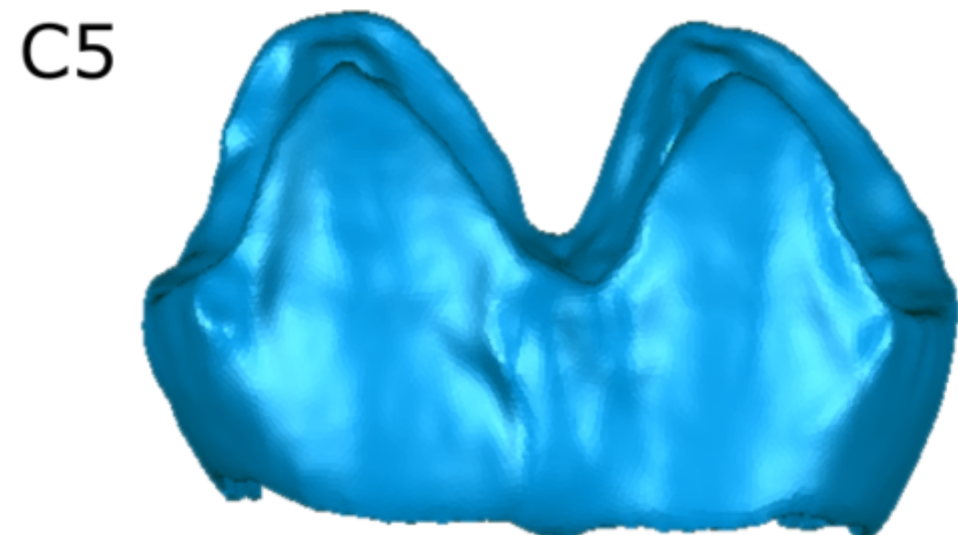
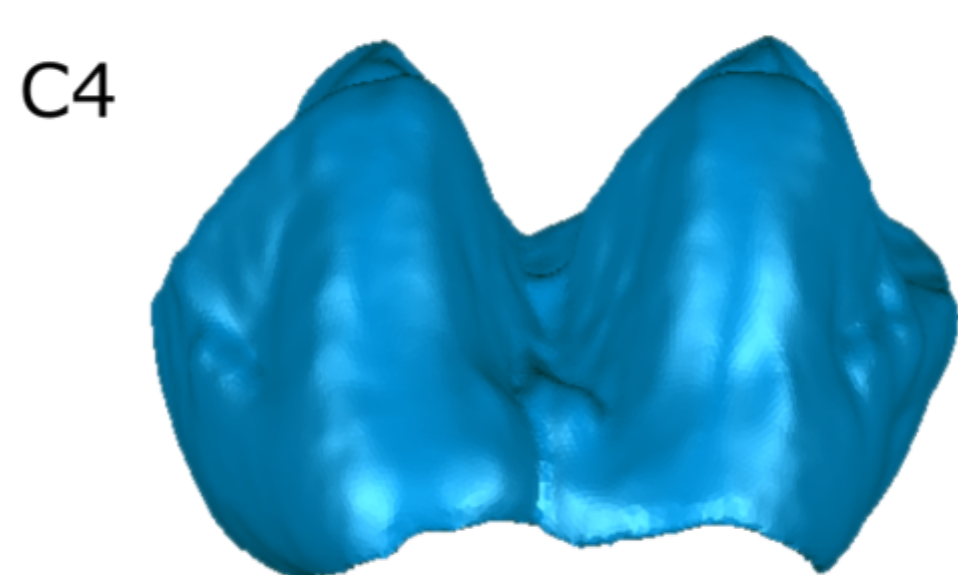
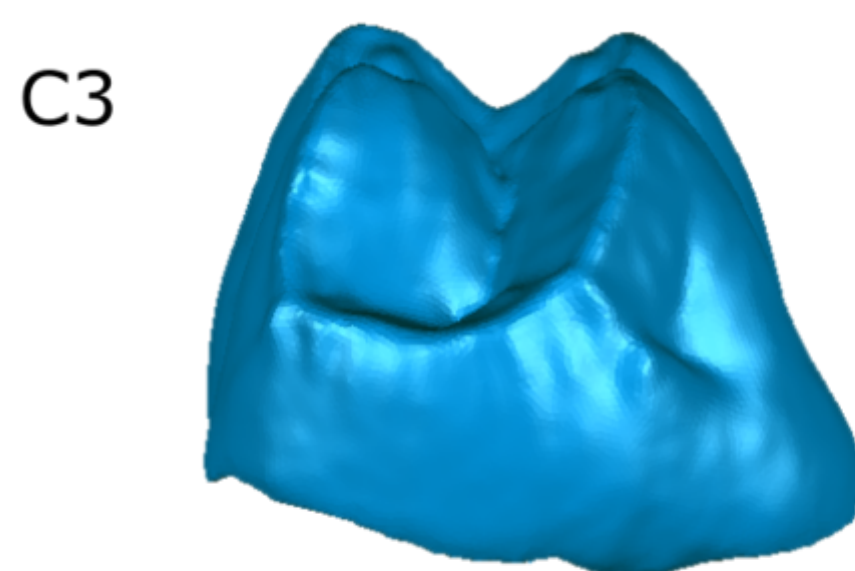
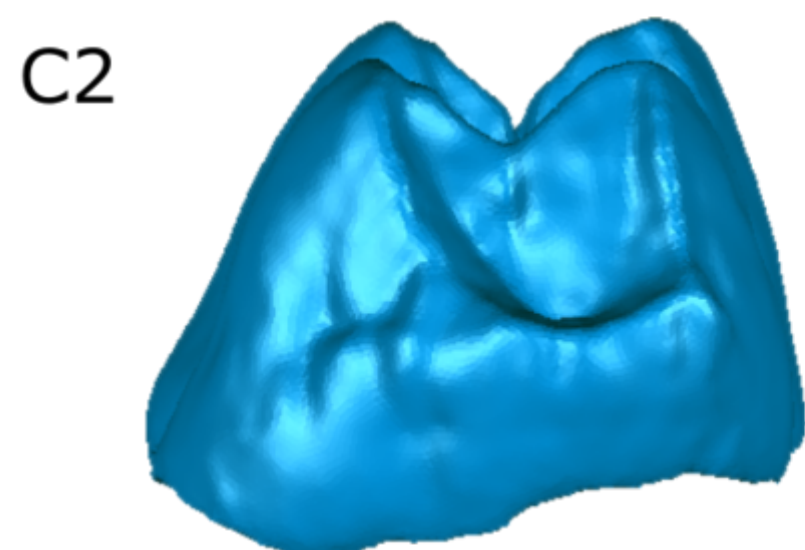
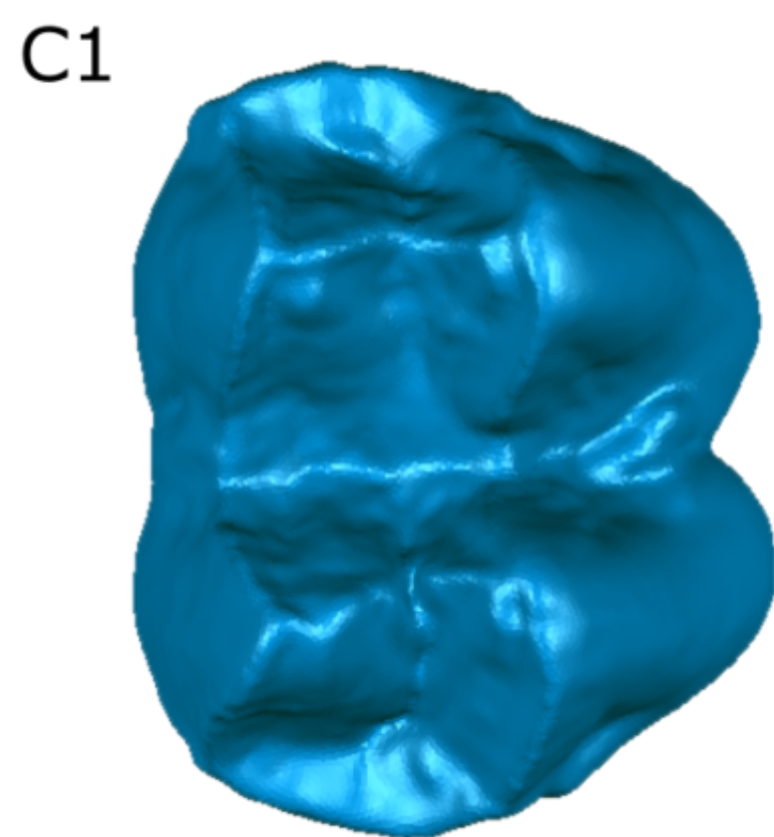
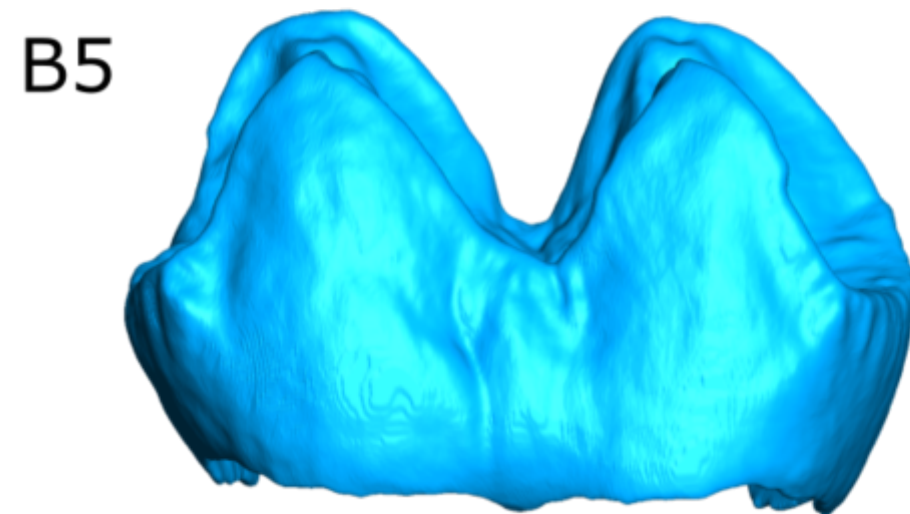
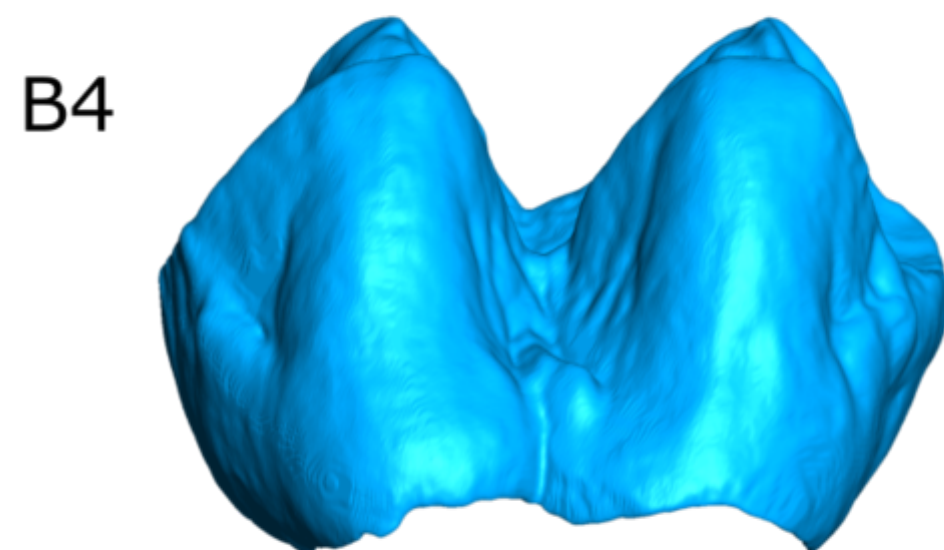
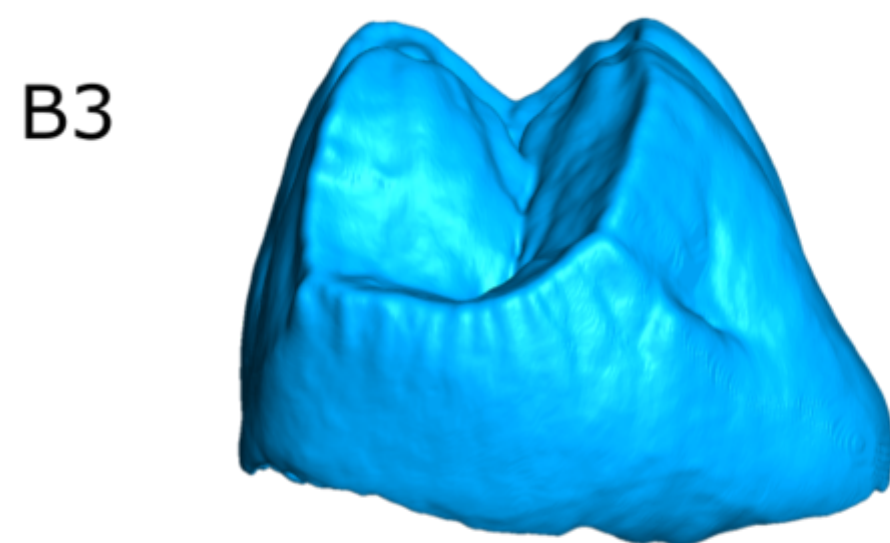
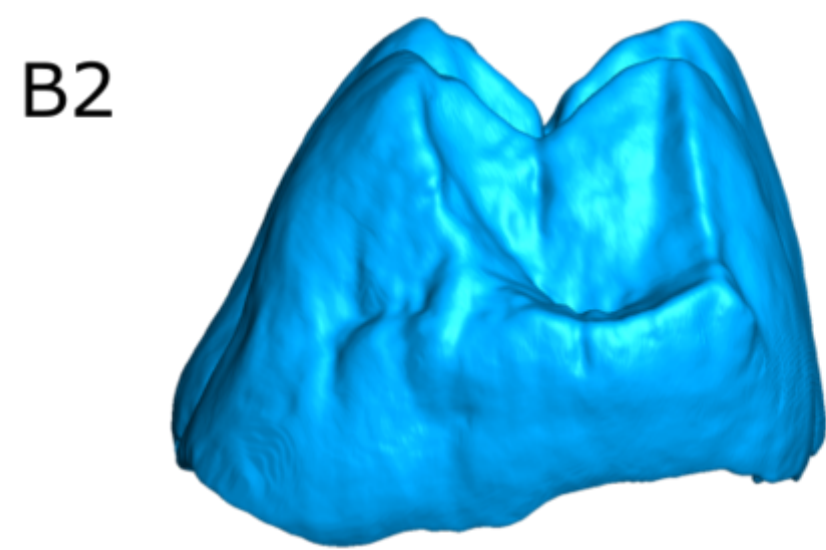
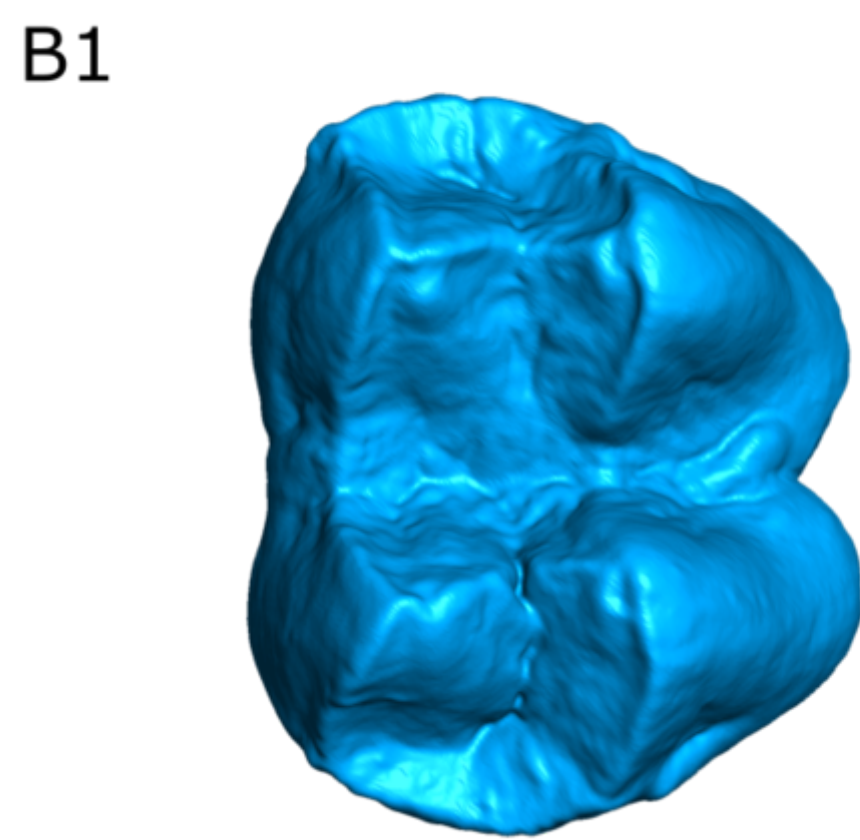
**Figure 6.** Bivariate plots (means with 95% confidence intervals) of complexity (Asfc) and anisotropy (epLsar) on Phase II and Phase I facets (green circles = African colobines, green diamonds = Asian colobines, squares = cercopithecines, triangles = papionins. *Dolichopithecus* fossil sample (red dot) is intermediate between highly folivorous species and more durophagous cercopithecids.

**Figure 7.** Boxplots of complexity (Asfc, left) and anisotropy (epLsar, right) on Phase II and Phase I dental wear facets within the fossil sample of *Dolichopithecus* across fossil localities. Individuals from some localities fall near the extreme limits of the sample range from Perpignan. The horizontal center line marks the median, the lower and upper bounds of the box mark the 25<sup>th</sup> and 75<sup>th</sup> percentiles, whiskers represent the minimum and maximum interquartiles (1.5\*interquartile range), and filled circles represent outliers.



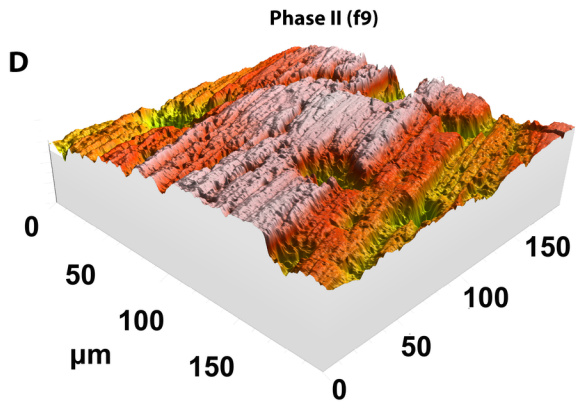
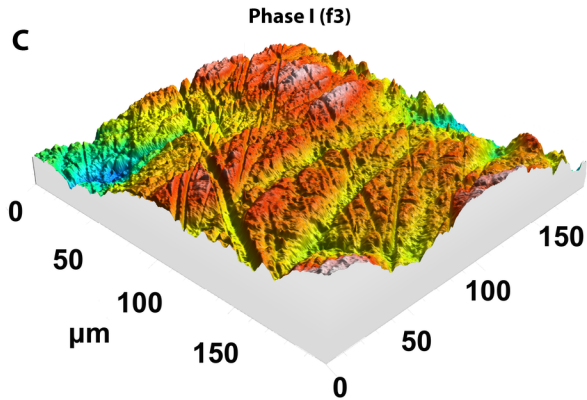
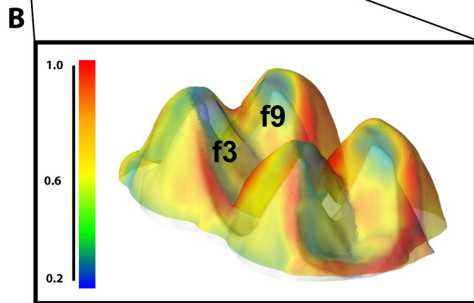
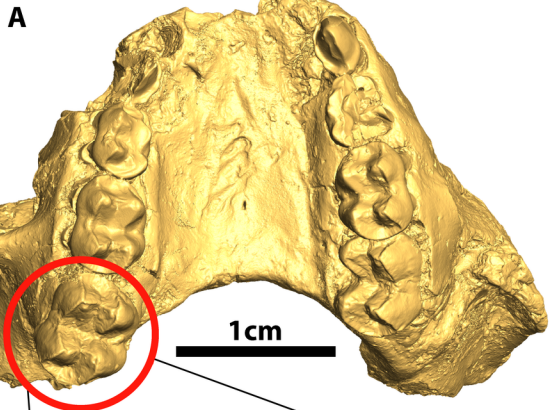


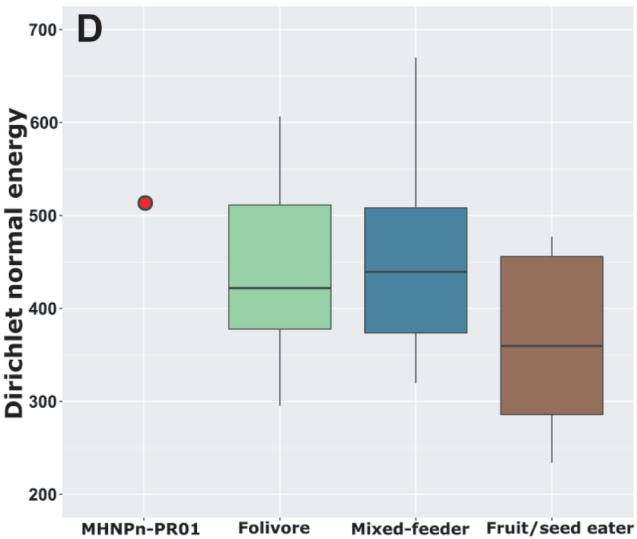
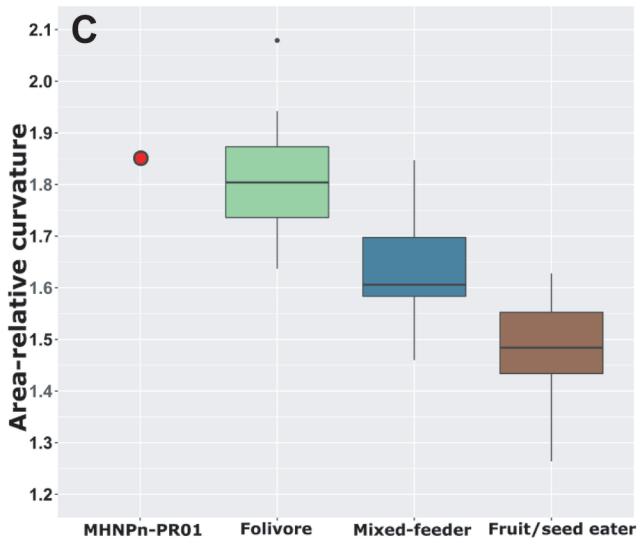
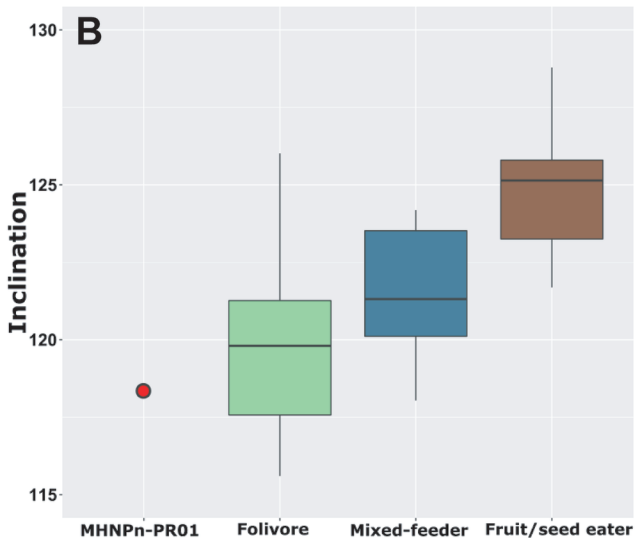
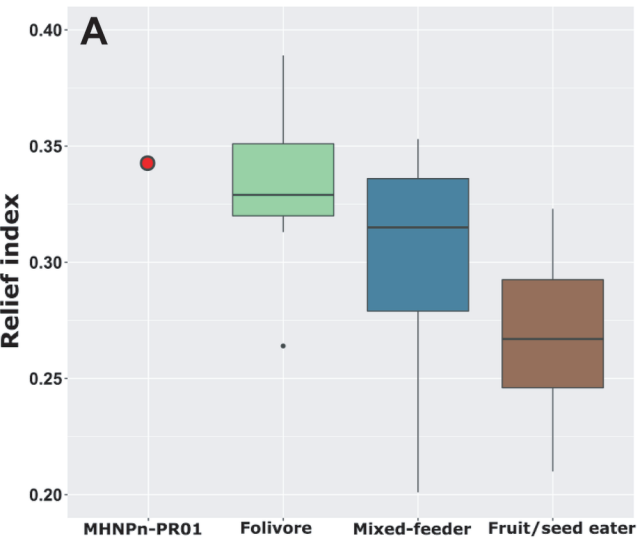
5cm

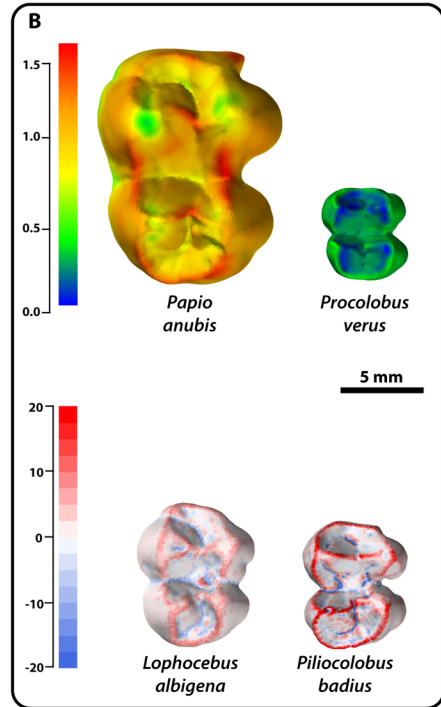
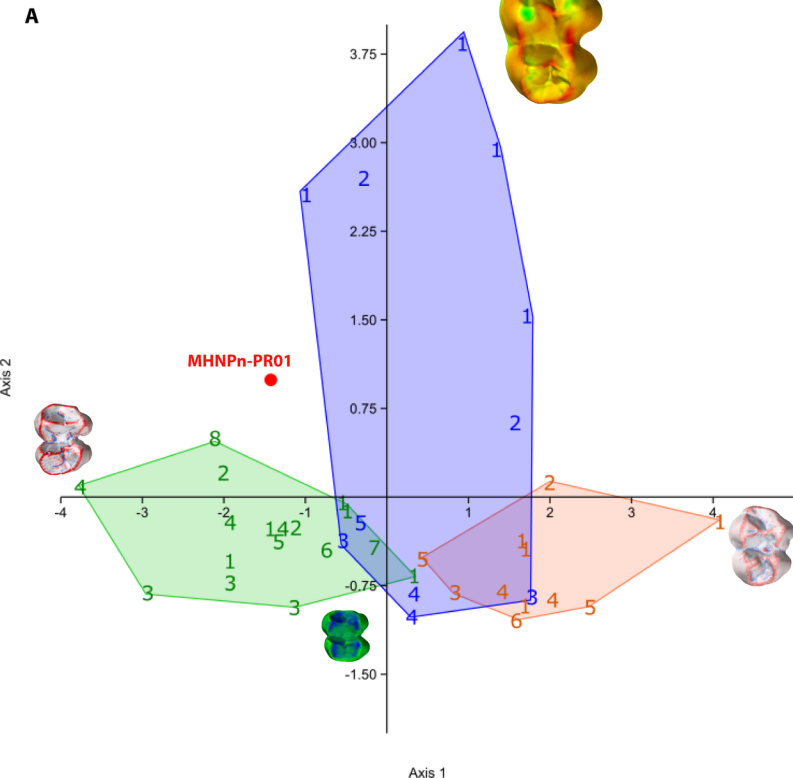


1cm

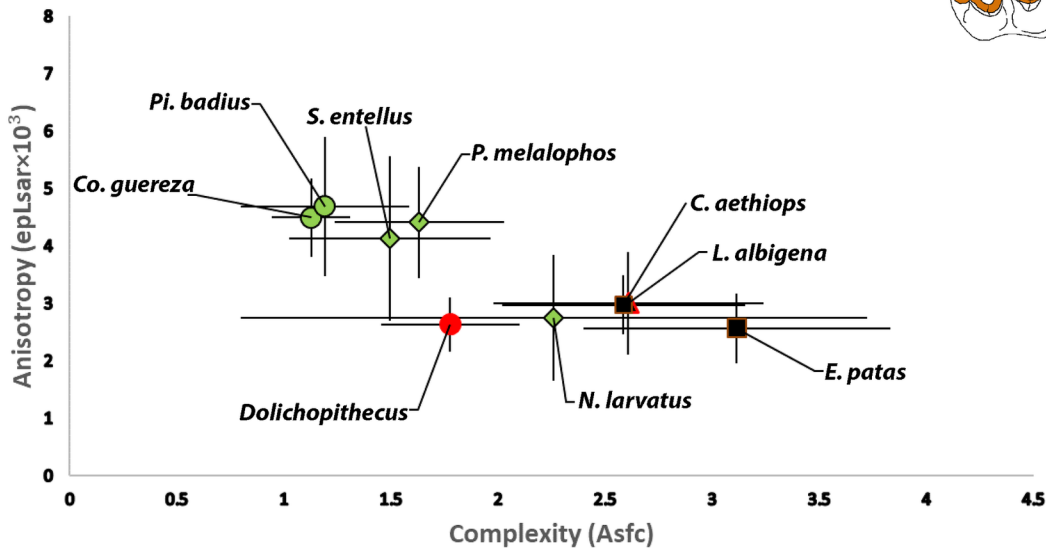




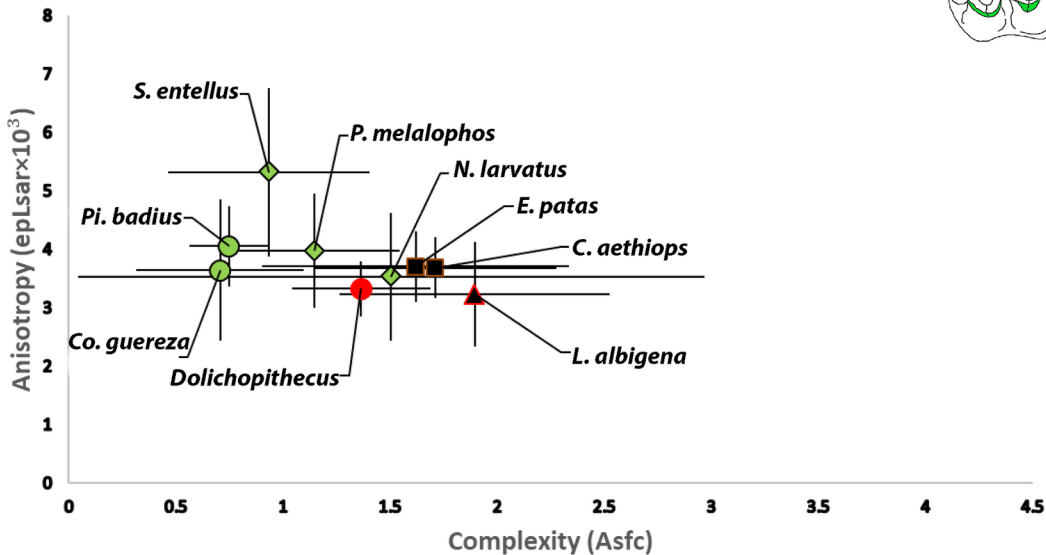




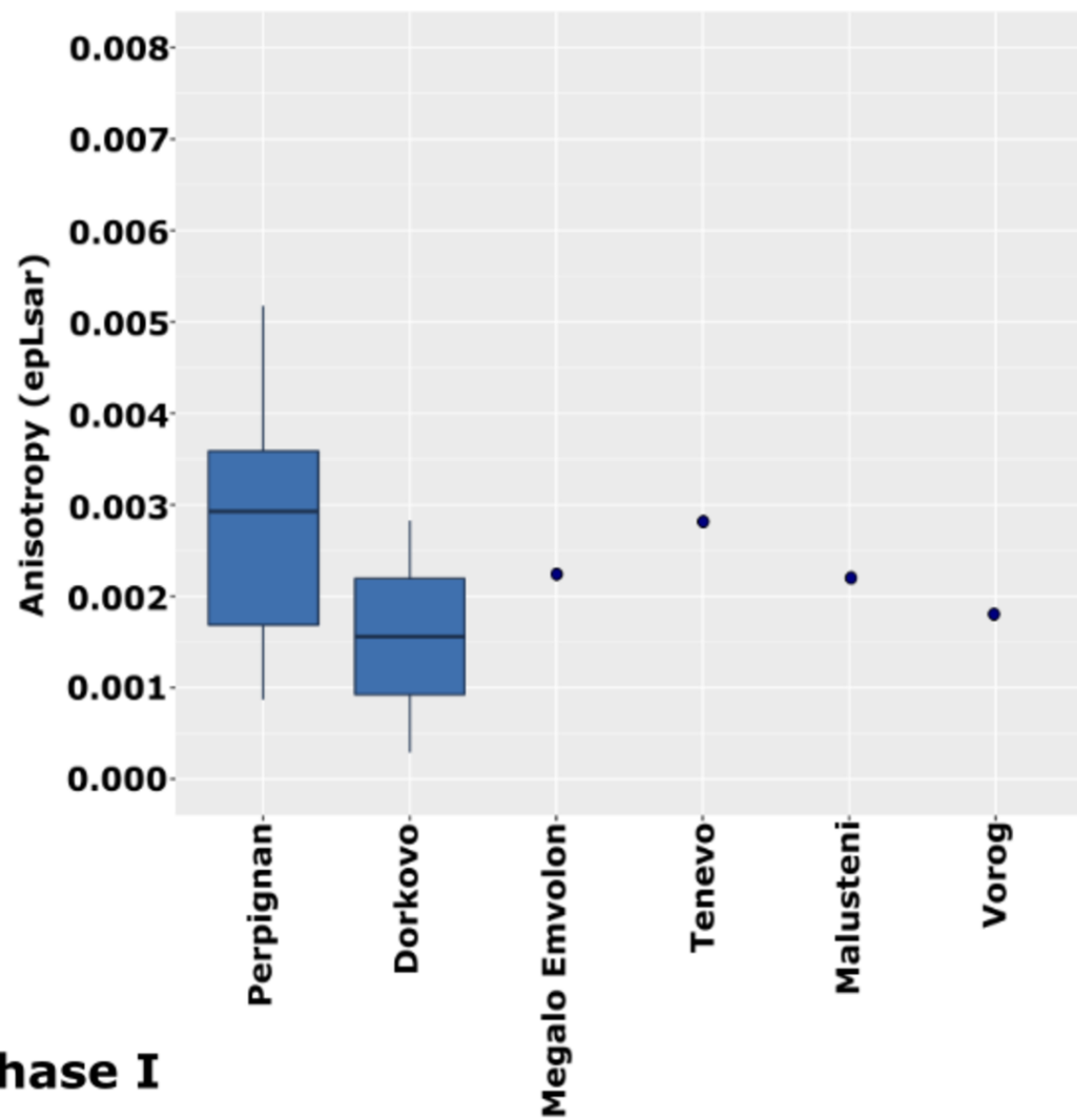
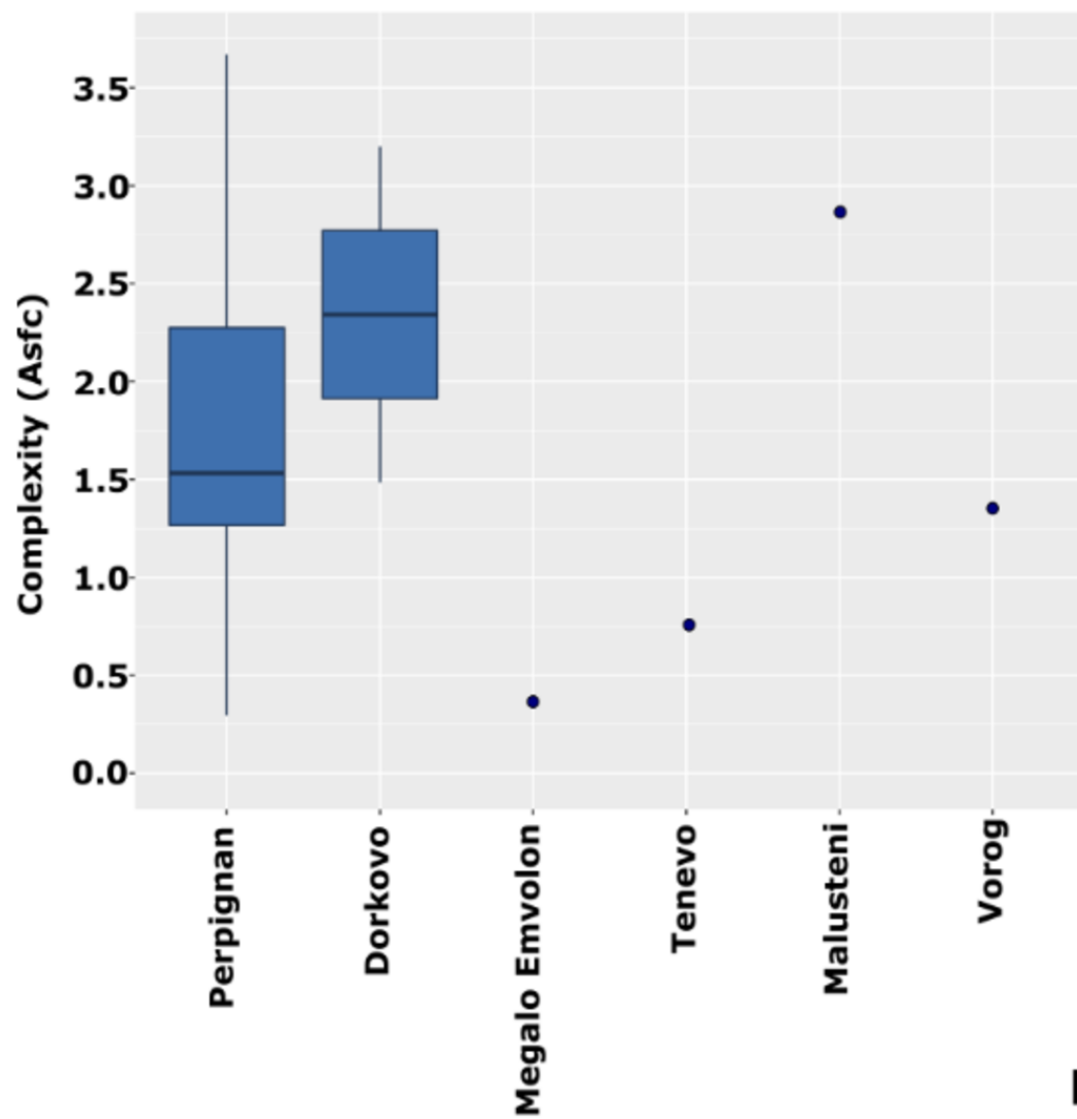
Phase II



Phase I



## Phase II



## Phase I

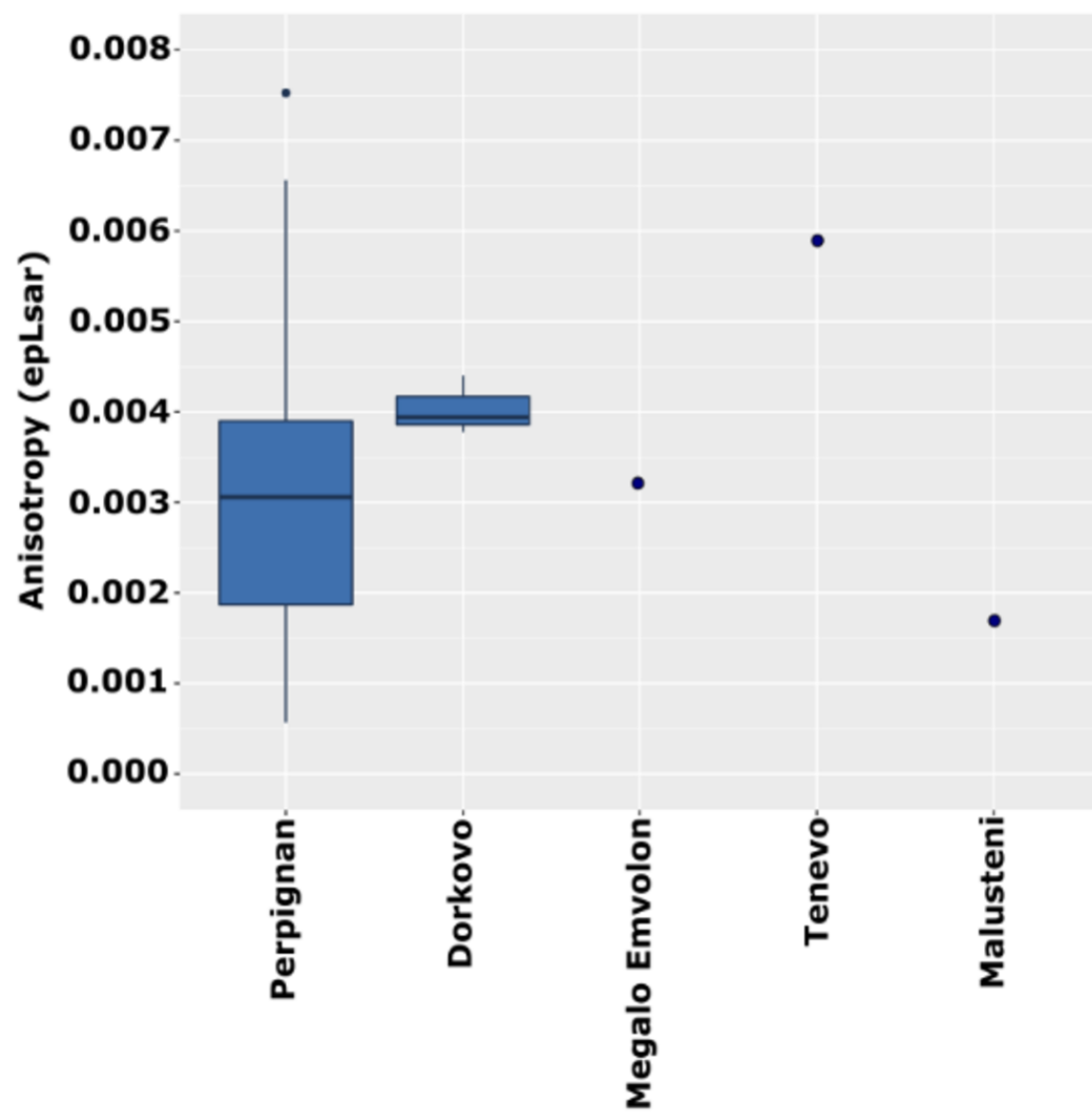
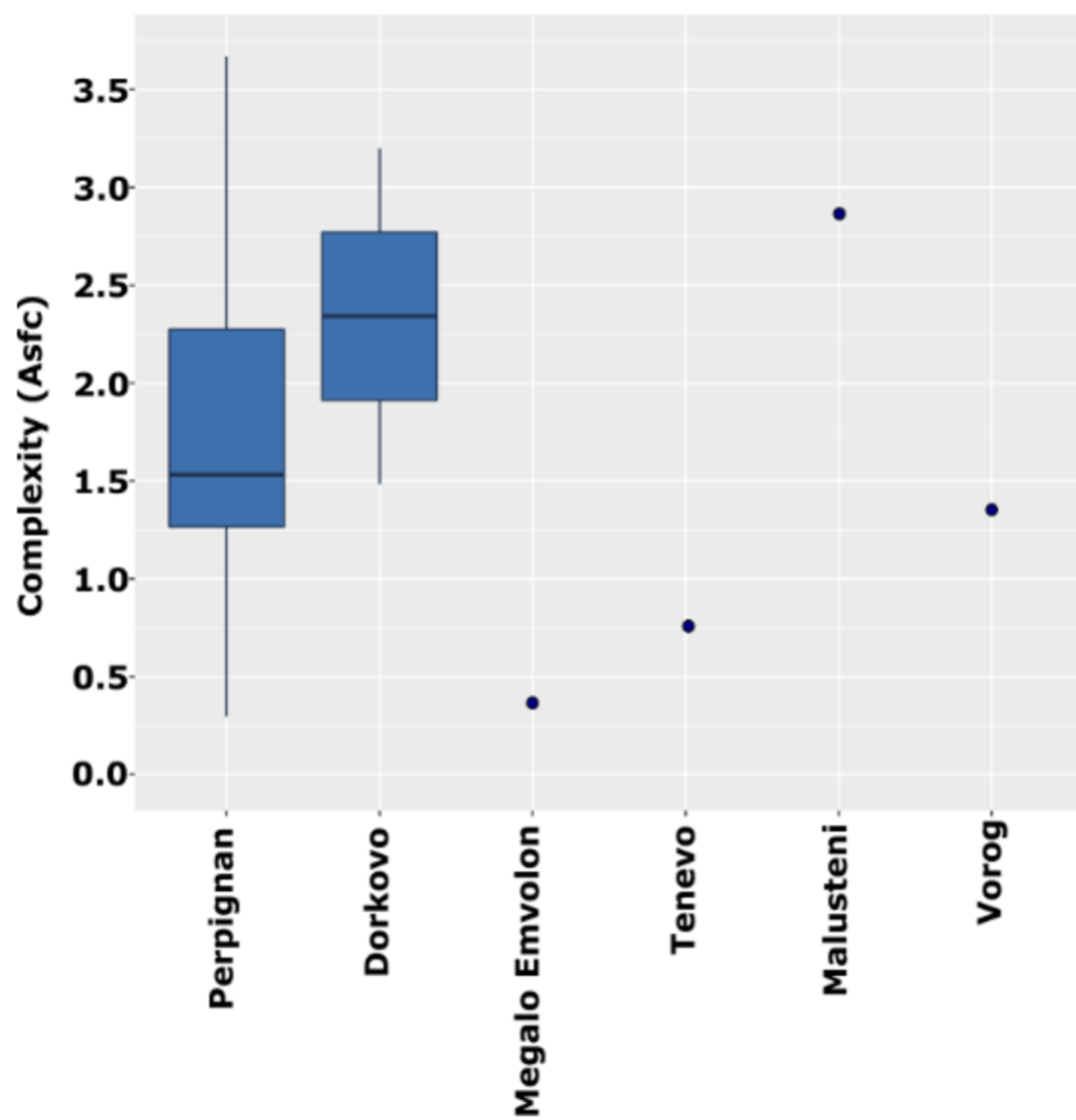


**Table 1**

Enamel thickness, dental topographic, and dental microwear texture variables used in this study.

Estimates	Abbreviation	Analysis	Biological meaning	Computation	References
3D (volumetric) relative enamel thickness	3DRETvol	Enamel thickness	The volume of enamel crown	Ratio between enamel volume and enamel-dentine junction surface, divided by the cubic root of coronal dentine	Kono (2004); Lambert et al. (2004); Olejniczak et al. (2008)
3D (geometric) relative enamel thickness	3DRETgeo	Enamel thickness	The distribution of enamel along the molar crown	Shortest normal distance from occlusal enamel surface to enamel-dentine junction surface	Thiery et al. (2017, 2019)
Absolute crown strength	ACS	Enamel thickness	Linear measure of average thickness of enamel on tooth modeled as a hemisphere	$\sqrt{(AET \cdot (BCD/2))}$ AET: average enamel thickness (mm). BCD: the 'radius' of the tooth's breadth (mm)	Schwartz et al. (2020)
Relief index	LRFI	Dental topography	Relative crown height	The logarithm of the ratio between the square root of the 3D area (OES3D) of the measured surface and the square root of its 2D projection (OES2D)	Boyer (2008)
Inclination		Dental topography		The angle between the vector normal to the polygon's surface in the z-direction and the horizontal xy plane	Guy et al. (2013, 2015)
Orientation patch-count rotated	OPCR	Dental topography	Complexity; number of dental tools on occlusal surface	Average orientation patch-count over eight orientations of 45°	Evans and Jernvall (2009)
Dirichlet normal energy	DNE	Dental topography	Tooth curviness or sharpness	Variability in surface curvature	Bunn et al. (2011)
Area-relative curvature	ARC	Dental topography	Tooth curviness or sharpness	Normalized version of mean curvature	Guy et al. (2013, 2017); Thiery et al. (2021)
Complexity	Asfc	DMTA <sup>a</sup>	Surface roughness	see Scott et al. (2006)	Ungar and Teaford (1996); Scott et al. (2005, 2012); Ungar et al. (2008, 2012); Merceron et al. (2009a, b); Williams and Holmes (2011, 2012); Engle et al. (2014); Shapiro et al. (2016); Percher et al. (2017, 2018); Ragni et al. (2017)
Anisotropy	epLsar	DMTA	Orientation/direction of surface roughness	See Scott et al. (2006)	
Scale of maximal complexity	Smc	DMTA		see Scott et al. (2006)	
Heterogeneity of complexity	Hasfc <sub>9,36,81</sub>	DMTA	Variation of surface roughness across tooth surface	see Scott et al. (2006)	
Textural fill volume	Tfv	DMTA	The total fill volume of a microwear surface	see Scott et al. (2006)	

<sup>a</sup> DMTA = Dental microwear texture analysis.

**Table 2**Phylogenetic generalized least squares correlations between enamel thickness and dental topographic variables.<sup>a</sup>

Variables	Pagel's $\lambda$			Slope		Std. error	t-value	AIC	logL	BIC	Multiple $r^2$	Adjusted $r^2$
	Value	Bounds	$p$ -value	Value	$p$ -value							
RETgeo-Inclination	0.000	1.000	<b>0.008</b>	7.490	<b>&lt;0.001</b>	1.371	5.460	-19.900	11.950	-17.909	0.623	0.602
		0.000	1.000									
RETvol-Inclination	0.000	1.000	1.000	6.829	<b>&lt;0.001</b>	1.399	4.878	-19.093	11.546	-17.101	0.569	0.545
		0.000	<b>0.001</b>									
LRFI-Inclination	0.391	1.000	1.000	-5.271	<b>&lt;0.001</b>	0.268	-19.64	-92.688	48.344	-90.697	0.955	0.952
		0.000	0.590									
ARC-Inclination	0.499	1.000	<b>0.005</b>	-2.568	<b>&lt;0.001</b>	0.647	-3.967	-58.445	31.222	-56.453	0.466	0.436
		0.000	0.362									
OES 2D-ACS	1.000	1.000	1.000	1.981	<b>&lt;0.001</b>	0.167	11.856	-15.104	9.552	-13.113	0.886	0.880
		0.000	<b>&lt;0.001</b>									
OES 2D-OPCR	0.000	1.000	<b>&lt;0.001</b>	1.945	<b>&lt;0.001</b>	0.375	5.185	14.152	-5.076	16.143	0.599	0.576
		0.000	1.000									
OES 2D-DNE	0.083	1.000	<b>0.008</b>	1.772	<b>0.001</b>	0.463	3.825	20.093	-8.046	22.084	0.448	0.417

		0.000	0.796									
OES 2D-RETvol	1.000	1.000	1.000	-1.408	<0.001	0.473	-2.977	20.399	-8.199	22.391	0.330	0.292
		0.000	<0.001									
RETgeo-LRFI	0.000	1.000	0.007	-1.388	<0.001	0.244	-5.67	-20.856	12.428	-18.865	0.641	0.621
		0.000	1.000									
OES 2D-RETgeo	0.992	1.000	0.853	-1.126	0.068	0.580	-1.940	24.478	-10.239	26.469	0.551	0.526
		0.000	0.004									
RETvol-LRFI	0.000	1.000	0.003	-1.228	<0.001	0.261	-4.701	-18.264	11.132	-16.273	0.878	0.871
		0.000	1.000									
RETvol-RETgeo	0.950	1.000	0.503	1.036	<0.001	0.090	11.416	-49.848	26.924	-47.857	0.794	0.782
		0.000	0.146									
DNE-OPCR	0.127	1.000	0.023	0.846	<0.001	0.101	8.334	-38.742	21.371	-36.70	0.455	0.421
		0.000	0.661									
OPCR-ACS	0.102	1.000	<0.001	0.525	0.001	0.135	3.879	-17.084	10.542	-15.092	0.469	0.439
		0.000	0.722									
ARC-LRFI	0.611	1.000	0.004	0.490	<0.001	0.122	3.989	-58.800	31.400	-56.809	0.219	0.175
		0.000	0.150									

RETvol-ACS	1.000	1.000	1.000	-0.401	<b>0.037</b>	0.178	-2.248	-12.415	8.207	-10.423	0.217	0.174
		0.000	<b>0.001</b>									
DNE-ACS	0.493	1.000	<b>0.001</b>	0.366	<b>0.038</b>	0.163	2.237	-13.135	8.567	-11.144	0.529	0.503
		0.000	0.257									
ARC-RETgeo	0.161	1.000	<b>&lt;0.001</b>	-0.281	<b>&lt;0.001</b>	0.062	-4.501	-57.963	30.981	-55.971	0.265	0.224
		0.000	0.736									
LRFI-DNE	1.000	1.000	1.000	0.239	<b>&lt;0.001</b>	0.093	2.551	-39.511	21.755	-37.520	0.340	0.303
		0.000	<b>&lt;0.001</b>									
ARC-RETvol	0.376	1.000	<b>&lt;0.001</b>	-0.221	<b>0.006</b>	0.072	-3.046	-53.555	28.777	-51.563	0.302	0.263
		0.000	0.315									
ARC-DNE	0.796	1.000	0.077	0.216	<b>0.011</b>	0.077	2.794	-52.946	28.473	-50.955	0.172	0.127
		0.000	<b>0.001</b>									
OES 2D-Inclination	0.948	1.000	0.401	-5.346	0.356	5.653	-0.945	27.358	-11.679	29.350	0.047	-0.005
		0.000	<b>0.024</b>									
DNE-Inclination	0.706	1.000	0.052	-4.173	0.063	2.112	-1.975	-12.401	8.200	-10.410	0.178	0.132
		0.000	0.075									

OPCR-Inclination	0.663	1.000	<b>0.025</b>	-1.833	0.455	2.402	-0.763	-7.064	5.532	-5.072	0.031	-0.022
		0.000	0.113									
OES 2D-ARC	0.938	1.000	0.490	0.905	0.525	1.399	0.646	27.934	-11.967	29.925	0.022	-0.031
		0.000	<b>0.036</b>									
OES 2D-LRFI	0.961	1.000	0.488	0.779	0.493	1.115	0.698	27.723	-11.816	29.715	0.026	-0.027
		0.000	<b>0.032</b>									
ACS-Inclination	0.963	1.000	0.506	-0.734	0.789	2.704	-0.271	-1.798	2.899	0.193	0.004	-0.051
		0.000	<b>0.012</b>									
RETvol-DNE	0.685	1.000	0.174	-0.321	0.180	0.230	-1.395	-9.351	6.675	-7.359	0.097	0.047
		0.000	<b>0.021</b>									
RETvol-OPCR	0.719	1.000	0.232	-0.268	0.241	0.221	-1.211	-8.909	6.454	-6.917	0.075	0.023
		0.000	<b>0.013</b>									
RETgeo-ACS	0.980	1.000	0.753	-0.222	0.221	0.175	-1.264	-13.388	8.694	-11.396	0.081	0.030
		0.000	<b>&lt;0.001</b>									
RETgeo-DNE	0.899	1.000	0.391	-0.163	0.447	0.210	-0.776	-12.193	8.096	-10.201	0.032	-0.021

		0.000	<b>&lt;0.001</b>									
ARC-OPCR	0.868	1.000	0.476	1.164	0.054	0.565	2.058	-9.995	6.997	-8.004	0.190	0.145
		0.000	<b>0.039</b>									
RETgeo-OPCR	0.925	1.000	0.447	-0.121	0.545	0.197	-0.615	-12.053	8.026	-10.061	0.020	-0.033
		0.000	<b>&lt;0.001</b>									
LRFI-OPCR	0.934	1.000	0.491	0.100	0.369	0.109	0.919	-35.538	19.769	-33.547	0.044	-0.008
		0.000	<b>&lt;0.001</b>									
ARC-ACS	0.676	1.000	<b>0.002</b>	0.042	0.569	0.073	0.579	-46.503	25.251	-44.512	0.018	-0.036
		0.000	<b>0.007</b>									
LRFI-ACS	0.916	1.000	0.255	0.003	0.977	0.102	0.029	-34.644	19.322	-32.652	0.0000476	-0.055
		0.000	<b>0.003</b>									

<sup>a</sup> Pagel's  $\lambda$  = is a measure of phylogenetic signal, with 1 representing a perfect fit between data and a Brownian motion model of change in values through evolution, and 0 representing no phylogenetic structuring; slope = an estimate that relates the two variables being regressed, values above 1.0 indicate that assumptions of Brownian motion are incorrect; std. error = standard error; t-value = the size of the difference relative to the variation in the sampled data (it can be either positive or negative), a t-value of 0 indicates that the sample results cannot reject the null hypothesis, the greater the magnitude of the t-value, the greater the evidence against the null hypothesis; AIC = Akaike information criterion; LogL = Log likelihood; BIC = Bayesian information criterion;  $r^2$  = Determination coefficient (higher values of  $r^2$  indicate stronger correlation, i.e., less dispersion of values).

<sup>b</sup> Pairs of variables that are significantly correlated are in bold ( $\alpha = 0.05$ ).

**Table 3**

Results of Kruskal-Wallis tests of enamel thickness and dental topographic variables among the three dietary categories.

<b>Variables</b>	<b>df</b>	<b><math>\chi^2</math></b>	<b><i>p</i>-value</b>
3DRETvol	2	21.887	<b>&lt;0.001</b>
3DRETgeo	2	24.879	<b>&lt;0.001</b>
ACS	2	4.978	0.082
LRFI	2	16.606	<b>&lt;0.001</b>
Inclination	2	17.634	<b>&lt;0.001</b>
OPCR	2	4.629	0.098
DNE	2	4.372	0.112
ARC	2	26.377	<b>&lt;0.001</b>

Abbreviations: df = degrees of freedom; 3DRETvol = 3D volumetric relative enamel thickness; 3DRETgeo = 3D geometric relative enamel thickness; ACS = absolute crown strength; LRFI = relief index; OPCR = orientation patch-count rotated; DNE = Dirichlet normal energy; ARC = area-relative curvature.

**Table 4**

Dunn's post-hoc tests of enamel thickness and dental topographic variables between the dietary categories proposed.

Variables	Comparisons between dietary categories		p-value	
			Significance <sup>a</sup>	Adjusted significance <sup>b</sup>
3DRETvol	Folivores	Fruit/seed eaters	<0.001	<0.001
	Fruit/seed eaters	Mixed feeders	0.008	0.024
3DRETgeo	Folivores	Fruit/seed eaters	<0.001	<0.001
	Folivores	Mixed feeders	0.005	0.015
LRFI	Folivores	Fruit/seed eaters	<0.001	<0.001
	Fruit/seed eaters	Mixed feeders	0.046	0.139
Inclination	Folivores	Fruit/seed eaters	<0.001	<0.001
	Folivores	Mixed feeders	0.050	0.150
	Fruit/seed eaters	Mixed feeders	0.043	0.130
ARC	Folivores	Fruit/seed eaters	<0.001	<0.001
	Folivores	Mixed feeders	0.004	0.013
	Fruit/seed eaters	Mixed feeders	0.045	0.136

Abbreviations: 3DRETvol = 3D volumetric relative enamel thickness; 3DRETgeo = 3D geometric relative enamel thickness; LRFI = relief index; ARC = area-relative curvature.

<sup>a</sup> Asymptotic significance (2-sided tests) are displayed with significance level set at 0.05.

<sup>b</sup> Significance values have been adjusted by the Bonferroni correction for multiple tests.

**Table 5**

Results of post-hoc pairwise comparisons of enamel thickness and dental topographic variables between the dietary categories proposed. Differences highlighted with Bonferroni adjustment are shown in bold.<sup>a</sup>

<b>Diet groups</b>	Fruit/seed eaters	Folivores	Mixed feeders
Fruit/seed eaters		<b>3DRETvol(-), 3DRETgeo(-), Inclination(-), LRFI(+), ARC(+)</b>	<b>3DRETvol(-), 3DRETgeo(-), LRFI(+), Inclination(-), ARC(+)</b>
Folivores	<b>3DRETvol(+), 3DRETgeo(+), Inclination(+), LRFI(-), ARC(-)</b>		<b>3DRETgeo(+), LRFI(-), Inclination(-), ARC(-)</b>
Mixed feeders	<b>3DRETvol(+), 3DRETgeo(+), LRFI(-), Inclination(+), ARC(-)</b>		

Abbreviations: 3DRETvol = 3D volumetric relative enamel thickness; 3DRETgeo = 3D geometric relative enamel thickness; LRFI = relief index; ARC = area-relative curvature.

<sup>a</sup> (-) and (+) indicate values that are either significantly lower or higher, respectively, for species in column compared to the one in the row.

**Table 6**

Combination of enamel thickness and topographic variables with probabilities of successful classification for linear discriminant analyses (LDAs) with classic dietary categories (mixed feeders, folivores, fruit/seed eaters) as factors. Best set of variables and their success rate indicated in bold.

Variables			(% Variance explained)		(% Correctly classified)	
			Axis 1	Axis 2	Normal	Resampling
3DRETvol	DNE	OES 3D	74.44	24.44	72.5	67.5
3DRETvol	OPCR	OES 3D	74.70	25.22	70.0	65.0
3DRETgeo	ACS	OES 3D	80.87	19.04	70.0	62.5
3DRETgeo	OPCR	OES 3D	81.77	18.09	77.5	62.5
LRFI	ACS	OES 3D	63.55	35.32	67.5	60.0.
LRFI	OPCR	OES 3D	63.57	35.79	67.5	62.5
DNE	Inclination	OES 3D	62.35	37.51	70.0	60.0
Inclination	OPCR	OES 3D	61.42	37.72	67.5	62.5
Inclination	ACS	OES 3D	62.35	34.84	72.5	65.0
ARC	OPCR	OES 3D	80.88	18.6	77.5	70.0
ARC	ACS	OES 3D	80.29	18.79	<b>77.5</b>	<b>72.5</b>

Abbreviations: 3DRETvol = 3D volumetric relative enamel thickness; 3DRETgeo = 3D geometric relative enamel thickness; ACS = absolute crown strength; LRFI = relief index; ARC = area-relative curvature; DNE = Dirichlet normal energy; OPCR = orientation patch-count rotated; OES 3D = 3D occlusal enamel surface.

**Table 7**Descriptive statistics for microwear texture variables on phase I and phase II facets of *Dolichopithecus* and the modern sample.

Taxa	<i>n</i>	Phase I							<i>n</i>	Phase II							
		Asfc	epLsar (x10 <sup>3</sup> )	Smc	Tfv	Hasfc <sub>9</sub>	Hasfc <sub>36</sub>	Hasfc <sub>81</sub>		Asfc	epLsar (x10 <sup>3</sup> )	Smc	Tfv	Hasfc <sub>9</sub>	Hasfc <sub>36</sub>	Hasfc <sub>81</sub>	
<i>Dolichopithecus</i>	Mean	25	1.36	3.32	68.04	35528.40	0.351	0.473	0.616	27	1.777	2.638	74.516	37661.75	0.305	0.418	0.557
	sd		0.859	1.735	54.637	11478.50	0.347	0.401	0.618		0.855	1.247	62.127	14167.91	0.175	0.166	0.226
	sem		0.172	0.347	10.927	2295.70	0.069	0.080	0.124		0.164	0.240	11.956	2726.61	0.034	0.032	0.043
<i>Nasalis larvatus</i>	Mean	7	1.505	3.531	0.346	25575.18	0.351	0.526	0.758	7	2.260	2.744	0.277	36665.23	0.308	0.450	0.563
	sd		1.551	1.797	0.196	10141.31	0.221	0.300	0.598		1.972	1.479	0.144	15936.64	0.178	0.220	0.239
	sem		0.586	0.679	0.074	3833.05	0.083	0.113	0.226		0.745	0.559	0.054	6023.48	0.067	0.083	0.090
<i>Semnopithecus entellus</i>	Mean	8	0.934	5.319	1.266	36114.45	0.390	0.580	0.743	8	1.497	4.131	22.733	34105.96	0.530	0.621	0.751
	sd		0.711	2.392	2.175	8126.46	0.195	0.254	0.374		0.679	2.076	38.339	12535.85	0.442	0.292	0.298
	sem		0.251	0.846	0.769	2873.13	0.069	0.090	0.132		0.240	0.734	13.555	4432.09	0.156	0.103	0.105
<i>Presbytis melalophos</i>	Mean	17	1.149	3.974	0.604	25434.82	0.280	0.406	0.538	19	1.632	4.411	21.362	35671.93	0.354	0.517	0.626
	sd		0.670	1.248	0.465	19868.65	0.151	0.198	0.253		0.832	2.048	86.470	16422.18	0.225	0.337	0.366
	sem		0.163	0.303	0.113	4818.85	0.037	0.048	0.061		0.202	0.497	20.972	3982.96	0.055	0.082	0.089
<i>Colobus guereza</i>	Mean	21	0.749	4.053	31.277	29588.78	0.268	0.391	0.506	25	1.128	4.495	0.370	30196.70	0.298	0.415	0.561
	sd		0.369	2.387	138.871	10703.93	0.164	0.174	0.213		0.467	1.755	0.154	9873.72	0.148	0.134	0.164
	sem		0.081	0.521	30.304	2335.79	0.036	0.038	0.047		0.093	0.351	0.031	1974.74	0.030	0.027	0.033
<i>Ptilocolobus</i>	Mean	12	0.706	3.639	0.674	34306.51	0.374	0.512	0.597	17	1.191	4.690	60.011	37329.29	0.349	0.479	0.589

<i>badius</i>																	
	sd		0.614	2.207	1.630	13649.04	0.321	0.362	0.380		0.825	2.540	170.449	17626.00	0.192	0.216	0.252
	sem		0.177	0.637	0.470	3940.13	0.093	0.105	0.110		0.200	0.616	41.340	4274.93	0.047	0.052	0.061
<i>Erythrocebus patas</i>																	
	Mean	13	1.619	3.703	29.923	41234.20	0.307	0.484	0.580	16	3.116	2.565	0.397	41359.01	0.370	0.511	0.629
	sd		0.885	2.510	102.391	7138.79	0.136	0.261	0.263		1.466	1.237	0.228	9775.96	0.172	0.213	0.216
	sem		0.245	0.696	28.398	1979.94	0.038	0.072	0.073		0.366	0.309	0.057	2443.99	0.043	0.053	0.054
<i>Chlorocebus aethiops</i>																	
	Mean	37	1.710	3.682	0.266	34543.57	0.374	0.510	0.674	37	2.586	2.975	10.359	35382.82	0.320	0.477	0.643
	sd		1.525	1.891	0.159	9862.58	0.443	0.499	0.611		1.764	1.615	60.013	14750.39	0.328	0.455	0.716
	sem		0.251	0.311	0.026	1621.44	0.073	0.082	0.100		0.290	0.265	9.866	2424.94	0.054	0.075	0.118
<i>Lophocebus albigena</i>																	
	Mean	15	1.895	3.229	3.558	36235.56	0.319	0.507	0.659	15	2.608	3.011	25.450	45004.68	0.400	0.586	0.719
	sd		1.046	1.366	8.045	13290.69	0.124	0.175	0.255		1.246	1.763	92.205	10906.67	0.184	0.194	0.262
	sem		0.270	0.353	2.077	3431.64	0.032	0.045	0.066		0.322	0.455	23.807	2816.09	0.047	0.050	0.068

Abbreviations: sd = standard deviation; sem = standard error of the mean; Asfc = area scale fractal complexity; epLsar = exact proportion length-scale anisotropy of relief; Smc = scale of maximal complexity; Tfv = textural fill volume; Hasfc<sub>9,36,81</sub> = heterogeneity of area-scale fractal complexity on 9, 36, and 81 cell.

**Table 8**

Results of Kruskal-Wallis tests among the eight extant species (*Co. guereza*, *Pi. badius*, *S. entellus*, *N. larvatus*, *P. melalophos*, *Ch. aethiops*, *L. albigena*, *E. patas*) and *Dolichopithecus* on both phase II and phase I facets with species as factor.

<b>Facets</b>	<b>Variable</b>	<b>df</b>	<b><math>\chi^2</math></b>	<b>p-value</b>
Phase II	Asfc	8	47.147	<b>&lt;0.001</b>
	Smc	8	51.484	<b>&lt;0.001</b>
	epLsar	8	30.880	<b>&lt;0.001</b>
	Tfv	8	15.032	0.058
	Hasfc <sub>9</sub>	8	13.377	0.099
	Hasfc <sub>36</sub>	8	15.675	<b>0.047</b>
	Hasfc <sub>81</sub>	8	12.307	0.138
Phase I	Asfc	8	30.154	<b>&lt;0.001</b>
	Smc	8	67.587	<b>&lt;0.001</b>
	epLsar	8	6.522	0.589
	Tfv	8	16.761	<b>0.032</b>
	Hasfc <sub>9</sub>	8	5.245	0.731
	Hasfc <sub>36</sub>	8	9.175	0.327
	Hasfc <sub>81</sub>	8	8.519	0.384

Abbreviations: df = degrees of freedom; Asfc = area-scale fractal complexity; epLsar = exact proportion length-scale anisotropy of relief; Smc = scale of maximal complexity; Tfv = textural fill volume; Hasfc<sub>9,36,81</sub> = heterogeneity of area-scale fractal complexity on 9, 36 and 81 cells.

**Table 9**

Dunn's post-hoc tests among the eight extant species (*Co. guereza*, *Pi. badius*, *S. entellus*, *N. larvatus*, *P. melalophos*, *Ch. aethiops*, *L. albigena*, *E. patas*) and *Dolichopithecus* on both phase II and phase I facets.

			<b>p-value</b>	
<b>Phase II</b>			<b>Significance<sup>a</sup></b>	<b>Adjusted significance<sup>b</sup></b>
Asfc	<i>Dolichopithecus</i>	<i>Co. guereza</i>	0.010	0.371
	<i>Co. guereza</i>	<i>Ch. aethiops</i>	<0.001	<0.001
	<i>Co. guereza</i>	<i>L. albigena</i>	<0.001	<0.001
	<i>Co. guereza</i>	<i>E. patas</i>	<0.001	<0.001
	<i>Dolichopithecus</i>	<i>Pi. badius</i>	<0.001	1.000
	<i>Pi. badius</i>	<i>Ch. aethiops</i>	<0.001	0.005
	<i>Pi. badius</i>	<i>L. albigena</i>	<0.001	0.004
	<i>Pi. badius</i>	<i>E. patas</i>	<0.001	0.001
	<i>L. albigena</i>	<i>S. entellus</i>	0.025	0.917
	<i>L. albigena</i>	<i>P. melalophos</i>	0.014	0.513
	<i>P. melalophos</i>	<i>Ch. aethiops</i>	0.038	1.000
	<i>P. melalophos</i>	<i>E. patas</i>	0.040	0.152
	<i>N. larvatus</i>	<i>E. patas</i>	0.050	1.000
	<i>Dolichopithecus</i>	<i>L. albigena</i>	0.028	0.992
	<i>Dolichopithecus</i>	<i>E. patas</i>	0.008	0.295
Smc	<i>L. albigena</i>	<i>N. larvatus</i>	0.020	0.724
	<i>P. melalophos</i>	<i>N. larvatus</i>	0.007	0.237
	<i>S. entellus</i>	<i>N. larvatus</i>	0.009	0.331
	<i>Dolichopithecus</i>	<i>N. larvatus</i>	<0.001	0.001
	<i>L. albigena</i>	<i>Ch. aethiops</i>	0.015	0.541
	<i>P. melalophos</i>	<i>Ch. aethiops</i>	0.002	0.064
	<i>S. entellus</i>	<i>Ch. aethiops</i>	0.008	0.300
	<i>Dolichopithecus</i>	<i>Ch. aethiops</i>	<0.001	<0.001
	<i>L. albigena</i>	<i>Co. guereza</i>	0.039	1.000
	<i>P. melalophos</i>	<i>Co. guereza</i>	0.008	0.274
	<i>S. entellus</i>	<i>Co. guereza</i>	0.018	0.656
	<i>Dolichopithecus</i>	<i>Co. guereza</i>	<0.001	<0.001
	<i>P. melalophos</i>	<i>E. patas</i>	0.022	0.786
	<i>S. entellus</i>	<i>E. patas</i>	0.033	1.000
	<i>Dolichopithecus</i>	<i>E. patas</i>	<0.001	0.001
<i>Dolichopithecus</i>	<i>Pi. badius</i>	0.001	0.051	
<i>Dolichopithecus</i>	<i>L. albigena</i>	0.028	1.000	

epLsar	<i>E. patas</i>	<i>S. entellus</i>	0.039	1.000	
	<i>E. patas</i>	<i>Pi. badius</i>	0.007	0.241	
	<i>E. patas</i>	<i>P. melalophos</i>	0.004	0.127	
	<i>E. patas</i>	<i>Co. guereza</i>	<0.001	0.014	
	<i>Dolichopithecus</i>	<i>S. entellus</i>	0.049	1.000	
	<i>Dolichopithecus</i>	<i>Pi. badius</i>	0.006	0.231	
	<i>Dolichopithecus</i>	<i>P. melalophos</i>	0.003	0.108	
	<i>Dolichopithecus</i>	<i>Co. guereza</i>	<0.001	0.007	
	<i>N. larvatus</i>	<i>Co. guereza</i>	0.027	0.988	
	<i>L. albigena</i>	<i>P. melalophos</i>	0.033	1.000	
	<i>L. albigena</i>	<i>Co. guereza</i>	0.007	0.249	
	<i>Ch. aethiops</i>	<i>Pi. badius</i>	0.023	0.823	
	<i>Ch. aethiops</i>	<i>P. melalophos</i>	0.012	0.421	
	<i>Ch. aethiops</i>	<i>Co. guereza</i>	0.001	0.034	
	Hasfc <sub>36</sub>	<i>L. albigena</i>	<i>Ch. aethiops</i>	0.002	0.076
		<i>S. entellus</i>	<i>Ch. aethiops</i>	0.014	0.488
<i>Dolichopithecus</i>		<i>L. albigena</i>	0.011	0.401	
<i>Dolichopithecus</i>		<i>S. entellus</i>	0.037	1.000	
<i>L. albigena</i>		<i>Co. guereza</i>	0.018	0.665	
<b>Phase I</b>					
Asfc	<i>Pi. badius</i>	<i>P. melalophos</i>	0.043	1.000	
	<i>Pi. badius</i>	<i>Dolichopithecus</i>	0.007	0.239	
	<i>Pi. badius</i>	<i>Ch. aethiops</i>	0.002	0.060	
	<i>Pi. badius</i>	<i>E. patas</i>	0.001	0.031	
	<i>Pi. badius</i>	<i>L. albigena</i>	<0.001	0.004	
	<i>Co. guereza</i>	<i>Dolichopithecus</i>	0.012	0.449	
	<i>Co. guereza</i>	<i>Ch. aethiops</i>	0.002	0.086	
	<i>Co. guereza</i>	<i>E. patas</i>	0.002	0.055	
	<i>Co. guereza</i>	<i>L. albigena</i>	<0.001	0.006	
	<i>S. entellus</i>	<i>E. patas</i>	0.027	0.970	
	<i>S. entellus</i>	<i>L. albigena</i>	0.009	0.316	
	<i>P. melalophos</i>	<i>L. albigena</i>	0.041	1.000	
	Smc	<i>Pi. badius</i>	<i>E. patas</i>	0.050	1.000
<i>Pi. badius</i>		<i>P. melaophos</i>	0.025	0.906	
<i>Pi. badius</i>		<i>S. entellus</i>	0.024	0.859	
<i>Pi. badius</i>		<i>L. albigena</i>	0.003	0.118	
<i>Pi. badius</i>		<i>Dolichopithecus</i>	<0.001	<0.001	
<i>Co. guereza</i>		<i>P. melaophos</i>	0.049	1.000	
<i>Co. guereza</i>		<i>S. entellus</i>	0.046	1.000	
<i>Co. guereza</i>		<i>L. albigena</i>	0.006	0.203	

	<i>Co. guereza</i>	<i>Dolichopithecus</i>	<0.001	<0.001
	<i>Ch. aethiops</i>	<i>P. melaophos</i>	0.033	1.000
	<i>Ch. aethiops</i>	<i>S. entellus</i>	0.037	1.000
	<i>Ch. aethiops</i>	<i>L. albigena</i>	0.003	0.095
	<i>Ch. aethiops</i>	<i>Dolichopithecus</i>	<0.001	<0.001
	<i>N. larvatus</i>	<i>Dolichopithecus</i>	<0.001	0.018
	<i>E. patas</i>	<i>Dolichopithecus</i>	<0.001	0.010
	<i>P. melalophos</i>	<i>Dolichopithecus</i>	<0.001	0.006
	<i>L. albigena</i>	<i>Dolichopithecus</i>	0.007	0.237
Tfv	<i>L. albigena</i>	<i>N. larvatus</i>	0.041	1.000
	<i>E. patas</i>	<i>N. larvatus</i>	0.005	0.176
	<i>L. albigena</i>	<i>P. melaophos</i>	0.040	1.000
	<i>E. patas</i>	<i>P. melaophos</i>	0.003	0.093
	<i>E. patas</i>	<i>Co.guereza</i>	0.004	0.147
	<i>E. patas</i>	<i>Ch. aethiops</i>	0.044	1.000

Abbreviations: Asfc = area-scale fractal complexity; epLsar = exact proportion length-scale anisotropy of relief; Smc = scale of maximal complexity; Tfv = textural fill volume; Hasfc<sub>9,36,81</sub> = heterogeneity of area-scale fractal complexity on 36 cells.

<sup>a</sup> Asymptotic significance (2-sided tests) are displayed with significance level set at 0.05.

<sup>b</sup> Significance values have been adjusted by the Bonferroni correction for multiple tests.

**Table 10**

Results of post-hoc pairwise comparisons of *Dolichopithecus* and extant species on phase II and phase I facets. Differences highlighted with Bonferroni adjustment are shown in bold<sup>a</sup>.

Species	<i>Dolichopithecus</i>		<i>Colobus guereza</i>		<i>Ptilocolobus badius</i>		<i>Semnopithecus entellus</i>		<i>Nasalis larvatus</i>		<i>Presbytis melalophos</i>		<i>Lophocebus albigena</i>		<i>Chlorocebus aethiops</i>		<i>Erythrocebus patas</i>		
Facet	II	I	II	I	II	I	II	I	II	I	II	I	II	I	II	I	II	I	
<i>Dolichopithecus</i>			Asfc(-) <b>epLsar(+)</b> Smc(-)	Asfc(-) <b>Smc(-)</b>	Asfc(-) epLsar(+) Smc(-)	Asfc(-) <b>Smc(-)</b>	Hasfc <sub>36</sub> (-)	Smc(-)	<b>Smc(-)</b>	<b>Smc(-)</b>	epLsar(+)	<b>Smc(-)</b>	Asfc(+) Smc(-) Smc(-) Hasfc <sub>36</sub> (-)	Smc(-)	<b>Smc(-)</b>	<b>Smc(-)</b>	Asfc(+) <b>Smc(-)</b>	<b>Smc(-)</b>	
<i>Colobus guereza</i>	Asfc(+) <b>epLsar(-)</b> Smc(+)	Asfc(+) <b>Smc(+)</b>					Smc(+)			epLsar(-)	Smc(+)	<b>Smc(+)</b>	Asfc(+) epLsar(-) Smc(+) Hasfc <sub>36</sub> (+)	<b>Asfc(+)</b>	<b>epLsar(-)</b>	Asfc(+)	<b>epLsar(-)</b>	Asfc(+) Tfv(+)	
<i>Ptilocolobus badius</i>	Asfc(+) epLsar(-) Smc(+)	Asfc(+) <b>Smc(+)</b>							Smc(+)			Asfc(+) Smc(+)	<b>Asfc(+)</b>	<b>Asfc(+)</b>	<b>Asfc(+)</b>	epLsar(-)	Asfc(+)	<b>Asfc(+)</b>	<b>Asfc(+)</b> Smc(+)
<i>Semnopithecus entellus</i>	Hasfc <sub>36</sub> (+)	Smc(+)	Smc(-)			Smc(-)					Smc(+)	Smc(+)	Asfc(+)	Asfc(+)	Smc(-) Hasfc <sub>36</sub> (-)	Smc(-)	Asfc(+) epLsar(-)	Asfc(+)	
<i>Nasalis larvatus</i>	<b>Smc(+)</b>	<b>Smc(+)</b>	epLsar(+)									Smc(+)	Smc(+)	Tfv(+)			epLsar(-) Smc(-)	Tfv(+)	
<i>Presbytis melalophos</i>	epLsar(-)	<b>Smc(+)</b>	Smc(-)	<b>Smc(-)</b>	Asfc(-) Smc(-)	Smc(-)			Smc(-)					Asfc(+) epLsar(-)	Asfc(+) Tfv(+)	Asfc(+) epLsar(-) Hasfc <sub>36</sub> (-)	<b>Smc(-)</b>	Asfc(+) epLsar(-)	
<i>Lophocebus albigena</i>	Asfc(-) Smc(+) Hasfc <sub>36</sub> (+)	Smc(+)	<b>Asfc(-)</b> epLsar(+) Smc(-) Hasfc <sub>36</sub> (-)	<b>Asfc(+)</b>	<b>Asfc(-)</b>	<b>Asfc(-)</b>	Asfc(-)	Asfc(-)	Smc(-)	Tfv(-)	Asfc(-) epLsar(+)	Asfc(-) Tfv(-)			Smc(-)	Smc(-)			
<i>Chlorocebus aethiops</i>	<b>Smc(+)</b>	<b>Smc(+)</b>	<b>Asfc(-)</b> <b>epLsar(+)</b>	Asfc(-)	<b>Asfc(-)</b> epLsar(+)	Asfc(-)	Smc(+) Hasfc <sub>36</sub> (+)	Smc(+)			Asfc(-) epLsar(+) Smc(+) Hasfc <sub>36</sub> (+)	<b>Smc(+)</b>	Smc(+)	Smc(+)					Tfv(+)
<i>Erythrocebus patas</i>	Asfc(-) <b>Smc(+)</b>	<b>Smc(+)</b>	<b>Asfc(-)</b> <b>epLsar(+)</b>	Asfc(-) Tfv(-)	<b>Asfc(-)</b> Smc(+)	<b>Asfc(-)</b> Smc(-)	Asfc(-) epLsar(+)	Asfc(-)	Asfc(-) epLsar(+) Smc(+)	Tfv(-)	Asfc(-) epLsar(+)					Tfv(-)			

Abbreviations: Asfc = area scale fractal complexity; epLsar = exact proportion length-scale anisotropy of relief; Smc = scale of maximal complexity; Tfv = textural fill volume; Hasfc<sub>36</sub> = heterogeneity of area-scale fractal complexity on 36 cells.

<sup>a</sup>(-) and (+) indicate values that are either significantly lower or higher, respectively, for species in column compared to the one in the row.